Supporting Information File

A Protodefluorinated Selectfluor® Heteroaggregate Photoinduces Direct C(sp^3)−H Fluorinations Without Photocatalyst

Shahboz Yakubov,[a] and Joshua P. Barham[a,b]*

[a]Fakultät für Chemie und Pharmazie, Universität Regensburg, Universitätsstr. 31, 93053 Regensburg, Germany

[b]Department of Pure & Applied Chemistry, University of Strathclyde, 295 Cathedral St., Glasgow G1 1XL, U.K.

*Corresponding Author. E-mail: Joshua-Philip.Barham@chemie.uni-regensburg.de

Table of Contents

1 Experimental 2
1.1 General Comments 2
2 Synthesis 13
2.1 Synthesis of Starting Materials 13
2.2 Synthesis of Fluorinated products 14
3 Mechanistic Studies 21
3.1 Radical Trapping 21
3.2 UV-visible Spectroscopy Studies 22
3.3 Luminescence Measurements 23
4 ^{1}H NMR, ^{13}C NMR and ^{19}F NMR Spectra 32
5 X-Ray Crystal Data and Experimental 54
6 References 62

1 Experimental

1.1 General Comments

Unless otherwise specified, all reactions were performed using dried, deoxygenated solvents. Purifications were conducted by column chromatography with silica gel (Macherey Nagel 0.063–0.2 mm) and the solvents were used after receiving without further purification. Syntheses of products were confirmed by comparisons with the literature data where possible, HR-MS and by ^{1}H and ^{19}F NMR spectra. The reactions were followed and pure fractions from column chromatography were detected by TLC using silica gel pre-coated aluminum sheets (Macherey Nagel: Alugram Xtra SIL G UV254 Nr. 818333, thickness 0.2 mm). TLC plates were analyzed under a UV-light (254 nm) and by potassium permanganate stain.

NMR spectra were recorded in $CDCl_3$ or CD_3CN on a Bruker Avance 400 (400 MHz for ^{1}H, 101 MHz for ^{13}C, 376 MHz for ^{19}F). For ^{1}H, ^{13}C and ^{19}F chemical shifts are presented in δ-scale as ppm (parts per million) with residual chloroform peak (7.26 ppm for ^{1}H and 77.00 ppm for ^{13}C), residual DMSO peak (2.54 ppm for ^{1}H and 40.45 ppm for ^{13}C), residual acetonitrile peak (1.96 ppm for ^{1}H and 118.26 and 1.79 ppm for ^{13}C) or residual water peak (4.79 ppm for ^{1}H) as an internal standard. For ^{19}F NMR, trifluorotoluene was used as the reference (-63.38 ppm), if not stated, no reference is used. NMR yields were calculated based on ^{19}F NMR using either trifluorotoluene or pentafluorobenzene as an Internal Standard. MestReNova v6.0.2-5475 was used to process NMR spectra. The description of multiplicity that were used is as follows: s = singlet, d = doublet, dd=doublet of doublet, ddd=doublet of doublet of doublet, dm=doublet of multiplet, t = triplet, q = quartet, p=pentet, m = multiplet.

UV-vis absorption spectra were recorded on an Agilent Cary 100 UV/Vis spectrometer (wavelength range: 200-800 nm) and using 0.10 mm thick 10 mm × 10 mm quartz cuvettes housing liquid samples at 25 °C.

HR-MS were recorded at the Central Analytical Department of the University of Regensburg and the spectra were measured on a JOEL AccuTOF GCx instrument for electron ionization (EI), Agilent Q-TOF 6540 UHD instrument for electrospray ionization (ESI) and atmospheric-pressure chemical ionization (APCI).

Figure S1. Typical photochemical reaction set-up using purple LEDs 3.8 W switched off (left) and on (right).

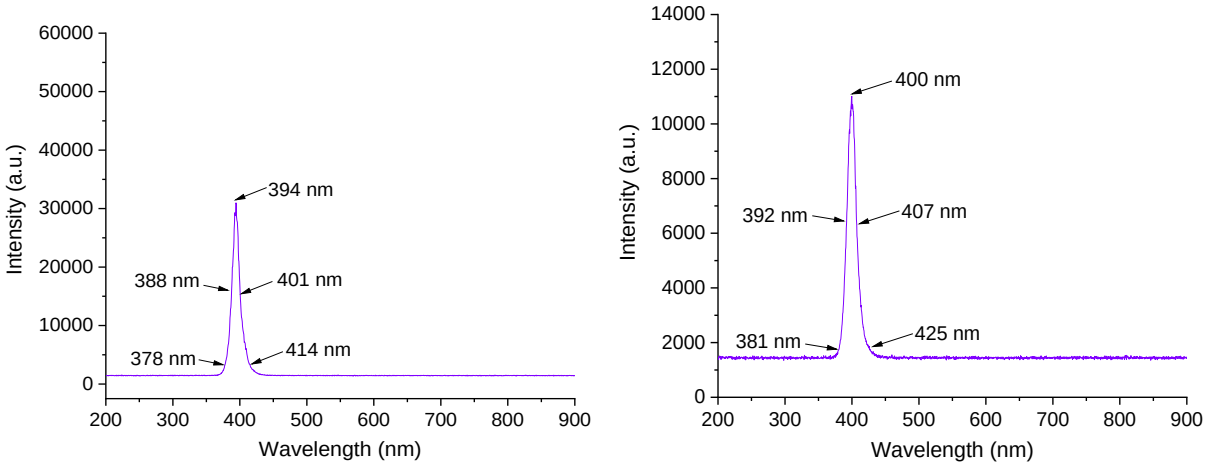

Figure S2. Relative LED intensities of 400 nm LEDs measured at a 30 cm distance directly above the LED. Input power of the higher intensity LED (left) = 3.8 W, input power of lower intensity LED (right) = 350 mW.

Figure S3. Gram-scale fluorination reactions were conducted by irradiation with LED Engine LZ4-40UB00-00U4 LEDs (λ = 395 nm, 14.8 V, 700 mA).

Initial screening of additives (2.0 eq.) with butylphenyl acetate revealed that **H-TEDA(BF$_4$)$_2$** afforded the highest product yield (Table S1, entry 1). Boc-Val-OH and dibenzoyl tartaric acid gave similar yields (entries 3 and 6), however these additives were not as generally applicable across photochemical C(sp^3)−H fluorinations of other substrates (Tables S1, S2 and S4).

Table S1. Fluorination of butylphenyl acetate with different additives.

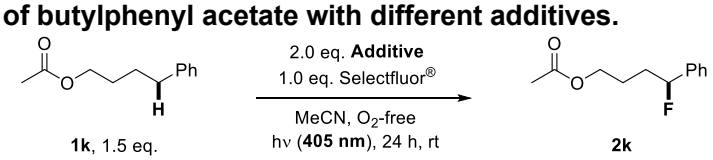

1k, 1.5 eq. **2k**

Entry	Additive (2.0 eq.)	NMR yield (%)
1	**H-TEDA(BF_4)$_2$**	64
2	TFA	43
3	Boc-Val-OH	63
4	L-*tert*-Leucine	37
5	2-(CF_3)phenylglycine	22
6	Dibenzoyl tartaric acid	60
7	Ditoluoyl tartaric acid	35
8	Dipivaloyl tartaric acid	36

Table S2. Fluorination of butylphenyl 4-fluorobenzoate with different additives.

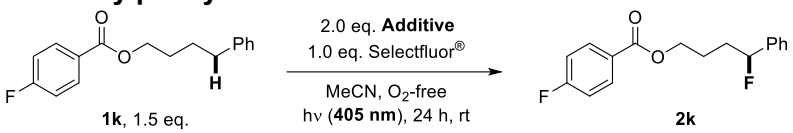

Entry	Additive (2.0 eq.)	NMR yield (%)
1	**H-TEDA(BF_4)$_2$**	85
2	Carbobenzyloxy-L-Valine	41
3	Boc-Val-OH	66
4	L-2-phenylglycine	63
5	Tartaric acid	68
6	Dibenzoyl tartaric acid	55
7	Ditoluoyl tartaric acid	traces
8	Dipivaloyl tartaric acid	65

Table S3. Fluorination of hexyl propionate with different amount of H-TEDA(BF_4)$_2$.

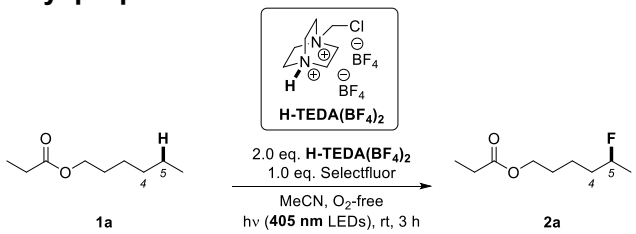

Entry	Additive	NMR yield (%)
1	-	0
2	0.1 eq. **H-TEDA(BF_4)$_2$**	48
3	0.5 eq. **H-TEDA(BF_4)$_2$**	53
4	1.0 eq. **H-TEDA(BF_4)$_2$**	43

5	1.5 eq. **H-TEDA(BF$_4$)$_2$**	91
6	2.0 eq. **H-TEDA(BF$_4$)$_2$**	91
7	2.5 eq. **H-TEDA(BF$_4$)$_2$**	88
8	3.0 eq. **H-TEDA(BF$_4$)$_2$**	81
9	3.5 eq. **H-TEDA(BF$_4$)$_2$**	96
10	4.0 eq. **H-TEDA(BF$_4$)$_2$**	67
11	6.0 eq. **H-TEDA(BF$_4$)$_2$**	91
12	8.0 eq. **H-TEDA(BF$_4$)$_2$**	95
13	10.0 eq. **H-TEDA(BF$_4$)$_2$**	97

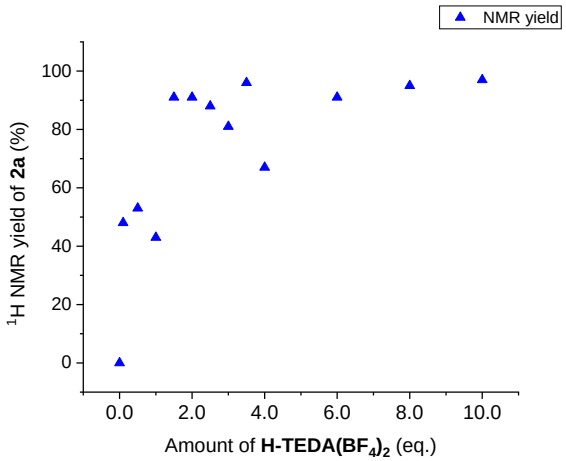

Figure S4. Plot of NMR yield of the reaction of **1a** vs equivalents of **H-TEDA(BF$_4$)$_2$** added.

In previous studies, hexyl propionate (**1a**) underwent C(sp^3)−H fluorination in a good (~70%) yield in the presence of methyl 4-fluorobenzoate as a photocatalyst,[1] and has no photoactive auxiliary (benzoyl group) nor activated benzylic position. Therefore, it was chosen as a suitable substrate for screening loading of **H-TEDA(BF$_4$)$_2$**. In general, increasing the equivalents of **H-TEDA(BF$_4$)$_2$** increased the yield. However, in order to strike a balance with mass intensity, we identified 2.0 eq. **H-TEDA(BF$_4$)$_2$** as optimal. Therefore, 2.0 eq. **H-TEDA(BF$_4$)$_2$**, 1.0 eq. **SF** and 1.5 eq. substrate under 405 nm LED irradiation and under inert atmosphere were deemed to be the optimal conditions, under which reactions were complete after only 3 h providing 91% yield (Table S3, entry 5). Without **H-TEDA(BF$_4$)$_2$** additive, the reaction does not proceed at all (Table S3, entry 1). In the presence of methyl 4-fluorobenzoate (1 mol%), the yield was 0% after 3 h and 73% after 24 h.

We examined further the robustness of the process (Table S4). We established that inert atmosphere and light are crucial for the reaction to proceed successfully (entries 2-4). Gratifyingly, the addition of three drops of water did not change the outcome of the reaction (entry 5), meaning that unlike most previously reported photocatalytic fluorination methods, where they use dry solvent,[2] our conditions do not require a dry solvent, which is economically desirable. However, a threshold level of water shuts down the reaction. For example, when using a 10:1 and 1:1 ratio of MeCN and water - where **H-TEDA(BF$_4$)$_2$** and **SF** were dissolved completely - this did not afford product (entries 6,7). We assume that water interferes with heteroaggregate formation thus preventing the activation of **SF**. A 1:1 ratio of MeCN and DMSO did not

provide any product (entry 8). Using **NFSI** instead of **SF** provided only 40% fluorinated product (entries 9). Next, we investigated the importance of **H-TEDA(BF$_4$)$_2$** and its structure. NH$_4$•BF$_4$ as a BF$_4$ source instead of **H-TEDA(BF$_4$)$_2$**, did not promote the reaction. To examine the importance of the N$^+$-H moiety of **H-TEDA(BF$_4$)$_2$**, we used substrate **TEDA•BF$_4$** that does not contain the N$^+$-H moiety. No product was formed. Instead of the BF$_4$ counter-anion, other counter-anions of **H-TEDA^{2+}** were examined such as Cl and PF$_6$. The former gave no reaction, and the latter gave a low yield (entries 12,13). At last, we used protodefluorinated Selectfluor II instead of **H-TEDA(BF$_4$)$_2$** that did not work. After the optimization process, we concluded that all the structural features of **H-TEDA(BF$_4$)$_2$** such as its N$^+$-H, BF$_4$, and the methylene Cl substituent are important for the **H-TEDA(BF$_4$)$_2$** to function as active species.

Table S4. Initial investigations and optimization of conditions.

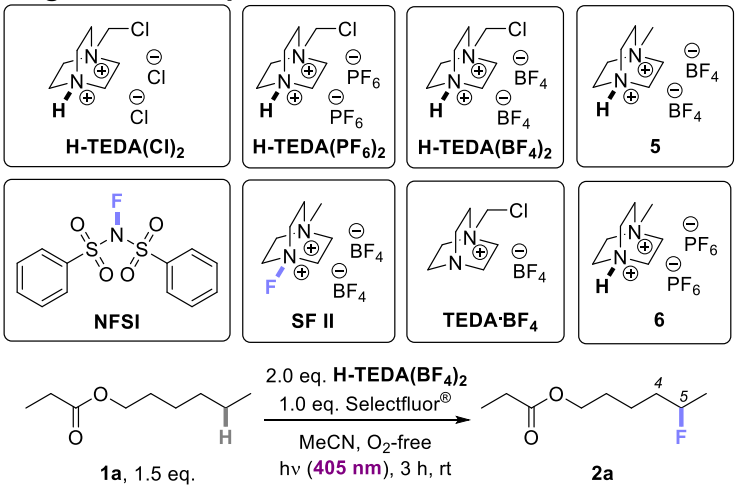

Entry	Deviation from the standard conditions	NMR yield (%)
1	None	91[a]
2	No light	0
3	No **H-TEDA(BF$_4$)$_2$**	0
4	Under air	0
5	+ 3 drops of water	90[a]
6	MeCN : H$_2$O = 10:1 as solvent	0
7	MeCN : H$_2$O = 1:1 as solvent	0
8	MeCN : DMSO = 1:1 as solvent	0
9	**NFSI** instead of **SF**	40[a]
10	**SF II** instead of **SF**	0
11	**NH$_4$•BF$_4$** instead of **H-TEDA(BF$_4$)$_2$**	0
12	**TEDA•BF$_4$** instead of **H-TEDA(BF$_4$)$_2$**	0
13	**H-TEDA(Cl)$_2$** instead of **H-TEDA(BF$_4$)$_2$**	0
14	**H-TEDA(PF$_6$)$_2$** instead of **H-TEDA(BF$_4$)$_2$**	13
15	**5** instead of **H-TEDA(BF$_4$)$_2$**	0
16	**6** instead of **H-TEDA(BF$_4$)$_2$**	traces
17	**Py-H•BF$_4$** instead of **H-TEDA(BF$_4$)$_2$**	70
18	**Imid-H•BF$_4$** instead of **H-TEDA(BF$_4$)$_2$**	62
19	**TFA** instead of **H-TEDA(BF$_4$)$_2$**	63
20	**Ph-Gly** instead of **H-TEDA(BF$_4$)$_2$**	15
21	**Tartaric acid** instead of **H-TEDA(BF$_4$)$_2$**	92

22	**Boc-Val-OH** instead of **H-TEDA(BF$_4$)$_2$**	70
23	**Acetic acid** instead of **H-TEDA(BF$_4$)$_2$**	0
24	**TEA-H·BF$_4$** instead of **H-TEDA(BF$_4$)$_2$**	35
25	**L-*tert*-Leucine** instead of **H-TEDA(BF$_4$)$_2$**	0
26	**2-(CF$_3$)phenylglycine** instead of **H-TEDA(BF$_4$)$_2$**	0
27	**Camphorsulfonic acid** instead of **H-TEDA(BF$_4$)$_2$**	0

Unless otherwise specified, substrate concentration was [0.15 M] and a 3.8 W 400 nm LED was employed. NMR yields were determined by ^{19}F NMR spectroscopy with pentafluorobenzene as an internal standard. [a] Combined yields of the regioisomers (C4 and C5 positions).

Synthesis of H-TEDA(BF$_4$)$_2$ from DABCO:

In order to make additive **H-TEDA(BF$_4$)$_2$** accessible for use, we considered three pathways for its synthesis: **Pathway A** (consists of 2 steps) and **Pathway B** (consists of 3 steps) and **Pathway C** (consists of 3 steps). The first step in all pathways is the same – alkylation of DABCO:

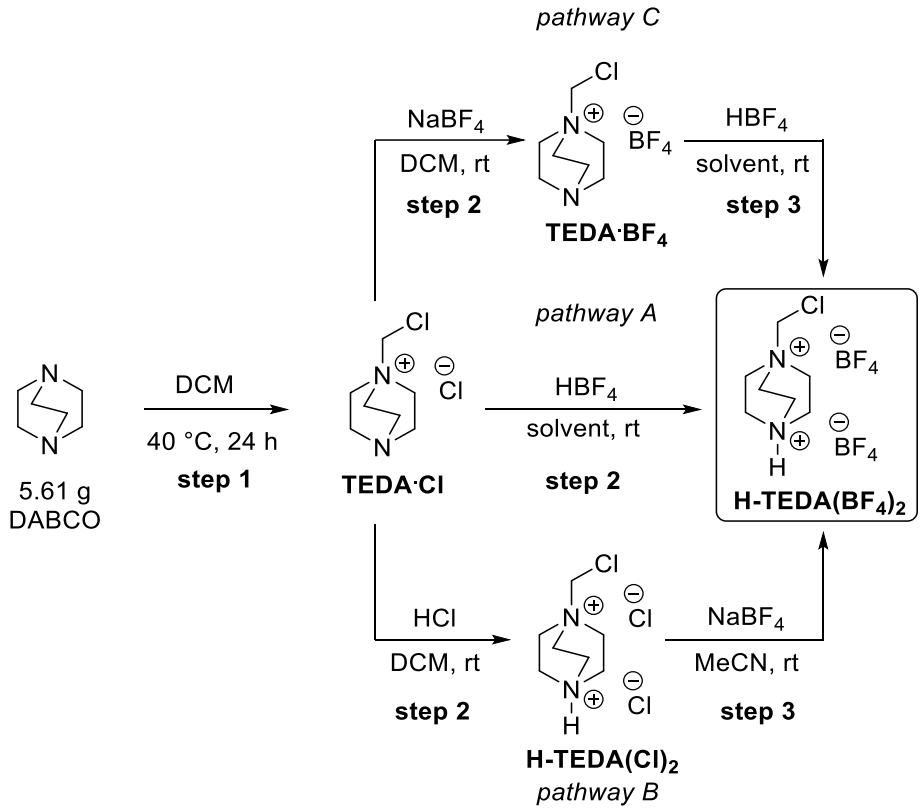

Scheme S1. Preparation of H-TEDA(BF$_4$)$_2$ and derivatives.

In order to examine the impact of derivatives of **H-TEDA(BF$_4$)$_2$** to understand which structural aspects were key for promotion of the 'photocatalyst'-free reactivity, we synthesized derivatives of **H-TEDA(BF$_4$)$_2$**. We synthesized **H-TEDA(BF$_4$)$_2$** and **TEDA·BF$_4$** with different counter-anions and compounds **5** - **7** and used them in fluorination reactions. However, none of those substrates showed any efficiency as initial **H-TEDA(BF$_4$)$_2$**, revealing the key importance of the $^{-}BF_4$ counter-anion, the N^{+}–H moiety and the CH_2Cl moiety in the heteroaggregate formation or reactivity.

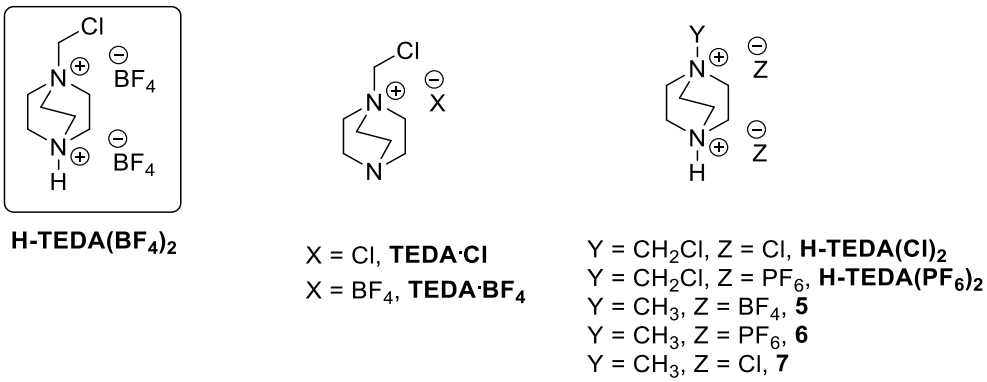

H-TEDA(BF_4)$_2$

Figure S5. Structures of derivatives of H-TEDA(BF_4)$_2$ synthesized.

Synthesis of H-TEDA(BF_4)$_2$:

Step 1 – alkylation: 1,4-diazabicyclo[2.2.2]octane (DABCO, also known as triethylenediamine (TEDA)) (5.61 g, 50.0 mmol, 1.0 eq.) was dissolved in DCM (100 mL) and refluxed under 40 °C for 24 h. The reaction mixture was used for the second step.

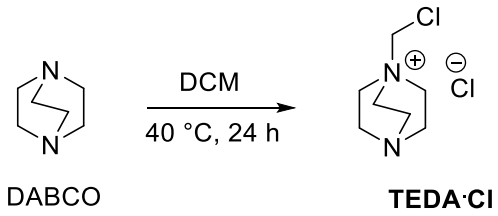

DABCO **TEDA·Cl**

Scheme S2. Alkylation of DABCO with DCM.

Pathway A: **Step 2** – counterion exchange and protonation:

- To the reaction mixture from *Step 1*, solution of tetrafluoroboric acid (48 wt.% in H_2O) (20.0 mL, 150 mmol, 3.0 eq.) was added. The reaction mixture was stirred for 1 h and concentrated *in vacuo* to afford **H-TEDA(BF_4)$_2$** (quantitative yield, 16.81 g, 50.0 mmol).
- To the reaction mixture from *Step 1* was concentrated *in vacuo* and the dry product was obtained. The product was dissolved in acetone (50 mL) and solution of tetrafluoroboric acid (48 wt.% in H_2O) (20.0 mL, 150 mmol, 3.0 eq.) was added. The reaction mixture was stirred for 1 h. The white solid that precipitated was filtered and dried *in vacuo* to afford **H-TEDA(BF_4)$_2$** (quantitative yield, 16.81 g, 49.96 mmol).

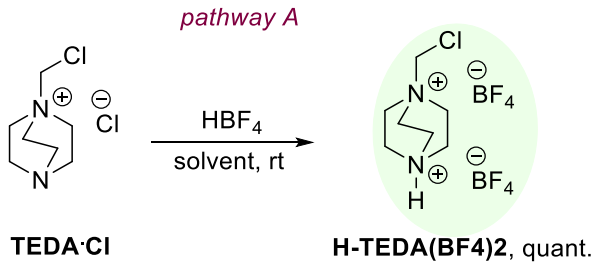

TEDA·Cl **H-TEDA(BF4)2**, quant.

Scheme S3. Counter-anion exchange and protonation of TEDA·Cl.

Pathway B: **Step 2** – protonation:

- To the reaction mixture from *Step 1*, solution of hydrochloric acid (12 M in H_2O) (8.3 mL, 100 mmol, 2.0 eq.) was added. The reaction mixture was stirred for 1 h and concentrated *in vacuo* to provide **H-TEDA(Cl)$_2$** as a white solid (quantitative yield, 11.67 g, 49.97 mmol).

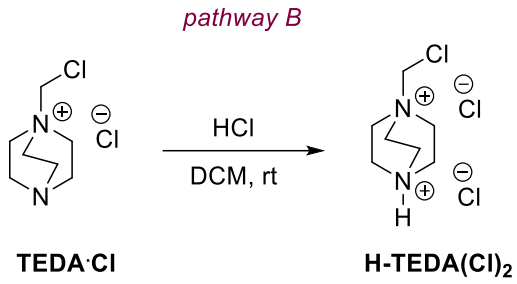

Scheme S4. Protonation of TEDA·Cl.

Step 3 – counterion exchange:

- The product from *Step 2 (Pathway B)* was added to the solution of $NaBF_4$ (11.53 g, 105.0 mmol, 2.1 eq.) in MeCN (100 mL). The reaction mixture was stirred for 1 hour. Sodium chloride was precipitated as a white solid that was filtered out and the filtrate was dried *in vacuo* to provide the desired product - **H-TEDA(BF$_4$)$_2$** (98% yield, 16,48 g, 49,0 mmol).

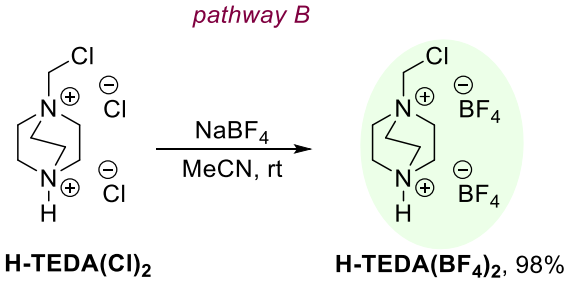

Scheme S5. Counter-anion exchange of H-TEDA(Cl)$_2$.

Pathway C: **Step 2** – counterion exchange:

- To the reaction mixture from *Step 1*, solution of $NaBF_4$ (55 mmol, 1.1 eq.) was added. The reaction mixture was stirred for 1 hour and then was concentrated *in vacuo* to provide white solid as the product (**TEDA·BF$_4$**).

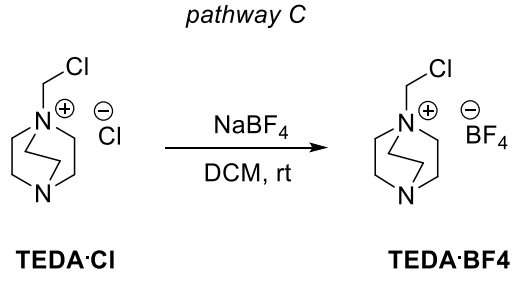

Scheme S6. Counter-anion exchange of TEDA·Cl.

Step 3 – counterion exchange and protonation:

- The product from *Step 2 (Pathway C)* was dissolved in acetonitrile (50 mL) and solution of tetrafluoroboric acid (48 wt.% in H2O) (10.0 mL, 75 mmol, 1.5 eq.) was added to the solution. The reaction mixture was stirred for 1 hour. A white solid was precipitated that was filtered and dried in vacuo to provide the desired product - **H-TEDA(BF$_4$)$_2$** (quantitative yield, 16.80 g, 49.96 mmol).

- The product *Step 2 (Pathway C)* was dissolved in acetone (50 mL) and solution of tetrafluoroboric acid (48 wt.% in H2O) (10.0 mL, 75 mmol, 1.5 eq.) was added to the solution. The reaction mixture was stirred for 1 hour. A white solid was precipitated that was filtered and dried in vacuo to provide the desired product - **H-TEDA(BF$_4$)$_2$** (quantitative yield, 16.81 g, 50.0 mmol).

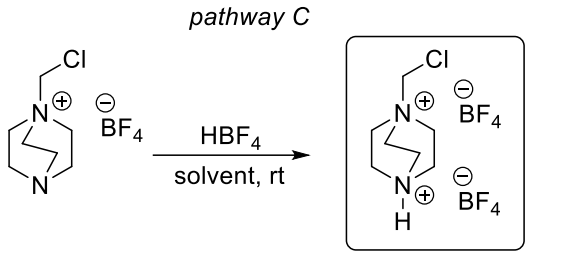

7 **H-TEDA(BF$_4$)$_2$**, 99%

Scheme S7. Protonation of TEDA·BF$_4$.

Isolation of H-TEDA(BF$_4$)$_2$ After Fluorination Reactions for Recycling:

Upon completion of fluorination reaction, diethyl ether was added to the reaction mixture, and instant precipitation of **H-TEDA(BF$_4$)$_2$** was observed. The mixture was filtered into a flask and the residue was washed with more diethyl ether. The residue was dried, and in all cases was deemed pure by NMR. This **H-TEDA(BF$_4$)$_2$** was used for further fluorination reactions.

1-(chloromethyl)-1,4-diazabicyclo[2.2.2]octane-1,4-diium ditetrafluoroborate (H-TEDA(BF$_4$)$_2$)

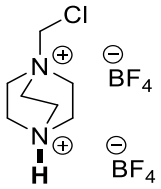

Yield: 97%; white solid; IR (neat) ν (cm^{-1}): 3179, 3060, 3012, 1480, 1409, 1338, 1290, 1036, 943, 895, 850, 798, 764, 731; ^{1}H NMR (400 MHz, CD_3CN) δ 7.45 (br. s, 1H), 5.20 (s, 2H), 3.82 (dt, *J* = 15.0, 6.7 Hz, 12H) ppm; ^{13}C NMR (101 MHz, CD_3CN) δ 70.1, 51.0, 45.1 ppm; ^{19}F NMR (377 MHz, CD_3CN) δ -150.0 (s), -150.1 (s) ppm; HRMS (ESI) (*m/z*) [M-H]$^+$: exact mass calc. for $C_7H_{14}ClN_2^+$: 161.0840; found: 161.0837.

1-(chloromethyl)-1,4-diazabicyclo[2.2.2]octan-1-ium chloride (TEDA·Cl)

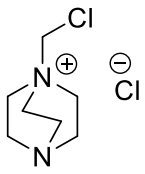

^{1}H NMR (400 MHz, DMSO) δ 5.67 (s, 2H), 3.62 – 3.50 (m, 6H), 3.18 – 3.01 (m, 6H) ppm; ^{13}C NMR (101 MHz, DMSO) δ 68.2, 51.3, 45.3 ppm; HRMS (ESI) (*m/z*) $[M]^+$: exact mass calc. for $C_7H_{14}ClN_2^+$: 161.0840; found: 161.0845.

1-(chloromethyl)-1,4-diazabicyclo[2.2.2]octane-1,4-diium dichloride (H-TEDA(Cl)$_2$)

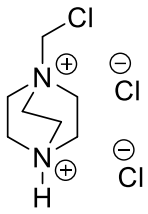

^{1}H NMR (400 MHz, D_2O) δ 5.48 (s, 2H), 4.19 – 4.07 (m, 6H), 4.03 – 3.91 (m, 6H) ppm; ^{13}C NMR (101 MHz, D_2O) δ 69.1, 50.2, 43.9 ppm; HRMS (ESI) (*m/z*) $[M]^+$: exact mass calc. for $C_7H_{14}ClN_2^+$: 161.0840; found: 161.0840.

1-(chloromethyl)-1,4-diazabicyclo[2.2.2]octan-1-ium tetrafluoroborate (TEDA·BF$_4$)

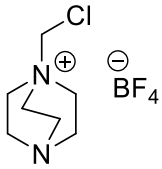

IR (neat) ν (cm^{-1}): 3630, 3049, 2974, 2900, 1636, 1469, 1364, 1327, 1290, 1047, 906, 842, 790, 686; ^{1}H NMR (400 MHz, DMSO) δ 5.29 (s, 2H), 3.48 – 3.35 (m, 6H), 3.20 – 3.06 (m, 6H) ppm; ^{13}C NMR (101 MHz, DMSO) δ 68.6, 51.7, 45.4 ppm; ^{19}F NMR (377 MHz, DMSO) δ -147.9 (s), -148.0 (s) ppm; HRMS (ESI) (*m/z*) $[M]^+$: exact mass calc. for $C_7H_{14}ClN_2^+$: 161.0841; found: 161.0839.

1-(chloromethyl)-1,4-diazabicyclo[2.2.2]octane-1,4-diium dihexafluorophosphate (H-TEDA(PF$_6$)$_2$)

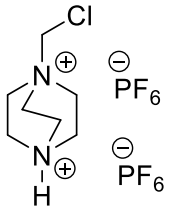

^{1}H NMR (400 MHz, CD_3CN) δ 6.07 – 5.28 (br. s, 1H), 5.16 (s, 2H), 3.82 (m, 6H), 3.71 (m, 6H) ppm; ^{13}C NMR (101 MHz, CD_3CN) δ 69.8, 50.7, 44.7 ppm; ^{19}F NMR (377 MHz, CD_3CN) δ -70.7 (s), -72.6 (s) ppm; ^{31}P NMR (162 MHz, CD_3CN) δ -143.1 (hept, *J* = 706.3 Hz) ppm; HRMS (ESI) (*m/z*) $[M]^+$: exact mass calc. for $C_7H_{14}ClN_2^+$: 161.0840; found: 161.0840.

1-methyl-1,4-diazabicyclo[2.2.2]octane-1,4-diium ditetrafluoroborate (5)

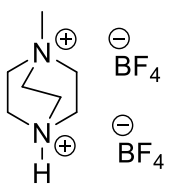

Prepared in two steps. *Step 1* was performed according to the literature procedure.[3] To a solution of DABCO (1 g, 8.9 mmol) in hexane (25 ml), methyl iodide (0.5 ml, 8.9 mmol) was added slowly at 0°C and stirred for

1 h at room temperature. The reaction mixture was concentrated in vacuo, and the residue was washed with hexanes (100 ml) and dried to yield a slightly yellow solid (2.06 g, 91%). The product was used directly for *Step 2*.

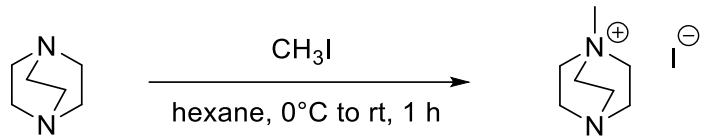

Step 2 is the same procedure that was used for **H-TEDA(BF$_4$)$_2$** synthesis, **Pathway A**, *Step 2*.

^{1}H NMR (400 MHz, CD_3CN) δ 6.97 (br. s, 1H), 3.73 (dq, *J* = 9.8, 6.2 Hz, 12H), 3.21 (s, 3H) ppm; ^{13}C NMR (101 MHz, CD_3CN) δ 53.4 – 53.0 (m), 44.9 (s) ppm; ^{19}F NMR (377 MHz, CD_3CN) δ -150.0 (s), -150.1 (s) ppm; HRMS (ESI) (*m/z*) $[M]^+$: exact mass calc. for $C_7H_{15}N_2^+$: 127.1230; found: 127.1238.

1-methyl-1,4-diazabicyclo[2.2.2]octane-1,4-diium dihexafluorophosphate (6)

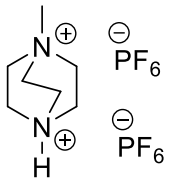

Prepared in two steps. *Step 1* is the same procedure that was used for synthesis of substrate **5**, *Step 1*.

Step 2 is the same procedure that was used for **H-TEDA(BF$_4$)$_2$** synthesis, **Pathway A**, *Step 2*, but using HPF_6 instead of HBF_4.

^{1}H NMR (400 MHz, CD_3CN) δ 7.17 (s, 1H), 3.66 (dq, *J* = 10.4, 6.5 Hz, 12H), 3.18 (s, 3H) ppm; ^{13}C NMR (101 MHz, CD_3CN) δ 53.5 – 53.0 (m), 44.7 (s) ppm; ^{19}F NMR (377 MHz, CD_3CN) δ -70.6 (s), -72.4 (s) ppm; ^{31}P NMR (162 MHz, CD_3CN) δ -143.1 (hept, *J* = 706.8 Hz) ppm; HRMS (ESI) (*m/z*) $[M]^+$: exact mass calc. for $C_7H_{15}N_2^+$: 127.1230; found: 127.1232.

1-methyl-1,4-diazabicyclo[2.2.2]octane-1,4-diium dichloride (7)

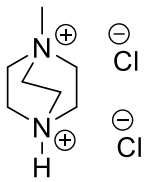

Prepared in two steps. *Step 1* is the same procedure that was used for synthesis of substrate **5**, *Step 1*.

Step 2 is the same procedure that was used for **H-TEDA(BF$_4$)$_2$** synthesis, **Pathway B**, *Step 2*.

^{1}H NMR (400 MHz, D_2O) δ 4.08 – 3.87 (m, 12H), 3.40 (s, 3H) ppm, ^{13}C NMR (101 MHz, D_2O) δ 53.2 – 52.9 (m), 52.8 – 52.5 (m), 44.0 (s) ppm; HRMS (ESI) (*m/z*) $[M]^+$: exact mass calc. for $C_7H_{15}N_2^+$: 127.1230; found: 127.1230.

2 Synthesis

2.1Synthesis of Starting Materials

General Procedure 1: Esterification

To a solution of DMAP (0.1 eq.), Et_3N (1.5 eq.) in DCM (0.2 M) alcohol (1.0 eq.) was added and the mixture was cooled to 0°C. Benzoyl chloride (1.2 eq.) was added dropwise to the reaction mixture and the reaction was stirred overnight at room temperature (rt). The solution was quenched with H_2O and extracted three times with DCM (20 mL). Combined organic layers were dried over $NaSO_4$, filtrated, and concentrated *in vacuo*. The residue was purified by column chromatography using silica gel and the specified eluent to yield the desired ester.

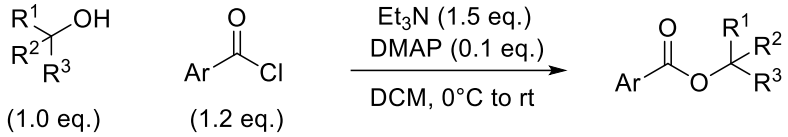

Scheme S8. Esterification of alcohols.

Methyl 2-(4-isobutylphenyl)propanoate (1m)

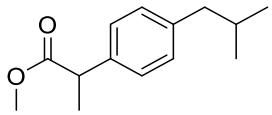

Prepared according to the literature procedure.[4] To the mixture of Ibuprofen (5.00 mmol, 1.0 eq.) and DMAP (0.50 mmol, 0.1 eq.) in 10 mL DCM, methanol (15.00 mmol, 3.0 eq.) was added at 0 °C and stirred for 5 min. DCC (5.50 mmol, 1.1 eq.) was added next and stirred at 0 °C for 5 more minutes. The reaction was allowed to reach rt and stirred for 3 h. The resulting precipitates were filtered, and the filtrate was treated with diluted HCl and the product was extracted three times with DCM. The organic layers were combined, dried over $MgSO_4$, filtered and concentrated *in vacuo*. The residue was purified by column chromatography using 5% EtOAc in pentane to provide the desired product.

Yield: 1.05 g, 95%; colorless liquid; ^{1}H NMR (400 MHz, $CDCl_3$) δ 7.20 (d, *J* = 8.1 Hz, 2H), 7.11 (d, *J* = 8.1 Hz, 2H), 3.70 (q, *J* = 7.2 Hz, 1H), 3.67 (s, 3H), 2.46 (d, *J* = 7.2 Hz, 2H), 1.86 (td, *J* = 13.6, 6.8 Hz, 1H), 1.51 (d, *J* = 7.2 Hz, 3H), 0.91 (d, *J* = 6.6 Hz, 6H) ppm. HRMS (ESI) (*m/z*) $[M]^+$: exact mass calc. for $C_{14}H_{20}O_2$: 220.1463, found: 220.1462.

The data are consistent with our published literature.[1]

4-Phenylbutyl acetate (1k)

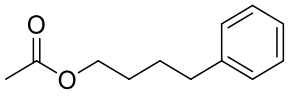

Prepared according to the **General Procedure 1**. Yield: 1.88 g, 98%, colorless oil; ^{1}H NMR (400 MHz, $CDCl_3$) δ 7.34 – 7.16 (m, 5H), 4.11 (dd, *J* = 8.6, 4.0 Hz, 2H), 2.66 (t, *J* = 7.2 Hz, 2H), 2.05 (s, 3H), 1.78 – 1.56 (m, 4H). HRMS (EI) (*m/z*) $[M]^+$: exact mass calc. for $C_{12}H_{16}O_2$: 192.1150, found: 192.1148.

The data are consistent with our published literature.[1]

Methyl (*R*)-4-((5*S*,8*R*,9*S*,10*S*,13*R*,14*S*,17*R*)-10,13-dimethyl-3,7,12-trioxohexadecahydro-1*H*-cyclopenta[a]phenanthren-17-yl)pentanoate (1p)

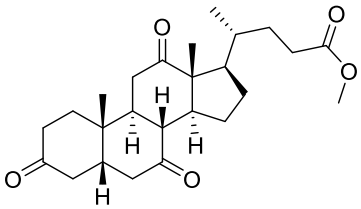

Prepared according to the literature procedure.[5] To a mixture of Dehydrocholic acid (5.00 mmol, 1.0 eq.) and Cs_2CO_3 (6.20 mmol 1.2 eq.) in 10 mL DMF, methyl iodide (28.50 mmol, 5.7 eq.) was added and the mixture was stirred at rt for 24 h. After the addition of water (40 mL), a white precipitate was obtained that was filtered and dried. Yield: 1.94 g, 93%; white solid, m.p. 150-152 °C; ^{1}H NMR (400 MHz, $CDCl_3$) δ 3.65 (d, *J* = 1.1 Hz, 3H), 2.96 – 2.75 (m, 3H), 2.44 – 2.16 (m, 8H), 2.13 (dd, *J* = 12.8, 5.9 Hz, 2H), 2.05 – 1.90 (m, 4H), 1.88 – 1.78 (m, 2H), 1.60 (tt, *J* = 11.6, 5.9 Hz, 1H), 1.41 – 1.22 (m, 7H), 1.06 (s, 3H), 0.83 (d, *J* = 6.5 Hz, 3H) ppm. HRMS (EI) (*m/z*) $[M]^+$: exact mass calc. for $C_{25}H_{36}O_5$: 416.2563, found: 416.2560.

The data are consistent with our published literature.[1]

2.2 Synthesis of Fluorinated products

General Procedure A

To a 5 mL clear crimp vial charged with a stir bar were added **SF** (0.2 mmol, 1.0 eq.), **H-TEDA(BF$_4$)$_2$** (0.4 mmol, 2.0 eq.), and anhydrous MeCN (2.0 mL). The starting material (0.3 mmol, 1.5 eq.) was added next, and the reaction mixture was degassed *via* three cycles of *Freeze-Pump-Thaw*. The reaction mixture was then irradiated using a 405 nm LED for 2 h at rt. Product identity and yields were determined by ^{19}F NMR spectroscopy with pentafluorobenzene as an internal standard. The reaction mixture was then diluted with diethyl ether, filtrated, concentrated, and purified by silica gel flash column chromatography using the specified eluent to provide the desired product.

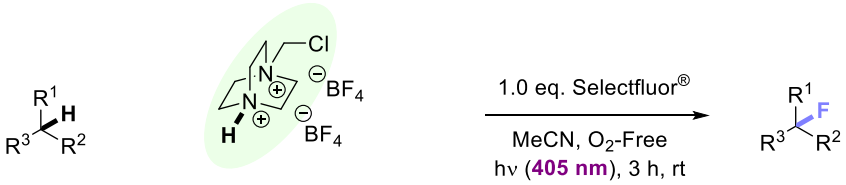

Scheme S9. Catalyst-free Photochemical C(sp^3)-H Fluorination

1-Fluorocyclooctane (2b)

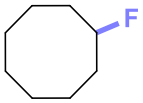

Prepared according to the **General Procedure A**. NMR yield: 93% (according to ^{19}F NMR with pentafluorobenzene as an internal standard); ^{19}F NMR (377 MHz, $CDCl_3$) δ –160.0 ppm (s). HRMS (EI) (*m/z*) $[M]^+$: exact mass calc. for $C_8H_{15}F$: 130.1158; found: 130.1160.

The data are consistent with our published literature.[1]

(3*s*,5*s*,7*s*)-1-Fluoroadamantane (2c)

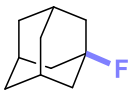

Prepared according to the **General Procedure A**. Yield: 18.0 mg, 58%; white solid, m.p. 230-232 °C; ^{1}H NMR (400 MHz, $CDCl_3$) δ 2.23 (br. s, 1H), 1.90 (dd, *J* = 5.6, 3.0 Hz, 2H), 1.70 – 1.58 (m, 2H) ppm; ^{19}F NMR (377 MHz, $CDCl_3$) δ -128.8 – -129.2 (m) ppm. HRMS (EI) (*m/z*) $[M]^+$: exact mass calc. for $C_{10}H_{15}F$: 154.1158, found: 154.1156.

The data are consistent with our published literature.[1]

Fluorocyclododecane (2d)

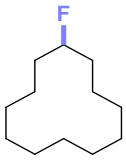

Prepared according to the **General Procedure A**. Yield: 34.0 mg, 91%; colorless solid, m.p. 48-50 °C; ^{1}H NMR (400 MHz, $CDCl_3$) δ 4.71 (dtt, *J* = 47.5, 7.2, 4.6 Hz, 1H), 1.88 – 1.71 (m, 2H), 1.62 (m, 2H), 1.46 – 1.25 (m, 18H) ppm; ^{13}C NMR (101 MHz, $CDCl_3$) δ 92.5 (d, *J* = 164.8 Hz), 29.9 (d, *J* = 21.0 Hz), 24.1 (s), 23.8 (s), 23.3 (s), 23.2 (s), 20.6 (d, *J* = 6.9 Hz) ppm; ^{19}F NMR (377 MHz, $CDCl_3$) δ -176.1 – -176.9 (m) ppm; HRMS (ESI) (*m/z*) $[M^+\text{-HF}]^+$: exact mass calc. for $C_{12}H_{22}$: 166.1716; found: 166.1722.
The data are consistent with the literature.[2b]

5-Fluorodecanedinitrile (2e)

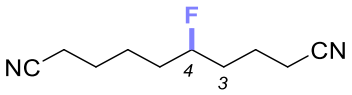

Prepared according to the **General Procedure A** (4F:3F=4:1 ratio). Yield: 25.5 mg, 70%; colorless oil; ^{1}H NMR (400 MHz, $CDCl_3$) δ 4.69 – 4.39 (m, 1H), 2.36 (ddd, *J* = 11.9, 9.6, 5.9 Hz, 4H), 1.90 – 1.44 (m, 10H) ppm; ^{19}F NMR (377 MHz, $CDCl_3$) δ -182.7 – -183.3 (m), -185.2 – -185.7 (m) ppm. HRMS (ESI) (*m/z*) $[M\text{-H}]^+$: exact mass calc. for $C_{10}H_{15}FN_2$: 181.1141, found: 181.1142.

The data are consistent with our published literature.[1]

1,10-dibromo-5-fluorodecane (2f)

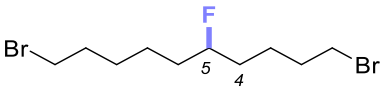

Prepared according to the **General Procedure A** (5F:4F=1.7:1 ratio). Yield: 48.0 mg, 75%; colorless oil; ^{1}H NMR (400 MHz, $CDCl_3$) δ 4.60 – 4.35 (m, 1H), 3.50 – 3.35 (m, 4H), 1.98 – 1.31 (m, 14H) ppm; ^{19}F NMR (377 MHz, $CDCl_3$) δ -181.2 – -181.6 (m), -181.5 – -181.9 (m) ppm. HRMS (ESI) (*m/z*) $[M\text{-HF}]^+$: exact mass calc. for $C_{10}H_{19}Br_2F$: 295.9770 found: 295.9776.

The data are consistent with our published literature.[1]

(3-bromo-1-fluoropropyl)benzene (2g)

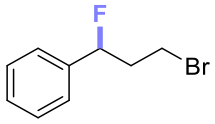

Prepared according to the **General Procedure A**. Yield: 30.0 mg, 69%; slightly yellow oil; ^{1}H NMR (400 MHz, $CDCl_3$) δ 7.55 – 7.33 (m, 5H), 5.70 (ddd, *J* = 47.8, 8.8, 3.9 Hz, 1H), 3.73 – 3.38 (m, 2H), 2.55 (m, 1H), 2.30 (m, 1H) ppm; ^{19}F NMR (377 MHz, $CDCl_3$) δ -176.8 – -177.2 (m) ppm. HRMS (EI) (*m/z*) $[M]^+$: exact mass calc. for $C_9H_{10}BrF$: 215.9950, found: 215.9942.

The data are consistent with our published literature.[1]

(4-chloro-1-fluorobutyl)benzene (2h)

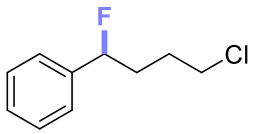

Prepared according to the **General Procedure A**. Yield: 25.0 mg, 67%; colorless oil; ^{1}H NMR (400 MHz, $CDCl_3$) δ 7.35 – 7.20 (m, 5H), 5.40 (ddd, *J* = 47.7, 7.9, 4.3 Hz, 1H), 3.67 – 3.38 (m, 2H), 2.12 – 1.74 (m, 4H) ppm; ^{13}C NMR (101 MHz, $CDCl_3$) δ 139.9 (d, *J* = 19.8 Hz), 128.6 (s), 128.4 (d, *J* = 1.8 Hz), 125.4 (d, *J* = 6.9 Hz), 93.8 (d, *J* = 171.4 Hz), 44.6 (s), 34.5 (d, *J* = 23.9 Hz), 28.2 (d, *J* = 3.8 Hz) ppm; ^{19}F NMR (377 MHz, $CDCl_3$) δ -176.2 – -176.7 (m) ppm; HRMS (EI) (*m/z*) $[M]^+$: exact mass calc. for $C_{10}H_{12}ClF$: 186.0612; found: 186.0606.

4-(3-Fluorobutyl)benzonitrile (2i)

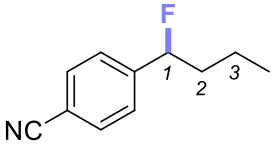

Prepared according to the **General Procedure A**. Yield: 31.0 mg, 87%; colorless oil; ^{1}H NMR (400 MHz, $CDCl_3$) δ 7.55 – 7.49 (m, 2H), 7.25 (d, *J* = 8.2 Hz, 2H), 4.76 – 4.39 (m, 1H), 2.76 (m, 2H), 1.99 – 1.84 (m, 1H), 1.84 – 1.66 (m, 1H), 1.30 (dd, *J* = 23.8, 6.2 Hz, 3H) ppm; ^{19}F NMR (377 MHz, $CDCl_3$) δ -172.92 – -173.56 (m), -179.11 (ddd, *J* = 48.1, 30.0, 18.3 Hz), -180.85 – -181.26 (m) ppm. HRMS (EI) (*m/z*) $[M]^+$: exact mass calc. for $C_{11}H_{12}FN$: 177.0954, found: 177.0953.
The data are consistent with our published literature.[1]

4-Fluoropentyl benzoate (2j)

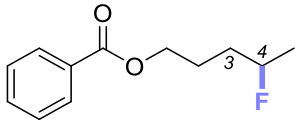

Prepared according to the **General Procedure A** (4F:3F=4:1 ratio). Yield: 36.0 mg, 85%; colorless oil; ^{1}H NMR (400 MHz, $CDCl_3$) δ 8.04 (d, *J* = 7.7 Hz, 53H), 7.56 (t, *J* = 7.4 Hz, 27H), 7.44 (t, *J* = 7.7 Hz, 55H), 4.87 – 4.44 (m, 30H), 4.43 – 4.28 (m, 54H), 2.19 – 1.50 (m, 121H), 1.36 (dd, *J* = 23.8, 6.2 Hz, 73H), 1.01 (t, *J* = 7.4 Hz, 4H)ppm; ^{19}F NMR (377 MHz, $CDCl_3$) δ -172.1 – -172.7 (m), -183.3 – -183.8 (m) ppm. HRMS (+APCI) (*m/z*) $[M+H]^+$: exact mass calc. for $C_{12}H_{15}FO_2$: 211.1129, found: 211.1130.

The data are consistent with our published literature.[1]

5-Fluorohexyl propionate (2a)

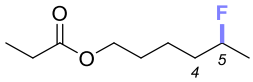

Prepared according to the **General Procedure A** (4F:5F=1:3 ratio). Yield: 31.0 mg, 88%; colorless oil; ^{1}H NMR (400 MHz, $CDCl_3$) δ 4.75 – 4.32 (m, 1H), 4.07 (t, *J* = 6.6 Hz, 2H), 2.31 (q, *J* = 7.6 Hz, 2H), 1.87 – 1.37 (m, 6H), 1.31 (dd, *J* = 23.9, 6.2 Hz, 2.3H), 1.13 (t, *J* = 7.6 Hz, 3H), 0.96 (t, *J* = 7.5 Hz, 0.7H) ppm; ^{19}F NMR (376 MHz, $CDCl_3$) δ -173.1 – -173.8 (m), -182.3 – -183.0 (m). HRMS (+APCI) (*m/z*) $[M+NH_4]^+$: exact mass calc. for $C_9H_{17}FO_2$: 194.1551, found: 194.1552.

The data are consistent with our published literature.[1]

4-fluoro-4-phenylbutyl acetate (2k)

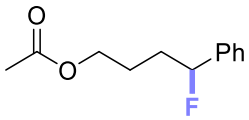

Prepared according to the **General Procedure A**. Yield: 33.6 mg, 80%; colorless oil; ^{1}H NMR (400 MHz, $CDCl_3$) δ 7.38 – 7.20 (m, 5H), 5.40 (ddd, *J* = 47.7, 8.2, 4.4 Hz, 1H), 4.12 – 3.96 (m, 2H), 1.98 – 1.95 (m, 3H), 1.97 – 1.60 (m, 4H) ppm; ^{19}F NMR (377 MHz, $CDCl_3$) δ -175.9 – -176.4 (m) ppm. HRMS (EI) (*m/z*) $[M]^+$: exact mass calc. for $C_{12}H_{15}FO_2$: 210.1056, found: 210.1057.

The data are consistent with our published literature.[1]

2-Fluoro-2-phenylethyl acetate (2l)

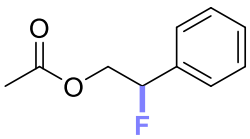

Prepared according to the **General Procedure A**. Yield: 13.0 mg, 36%; colorless oil; ^{1}H NMR (400 MHz, $CDCl_3$) δ 7.50 – 7.31 (m, 5H), 5.81 – 5.51 (m, 1H), 4.50 – 4.30 (m, 2H), 2.11 (s, 3H) ppm; ^{19}F NMR (377 MHz, $CDCl_3$) δ -182.67 – -183.07 (m) ppm. HRMS (+APCI) (*m/z*) $[M+NH_4]^+$: exact mass calc. for $C_{10}H_{11}FO_2$: 200.1081, found: 200.1082.

The data are consistent with our published literature.[1]

Methyl 2-(4-(1-fluoro-2-methylpropyl)phenyl)propanoate (2m)

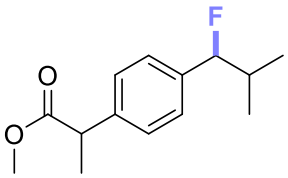

Prepared according to the **General Procedure A**. Yield: 28.6 mg, 60%; colorless oil; ^{1}H NMR (400 MHz, $CDCl_3$) δ 7.35 – 7.19 (m, 5H), 5.08 (dd, *J* = 47.0, 6.8 Hz, 1H), 3.73 (q, *J* = 7.2 Hz, 1H), 3.66 (s, 3H), 2.21 – 1.94 (m, 1H), 1.50 (d, *J* = 7.2 Hz, 3H), 1.02 (d, *J* = 6.6 Hz, 3H), 0.85 (d, *J* = 6.9 Hz, 3H) ppm; ^{19}F NMR (377 MHz, $CDCl_3$) δ -180.1 (ddd, *J* = 47.0, 17.1, 8.0 Hz) ppm. HRMS (EI) (*m/z*) $[M]^+$: exact mass calc. for $C_{14}H_{19}FO_2$: 238.1369, found: 238.1368.

The data are consistent with our published literature.[1]

(3a*R*,9a*S*,9b*R*)-8-Fluoro-3a,6,6,9a-tetramethyldecahydronaphtho[2,1-b]furan-2(1*H*)-one (2o)

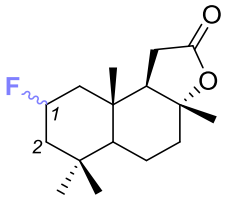

Prepared according to the **General Procedure A**. Yield: 45.6 mg, 84%; white solid, m.p. 118-120 °C; ^{1}H NMR (400 MHz, $CDCl_3$) δ 5.00 – 4.11 (m, 1H), 2.51 – 2.33 (m, 1H), 2.22 (dddd, *J* = 10.2, 8.0, 5.7, 1.9 Hz, 1H), 2.12 – 2.00 (m, 2H), 2.00 – 1.88 (m, 3H), 1.88 – 1.78 (m, 1H), 1.66 (t, *J* = 12.3 Hz, 1H), 1.56 – 1.40 (m, 1H), 1.29 (t, *J* = 3.9 Hz, 5H), 1.11 (dd, *J* = 21.8, 11.8 Hz, 2H), 0.96 (s, 3H), 0.92 (s, 3H), 0.86 (s, 3H), 0.81 (s, 1H) ppm; ^{19}F NMR (377 MHz, $CDCl_3$) δ -178.6 (dtt, *J* = 48.1, 11.1, 5.6 Hz), -186.6 – -187.8 (m) ppm. HRMS (ESI) (*m/z*) $[M+H]^+$: exact mass calc. for $C_{16}H_{25}FO_2$: 269.1911, found: 269.1913.

The data are consistent with our published literature.[1]

Methyl (4*R*)-4-((5*S*,8*S*,9*S*,10*S*,13*R*,14*S*,17*R*)-1-fluoro-10,13-dimethyl-3,7,12-trioxohexadecahydro-1*H*-cyclopenta[a]phenanthren-17-yl)pentanoate (2p)

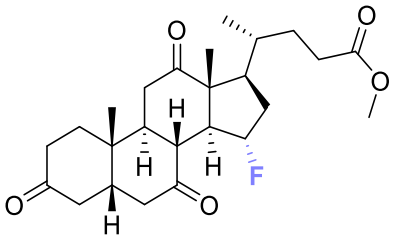

Prepared according to the **General Procedure A**. Yield: 67.0 mg, 77%; white solid, m.p. 133-134 °C; ^{1}H NMR (400 MHz, $CDCl_3$) δ 5.01 – 4.75 (m, 1H), 3.64 (s, 3H), 3.11 (t, *J* = 11.7 Hz, 1H), 2.93 (dd, *J* = 13.0, 5.8 Hz, 1H), 2.78 (t, *J* = 12.8 Hz, 1H), 2.38 – 2.33 (m, 2H), 2.32 – 2.24 (m, 3H), 2.25 – 2.18 (m, 5H), 2.14 (dd, *J* = 7.1, 5.2 Hz, 2H), 2.08 (dd, *J* = 13.1, 2.9 Hz, 1H), 1.92 (ddd, *J* = 18.7, 9.2, 5.1 Hz, 2H), 1.84 – 1.76 (m, 1H), 1.60 (td, *J* = 14.1, 5.2 Hz, 1H), 1.42 – 1.34 (m, 4H), 1.31 – 1.22 (m, 1H), 1.08 (s, 3H), 0.81 (d, *J* = 6.6 Hz, 3H) ppm; ^{19}F NMR (377 MHz, $CDCl_3$) δ -169.2 – -169.7 (m). HRMS (ESI) (*m/z*) $[M+H]^+$: exact mass calc. for $C_{25}H_{35}FO_5$: 435.2541, found: 435.2545.

The data are consistent with our published literature.[1]

(2R,5R)-2-(2-fluoropropan-2-yl)-5-methylcyclohexan-1-one (2q)

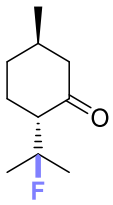

Prepared according to the **General Procedure A**. Yield: 26.0 mg, 75%; colorless oil; ^{1}H NMR (400 MHz, $CDCl_3$) δ 2.66 – 2.57 (m, 1H), 2.35 – 2.27 (m, 2H), 1.60 – 1.50 (m, 1H), 1.46 (d, *J* = 23.5 Hz, 3H), 1.42 – 1.31 (m, 6H), 1.01 (d, *J* = 6.3 Hz, 3H), 0.99 – 0.97 (m, 1H) ppm; ^{13}C NMR (101 MHz, $CDCl_3$) δ 209.5 (d, *J* = 10.7 Hz), 95.8 (d, *J* = 164.5 Hz), 58.8 (d, *J* = 22.7 Hz), 51.6 (d, *J* = 3.9 Hz), 36.0 (s), 33.8 (s), 27.8 (d, *J* = 4.8 Hz), 27.0 (d, *J* = 23.4 Hz), 22.4 (d, *J* = 23.2 Hz), 22.3 (s) ppm; ^{19}F NMR (377 MHz, $CDCl_3$) δ -134.5 (heptd, *J* = 23.8, 8.2 Hz) ppm; HRMS (EI) (*m/z*) $[M]^+$: exact mass calc. for $C_{10}H_{17}FO$: 172.1263; found: 172.1265.

The data are consistent with the literature.[2b]

3-Fluoro-2,3-dihydro-1*H*-inden-1-one (2r)

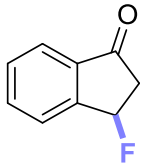

Prepared according to the **General Procedure A**. Yield: 21.0 mg, 70%; colorless oil; ^{1}H NMR (400 MHz, CD_3CN) δ 7.82 – 7.71 (m, 3H), 7.60 – 7.55 (m, 1H), 6.18 (ddd, *J* = 55.4, 6.6, 1.9 Hz, 1H), 3.12 (ddd, *J* = 19.0, 12.3, 6.6 Hz, 1H), 2.88 (ddd, *J* = 23.9, 19.2, 2.2 Hz, 1H) ppm; ^{13}C NMR (101 MHz, CD_3CN) δ 195.9 (d, *J* = 1.5 Hz), 144.9 (d, *J* = 17.6 Hz), 130.1 (d, *J* = 2.8 Hz), 125.5 (d, *J* = 3.2 Hz), 121.4 (d, *J* = 1.8 Hz), 118.1 (d, *J* = 1.7 Hz), 82.7 (d, *J* = 177.6 Hz), 38.7 (d, *J* = 21.1 Hz) ppm; ^{19}F NMR (377 MHz, CD_3CN) δ -172.7 (ddd, *J* = 55.5, 23.9, 12.3 Hz) ppm. HRMS (EI) (*m/z*) $[M]^+$: exact mass calc. for C_9H_7FO: 150.0481; found: 150.0483.
The data are consistent with our published literature.[1]

Fluorinated 4-butylacetophenone (2t)

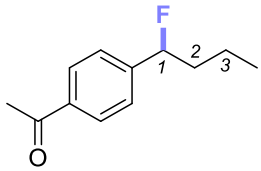

Prepared according to the **General Procedure A** (1F:3F:2F=3.6:2:1). Yield: 25.0 mg, 65%; colorless oil; ^{1}H NMR (400 MHz, $CDCl_3$) δ 7.96 (d, *J* = 8.0 Hz, 2H), 7.41 (d, *J* = 8.5 Hz, 2H), 5.50 (ddd, *J* = 47.9, 8.1, 4.7 Hz, 1H), 2.61 (s, 3H), 1.88 – 1.74 (m, 2H), 1.55 – 1.40 (m, 2H), 0.96 (t, *J* = 7.4 Hz, 3H) ppm; ^{13}C NMR (101 MHz, $CDCl_3$) δ 197.7 (s), 145.8 (d, *J* = 19.9 Hz), 136.7 (d, *J* = 1.5 Hz), 128.5 (s), 125.4 (d, *J* = 7.3 Hz), 93.7 (d, *J* = 172.0 Hz), 39.3 (d, *J* = 23.0 Hz), 26.7 (s),18.2 (d, *J* = 4.4 Hz), 13.8 (s) ppm; ^{19}F NMR (377 MHz,

$CDCl_3$) δ -179.4 (ddd, *J* = 47.6, 29.2, 18.1 Hz) ppm; HRMS (EI) (*m/z*) $[M]^+$: exact mass calc. for $C_{12}H_{15}FO$: 194.1107; found: 194.1105.

The data are consistent with the literature.[6]

Fluorinated 4-butylacetophenone (2u)

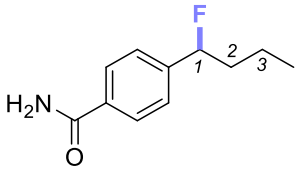

Prepared according to the **General Procedure A** (1F:3F:2F=5:2:1). This compound was not isolated but its identity confirmed by comparison with published literature.[1] NMR yield: 91% (according to ^{19}F NMR with pentafluorobenzene as an internal standard); ^{19}F NMR (377 MHz, CD_3CN) δ -172.35 – -172.88 (m), -174.74 – -175.20 (m), -175.76 – -176.07 (m) ppm; HRMS (EI) (*m/z*) $[M]^+$: exact mass calc. for $C_{11}H_{14}FNO$: 195.1059; found: 195.1057.

The data are consistent with our published literature.[1]

Fluorinated hexanone-2 (2v)

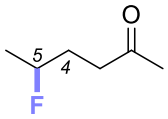

Prepared according to the **General Procedure A** (5F:4F=1.3:1). This compound was not isolated but its identity confirmed by comparison with published literature.[2b] NMR yield: 92% (according to ^{19}F NMR with pentafluorobenzene as an internal standard); Isolated yield: 74% (due to high volatility); ^1H NMR (600 MHz, $CDCl_3$) δ 4.89 (dddd, *J* = 16.1, 12.2, 8.1, 4.6 Hz, 0.4H), 4.72 – 4.58 (m, 0.6H), 2.66 – 2.50 (m, 2H), 2.20 (s, 1.5H), 2.16 (s, 2H), 1.88 – 1.74 (m, 1H), 1.74 – 1.60 (m, 1H), 1.36 – 1.24 (m, 3H) ppm; ^{13}C NMR (151 MHz, $CDCl_3$) δ 208.0 (s), 205.8 (d, *J* = 3.8 Hz), 90.7 (t, *J* = 167.0 Hz), 60.4 (s), 48.4 (d, *J* = 22.9 Hz), 38.9 (d, *J* = 3.6 Hz), 30.9 (d, *J* = 1.1 Hz), 30.7 (d, *J* = 21.0 Hz), 30.0 (s), 28.1 (d, *J* = 21.2 Hz), 21.1 (s), 21.1 (s), 21.0 (s), 9.2 (d, *J* = 5.6 Hz) ppm; ^{19}F NMR (377 MHz, $CDCl_3$) δ -176.1 – -176.8 (m), -182.1 – -182.7 (m) ppm; HRMS (EI) (*m/z*) $[M]^+$: exact mass calc. for $C_6H_{11}FO$: 118.0794; found: 118.0798.

The data are consistent with the literature.[2b]

1-((1*r*,3*s*,5*R*,7*S*)-3-Fluoroadamantan-1-yl)ethan-1-one (2x)

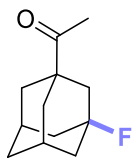

Prepared according to the **General Procedure A**. Yield: 29.0 mg, 74%; white solid, m.p. 59-61 °C; ^1H NMR (400 MHz, $CDCl_3$) δ 2.28 (m, 2H), 2.03 (s, 3H), 1.83 (d, *J* = 5.9 Hz, 2H), 1.78 (m, 4H), 1.69 – 1.57 (m, 4H), 1.55 – 1.48 (m, 2H) ppm; ^{19}F NMR (377 MHz, $CDCl_3$) δ -132.50 (br. s). HRMS (EI) (*m/z*) $[M]^+$: exact mass calc. for $C_{12}H_{17}FO$: 196.1263, found: 196.1260.

The data are consistent with our published literature.[1]

1-((1r,3R,5S,7r)-3,5-difluoroadamantan-1-yl)ethan-1-one (2y)

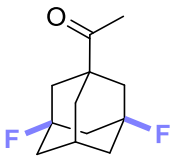

Prepared according to the **General Procedure A**. Yield: 30.0 mg, 70%; white solid, m.p. 51-53 °C; IR (neat) ν (cm^{-1}): 2922, 2870, 1703, 1457, 1357, 1334, 1245, 1211, 1114, 1086, 995, 947, 861, 824, 772; ^{1}H NMR (400 MHz, $CDCl_3$) δ 2.58 – 2.51 (m, 1H), 2.14 (s, 3H), 2.09 (t, *J* = 5.5 Hz, 2H), 1.90 (t, *J* = 3.6 Hz, 4H), 1.86 – 1.77 (m, 4H), 1.62 (br. s, 2H) ppm; ^{13}C NMR (101 MHz, $CDCl_3$) δ 209.0 (t, *J* = 1.8 Hz), 94.0 (d, *J* = 13.7 Hz), 92.1 (d, *J* = 13.7 Hz), 51.6 (t, *J* = 9.4 Hz), 47.4 (t, *J* = 19.1 Hz), 42.2 (dt, *J* = 11.3, 6.6 Hz), 40.5 (dt, *J* = 11.0, 7.0 Hz), 35.9 (t, *J* = 1.9 Hz), 30.6 (t, *J* = 10.5 Hz), 24.8 (s) ppm; ^{19}F NMR (377 MHz, $CDCl_3$) δ -137.2 (s) ppm; HRMS (EI) (*m/z*) [M]$^{+}$: exact mass calc. for $C_{12}H_{16}F_2O$: 214.1169; found: 214.1171.

3 Mechanistic Studies

3.1 Radical Trapping

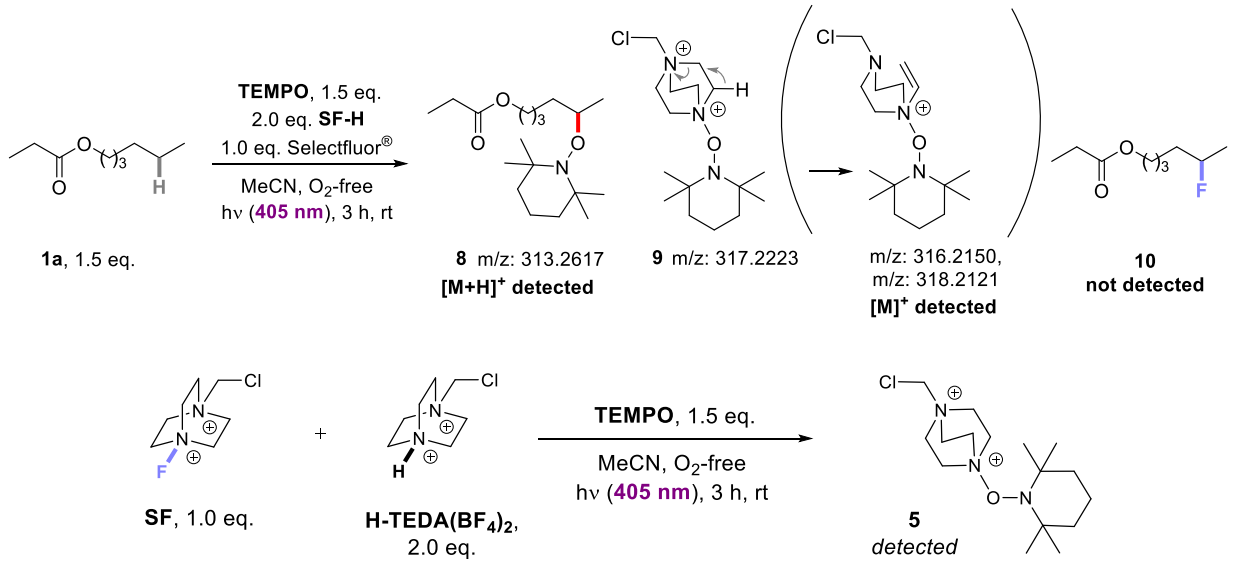

Scheme S10. Radical trapping reactions with TEMPO. **Top:** with **1a**. **Bottom:** in absence of **1a**.

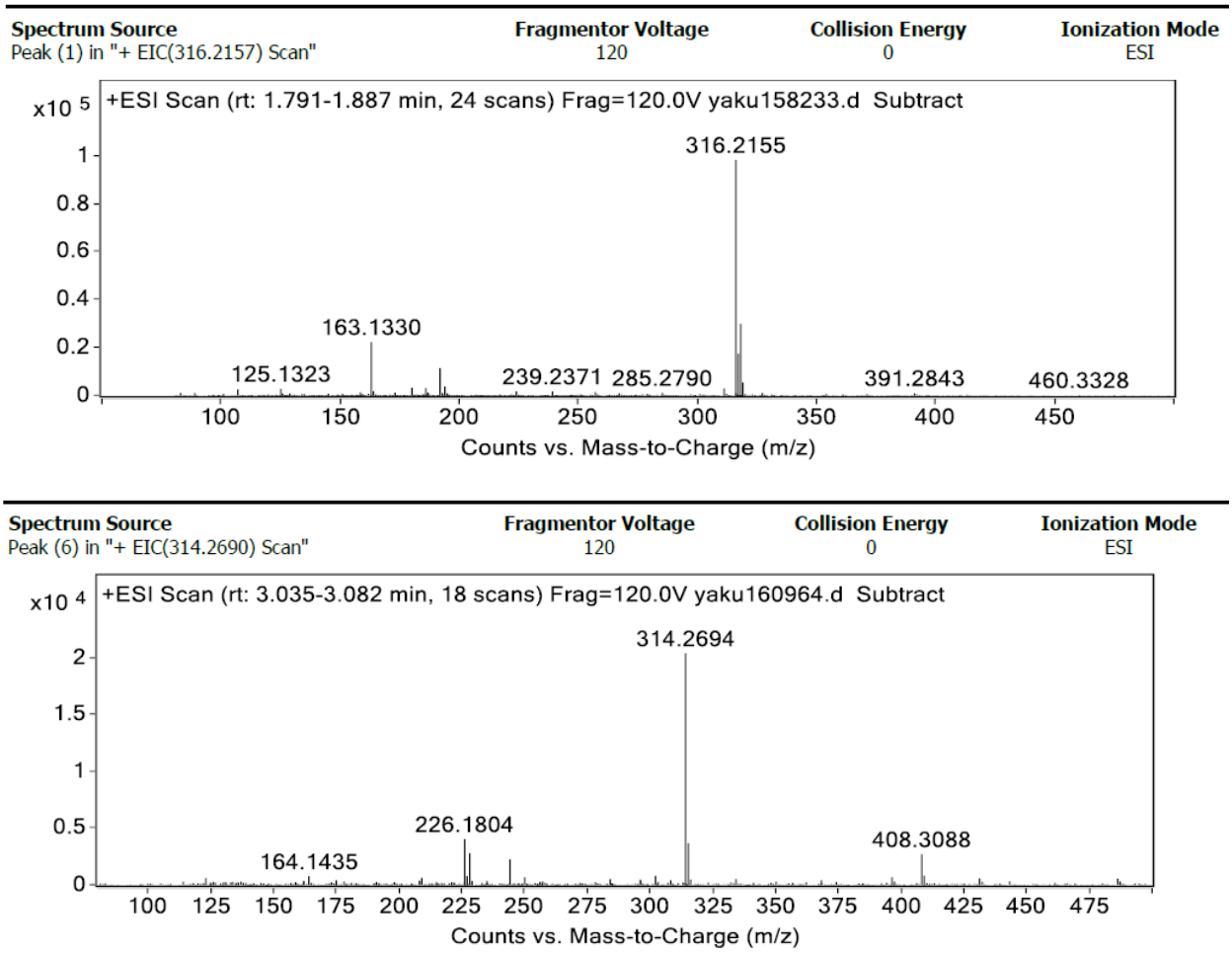

Figure S6. Mass spectra for TEMPO-trapped radicals from LC-MS analysis.

3.2 UV-visible Spectroscopy Studies

We elected to measure UV-vis absorption spectra of individual reaction components both separately and as reaction mixtures (Figure S7). As can be seen below, under these conditions the absorption of the reaction mixture resembled to that of **H-TEDA(BF$_4$)$_2$**. Due to the limited solubility of **H-TEDA(BF$_4$)$_2$**, we were not able to measure the UV-vis of the reaction mixture with increasing **H-TEDA(BF$_4$)$_2$** concentration.

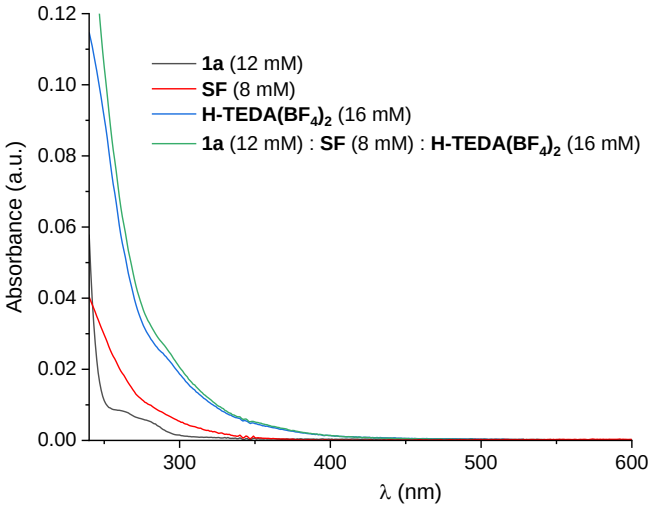

Figure S7. UV-vis spectra of separate reaction components and reaction mixture.

We chose TFA as another additive that proved effective in fluorination reactions, as it is well soluble in acetonitrile. We measured UV-vis of TFA and **SF** both separately and as mixture of both. It was observed that with increasing concentration of TFA, a new absorption peak emerged ((λ_{max} = 358 nm) tailing into <400nm, that was notably higher than any individual reaction component. With increasing TFA concentration, the absorption was increased.

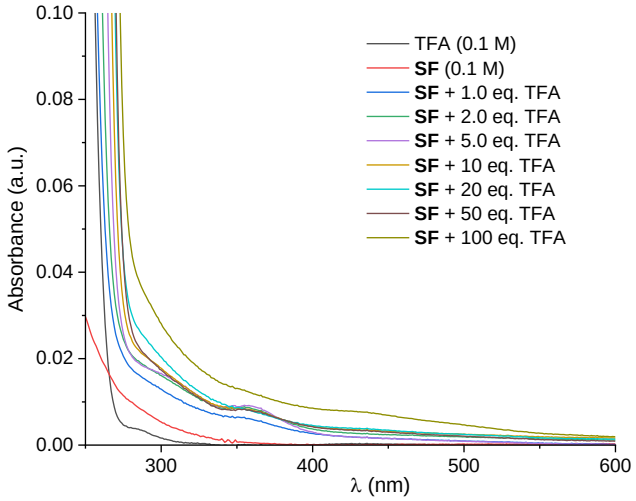

Figure S8. UV-vis spectra of TFA, **SF**, and **SF** with increasing concentrations of TFA.

We also measured UV-vis of TFA, substrate **1a** and **SF** both separately and as reaction mixture with increasing TFA concentration. In this case, it was also observed that with increasing concentration of TFA in the reaction mixture, a new absorption peak emerged ((λ_{max} = 355 nm) tailing into <400nm. This absorption peak was notably higher than any individual reaction component, and with increasing TFA concentration, this absorption peak also increased.

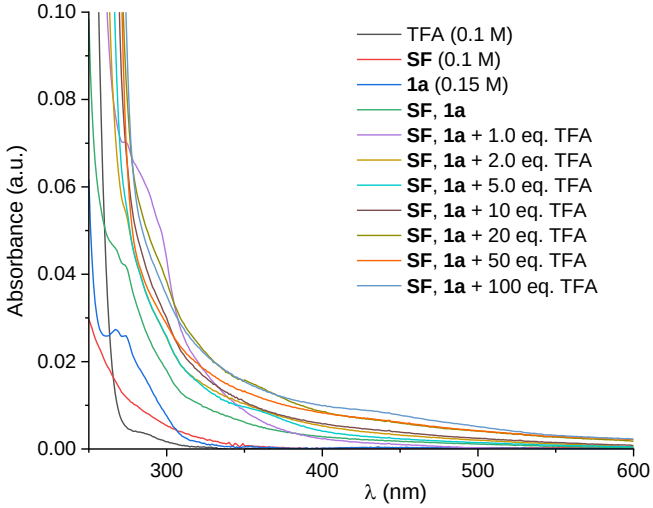

Figure S9. UV-vis spectra of TFA, **SF**, substrate **1a**, and **SF**+**1a** with increasing concentrations of TFA.

3.3 Luminescence Measurements

To gain more insight about an interaction between **SF** and **H-TEDA(BF$_4$)$_2$** and their excited state deactivation, steady-state luminescence measurement was carried out. We measured luminescence of **SF** and **H-TEDA(BF$_4$)$_2$** both as an individual component and as their mixtures of different ratios.

For steady-state luminescence measurements, a 15 mM concentration of **SF** and 15 mM concentration of **H-TEDA(BF$_4$)$_2$** were used. Spectroscopic concentrations had to be kept lower than reaction concentrations to i) ensure full solubility of **SF**, and ii) ensure that luminescence-derived photon counts did not saturate the detector.

We wanted to know the photostability of **SF** and **H-TEDA(BF$_4$)$_2$**. On its own, **SF** (15 mM) displayed a slight decrease in emission intensity after 5 min interval, and this continued to decrease with repeated measurements every 5 min until 20 min (Table S5, Figure S10). The same kind of decrease in emission intensity was observed when measuring **H-TEDA(BF$_4$)$_2$**, on its own, successively every 5 min until 20 min (Table S6, Figure S11).

Steady-state luminescence of **SF** with increasing **H-TEDA(BF$_4$)$_2$** concentration and **H-TEDA(BF$_4$)$_2$** with increasing **SF** concentration were measured. All of the samples prepared, were measured repeatedly 4-5 times over 5 min interval.

Note: *The sharp peak at λ = 416 nm is an instrumental artefact.*

Table S5. Steady state luminescence measurement of **SF** (15 mM) over time, see Figure S10, right.

Entry	Time (min)	Intensity at 467 nm (CPS)	Ln$_{[\text{Emission intensity}]}$ at 467 nm
1	0	21947	9.99639
2	5	20837	9.94449
3	10	20434	9.92496
4	15	20152	9.91106
5	20	19858	9.89636

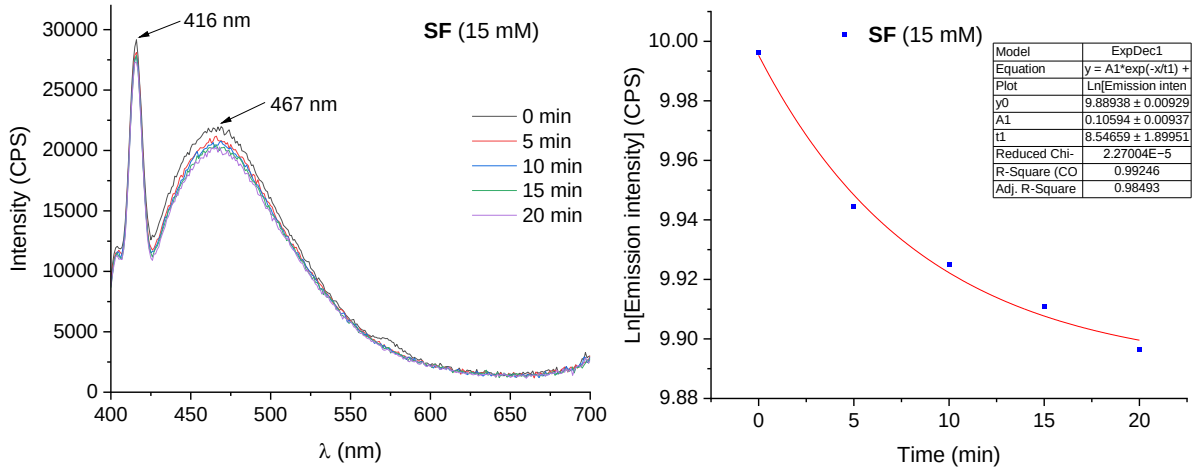

Figure S10. **SF** photostability (left) and λ_{max} = 467 nm peak height (right) measured repeatedly over time.

Table S6. Steady state luminescence measurement of **H-TEDA(BF$_4$)$_2$** (15 mM) over time, see Figure S11, right.

Entry	Time (min)	Intensity at 452 nm	Ln$_{[\text{Emission intensity}]}$ at 452 nm

1	0	41807	10.64082
2	5	38659	10.56253
3	10	38198	10.55054
4	15	37492	10.53188
5	20	37322	10.52734

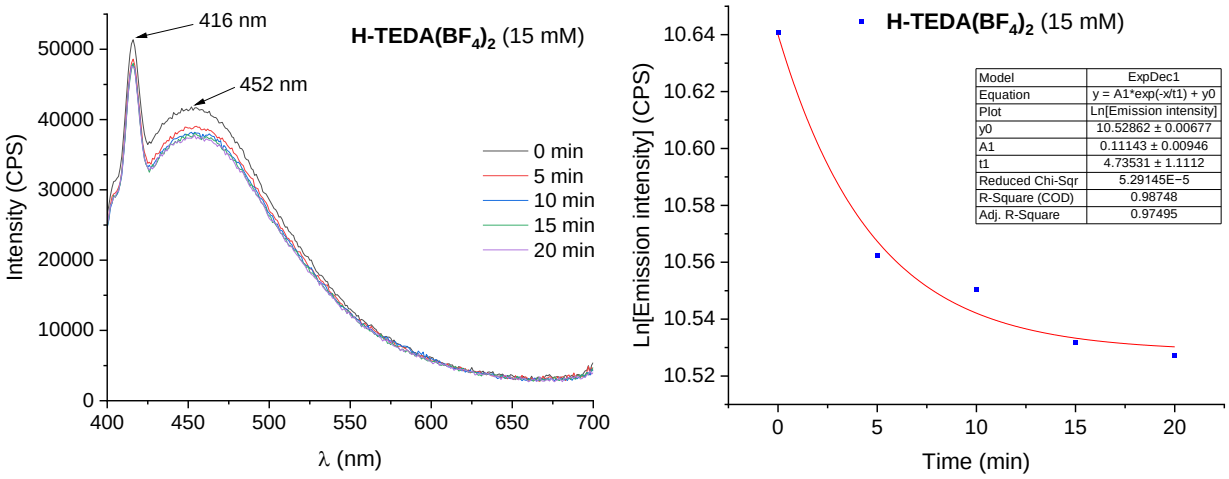

Figure S11. **H-TEDA(BF$_4$)$_2$** photostability (left) and λ_{max} = 452 nm peak height (right) measured repeatedly over time.

Table S7. Steady state luminescence measurement of the mixture of 1 : 1 ratio of **SF** (10 mM) and **H-TEDA(BF$_4$)$_2$** (10 mM) over time, see Figure S12, right.

Entry	**SF** : **H-TEDA(BF$_4$)$_2$** (10 mM : 10 mM) Over time (min)	Intensity at 463 nm	Ln$_{[Emission intensity]}$ at 463 nm
1	0	51588	10.85104
2	5	47674	10.77214
3	10	45656	10.72889
4	15	44628	10.70612

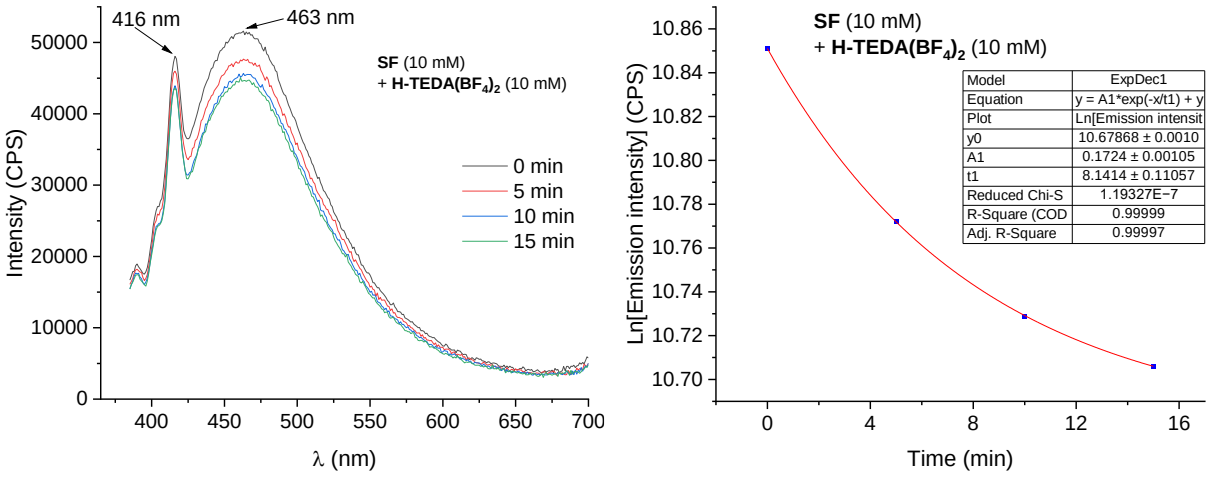

Figure S12. Emission of the mixture of 1 : 1 ratio of **SF** (10 mM) and **H-TEDA(BF$_4$)$_2$** (10 mM) (left) and peak height at λ_{max} = 463 nm over time.

Table S8. Steady state luminescence measurement of the mixture of 1 : 2 ratio of **SF** (10 mM) and **H-TEDA(BF$_4$)$_2$** (20 mM) over time, see Figure S13, right.

Entry	**SF** : **H-TEDA(BF$_4$)$_2$** (10 mM : 20 mM) Over time (min)	Intensity at 463 nm	Ln$_{[Emission intensity]}$ at 463 nm
1	0	80789	11.29960
2	5	70834	11.16809
3	10	67134	11.11445
4	15	66568	11.10598

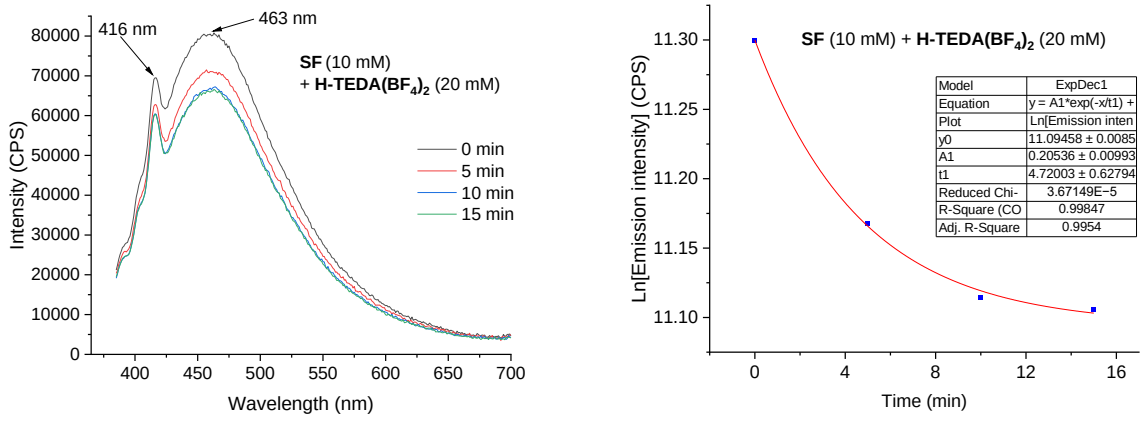

Figure S13. Emission of the mixture of 1 : 2 ratio of **SF** (10 mM) and **H-TEDA(BF$_4$)$_2$** (20 mM) (left) and λ_{max} = 463 nm peak height (right) measured repeatedly over time.

Table S9. Steady state luminescence measurement of the mixture of 1 : 4 ratio of **SF** (10 mM) and **H-TEDA(BF$_4$)$_2$** (40 mM) over time, see Figure S14, right.

Entry	**SF** : **H-TEDA(BF$_4$)$_2$** (10 mM : 40 mM) Over time (min)	Intensity at 467 nm	Ln$_{[Emission\ intensity]}$ at 467 nm
1	0	129410	11.77074
2	5	118443	11.68219
3	10	107796	11.58800
4	15	104552	11.55744

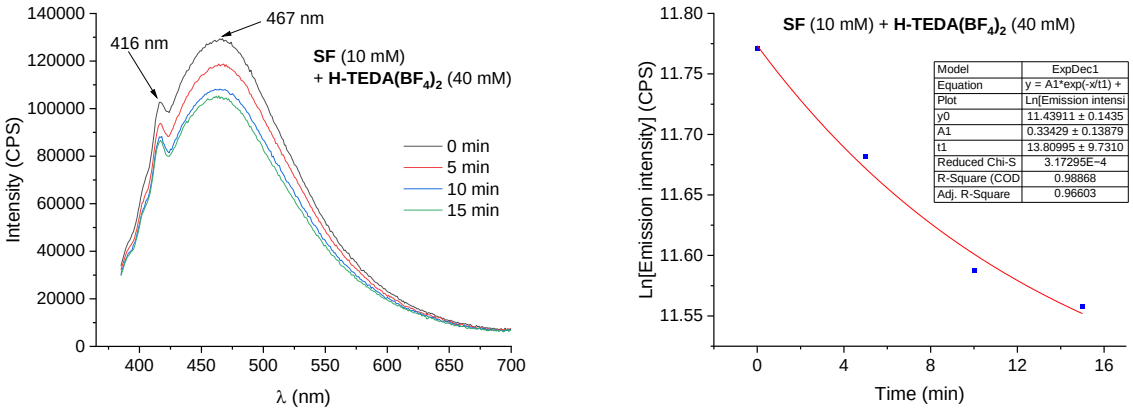

Figure S14. Emission of the mixture of 1 : 4 ratio of **SF** (10 mM) and **H-TEDA(BF$_4$)$_2$** (40 mM) (left) and λ_{max} = 467 nm peak height (right) measured repeatedly over time.

Table S10. Steady state luminescence measurement of the mixture of 1 : 8 ratio of **SF** (5 mM) and **H-TEDA(BF$_4$)$_2$** (40 mM) over time, see Figure S15, right.

Entry	**SF** : **H-TEDA(BF$_4$)$_2$** (5 mM : 40 mM) Over time (min)	Intensity at 463 nm	Ln$_{[Emission\ intensity]}$ at 463 nm
1	0	138261	11.83690
2	5	122397	11.71503
3	10	116862	11.66875
4	15	115792	11.65955
5	20	115700	11.65876

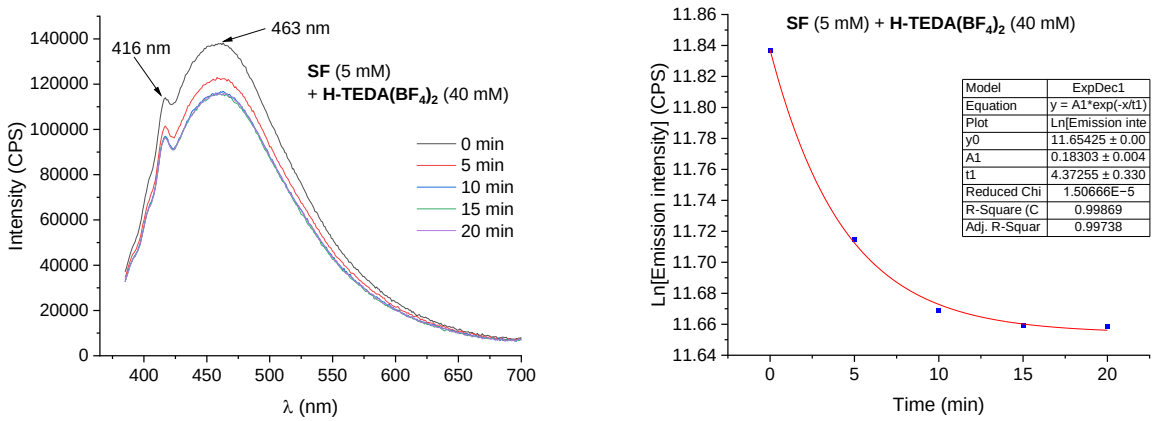

Figure S15. Emission of the mixture of 1 : 8 ratio of **SF** (5 mM) and **H-TEDA(BF$_4$)$_2$** (40 mM) (left) and λ_{max} = 463 nm peak height (right) measured repeatedly over time.

Table S11. Steady state luminescence measurement of the mixture of 1 : 16 ratio of **SF** (2 mM) and **H-TEDA(BF$_4$)$_2$** (32 mM) over time, see Figure S16, right.

Entry	**SF** : **H-TEDA(BF$_4$)$_2$** (2 mM : 32 mM) Over time (min)	Intensity at 463 nm	Ln$_{[Emission\ intensity]}$ at 463 nm
1	0	114571	11.64895
2	5	105069	11.56237
3	10	101445	11.52727
4	15	102767	11.54022
5	20	102278	11.53545

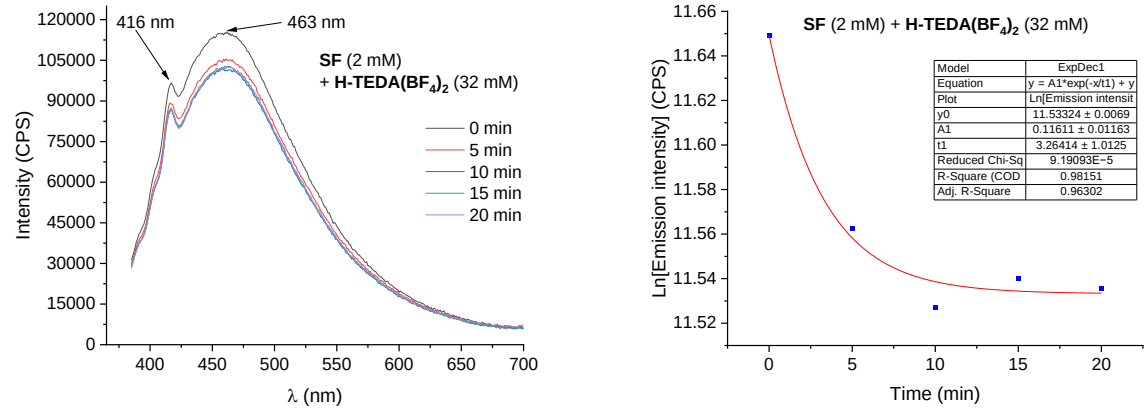

Figure S16. Emission of the mixture of 1 : 16 ratio of **SF** (2 mM) and **H-TEDA(BF$_4$)$_2$** (32 mM) (left) and λ_{max} = 463 nm peak height (right) measured repeatedly over time.

Table S12. Steady state luminescence measurement of the mixture of 2 : 1 ratio of **SF** (20 mM) and **H-TEDA(BF$_4$)$_2$** (10 mM) over time, see Figure S17, right.

Entry	**SF** : **H-TEDA(BF$_4$)$_2$** (20 mM : 10 mM) Over time (min)	Intensity at 475 nm	Ln$_{[Emission\ intensity]}$ at 475 nm
1	0	44699	10.70771
2	5	39948	10.59533
3	10	34518	10.44924
4	15	33202	10.41037

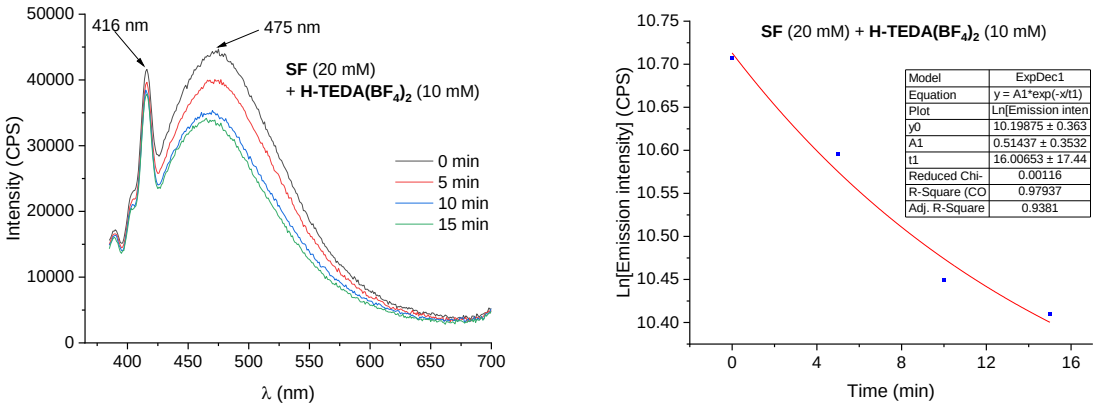

Figure S17. Emission of the mixture of 2 : 1 ratio of **SF** (20 mM) and **H-TEDA(BF$_4$)$_2$** (10 mM) (left) and λ_{max} = 475 nm peak height (right) measured repeatedly over time.

Table S13. Steady state luminescence measurement of the mixture of 4 : 1 ratio of **SF** (40 mM) and **H-TEDA(BF$_4$)$_2$** (10 mM) over time, see Figure S18, right.

Entry	**SF** : **H-TEDA(BF$_4$)$_2$** (40 mM : 10 mM) Over time (min)	Intensity at 490 nm	Ln$_{[Emission\ intensity]}$ at 490 nm
1	0	34266	10.44191
2	5	24227	10.09522
3	10	21395	9.970913
4	15	18988	9.851562

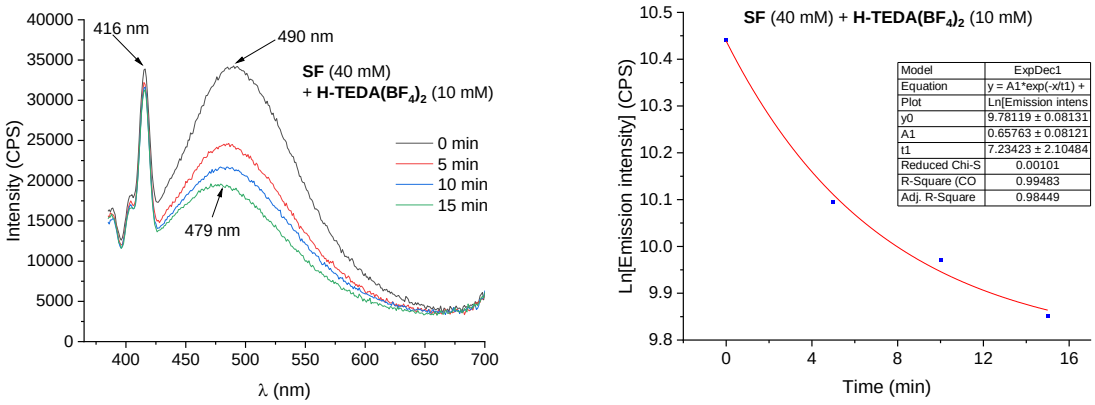

Figure S18. Emission of the mixture of 4 : 1 ratio of **SF** (40 mM) and **H-TEDA(BF$_4$)$_2$** (10 mM) (left) and λ_{max} = 490 nm peak height (right) measured repeatedly over time.

Table S14. Steady state luminescence measurement of the mixture of 8 : 1 ratio of **SF** (80 mM) and **H-TEDA(BF$_4$)$_2$** (10 mM) over time, see Figure S19, right.

Entry	**SF** : **H-TEDA(BF$_4$)$_2$** (80 mM : 10 mM) Over time (min)	Intensity at 490 nm	Ln$_{[Emission intensity]}$ at 490 nm
1	0	10494	9.25856
2	5	8404	9.03646
3	10	7408	8.91032
4	15	6958	8.84765

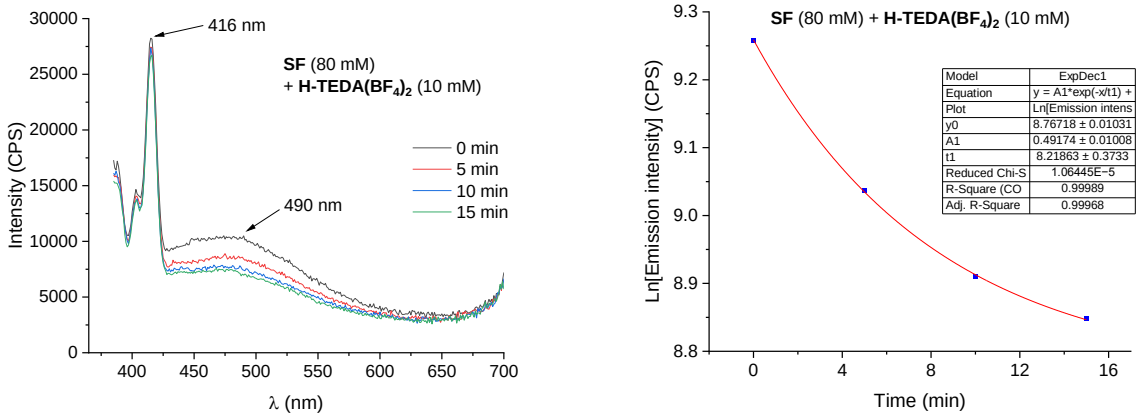

Figure S19. Emission of the mixture of 8 : 1 ratio of **SF** (80 mM) and **H-TEDA(BF$_4$)$_2$** (10 mM) (left) and λ_{max} = 490 nm peak height (right) measured repeatedly over time.

Steady state luminescence measurement of **H-TEDA(BF$_4$)$_2$** (10 mM) with increasing [**SF**] (up to 80 mM) was conducted. The emission peak intensity decreased with increasing [**SF**], and this led to bathochromic shift from 463 nm to 490 nm. Steady state luminescence measurement of **SF** (10 mM) with increasing [**H-**

TEDA(BF$_4$)$_2$] (up to 40 mM, due to its limited solubility) was also conducted. The emission peak intensity increased up to 2.7 times with increasing [**H-TEDA(BF$_4$)$_2$**]. Conversely, this did not lead to a change in wavelength (Figure S20).

Table S15. Steady state luminescence measurement of different ratios of **SF : H-TEDA(BF$_4$)$_2$**, see Figure S20, left.

Entry	**SF** : **H-TEDA(BF$_4$)$_2$** ratios and concentrations (mM)	Intensity at 463 nm
1	1 : 1 (10 mM : 10 mM)	51588
2	1 : 2 (10 mM : 20 mM)	80789
3	1 : 4 (10 mM : 40 mM)	129410
4	1 : 8 (5 mM : 40 mM)	138260

Table S16. Steady state luminescence measurement of different ratios of **SF : H-TEDA(BF$_4$)$_2$**, see Figure S20, right.

Entry	**SF** : **H-TEDA(BF$_4$)$_2$** ratios and concentrations (mM)	Intensity at 467 nm
1	1 : 1 (10 mM : 10 mM)	51404
2	2 : 1 (20 mM : 10 mM)	43597
3	4 : 1 (40 mM : 10 mM)	30577
4	8 : 1 (80 mM : 10 mM)	10230

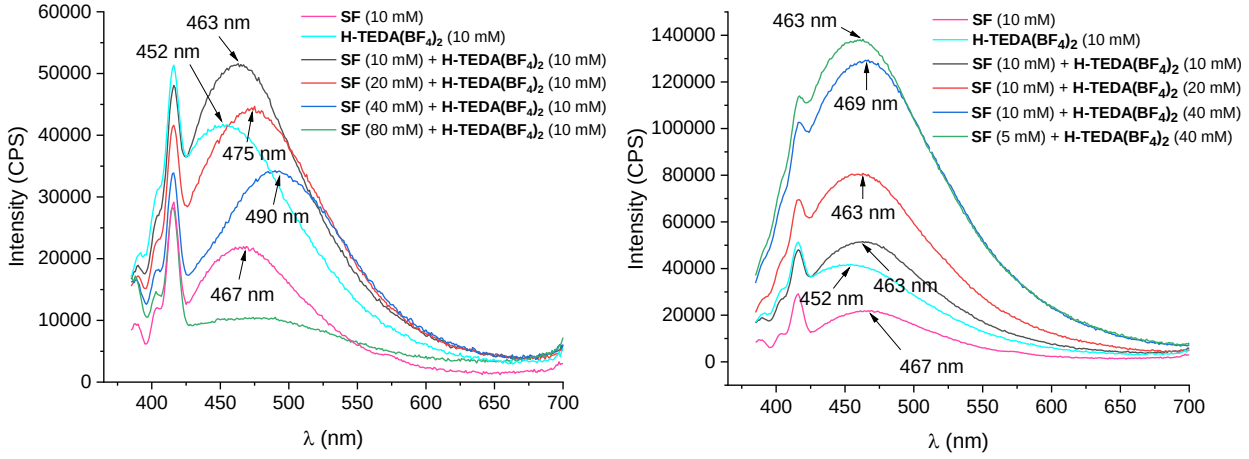

Figure S20. Steady state luminescence measurement of **H-TEDA(BF$_4$)$_2$** (10 mM) with increasing [**SF**] (left) (peak decreases with increasing [**SF**]). Steady state luminescence measurement of **SF** (10 mM) with increasing [**H-TEDA(BF$_4$)$_2$**] (right) (peak increases with increasing [**H-TEDA(BF$_4$)$_2$**]).

4 ^{1}H NMR, ^{13}C NMR and ^{19}F NMR Spectra

^{1}H NMR of compound **H-TEDA(BF$_4$)$_2$** in CD_3CN

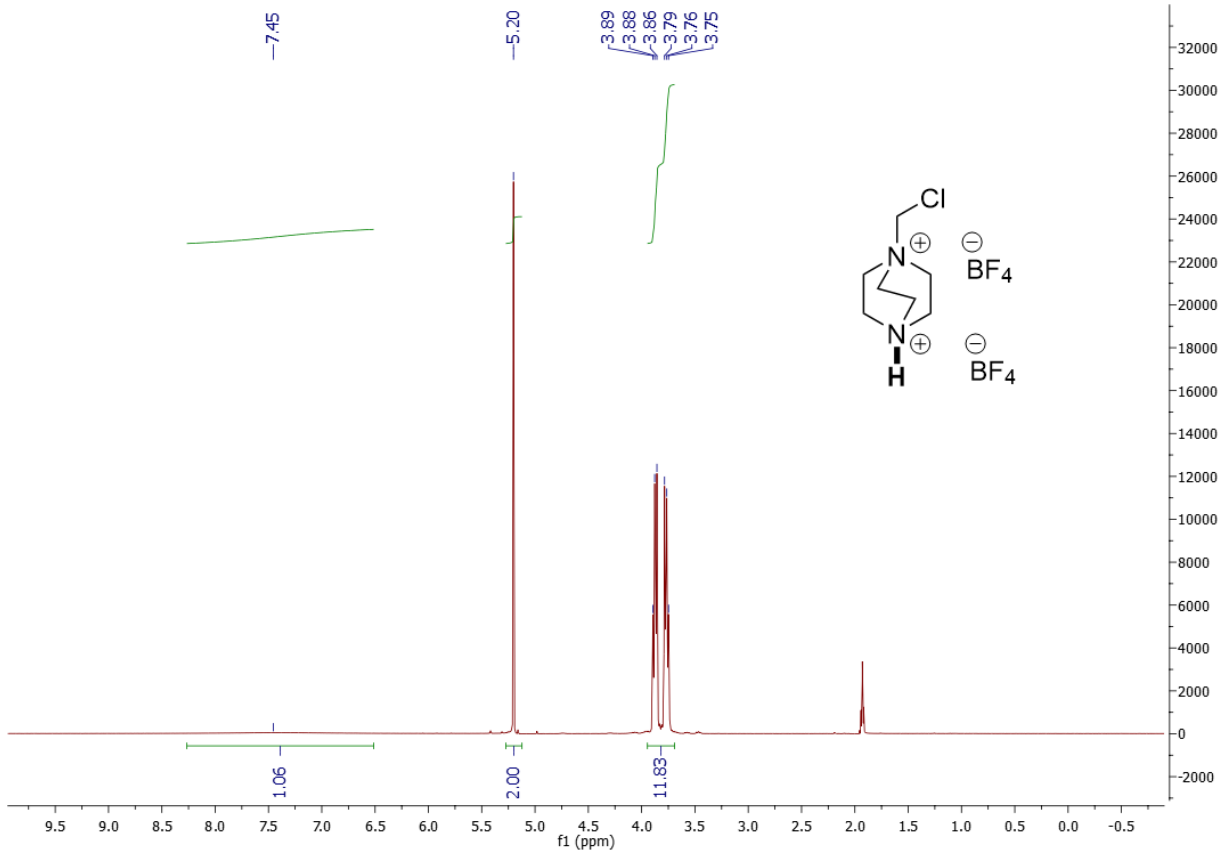

^{13}C NMR of compound **H-TEDA(BF$_4$)$_2$** in CD_3CN

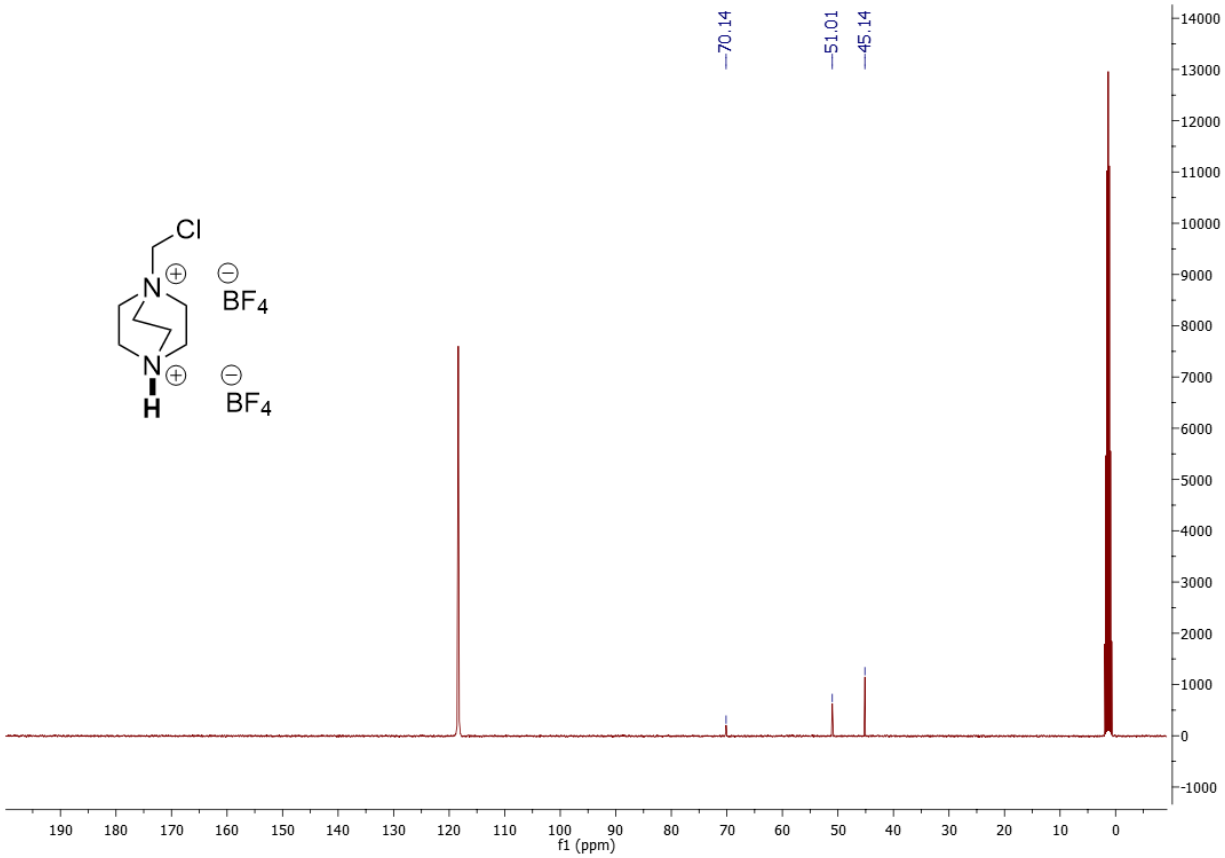

^{19}F NMR of compound **H-TEDA(BF$_4$)$_2$** in CD$_3$CN

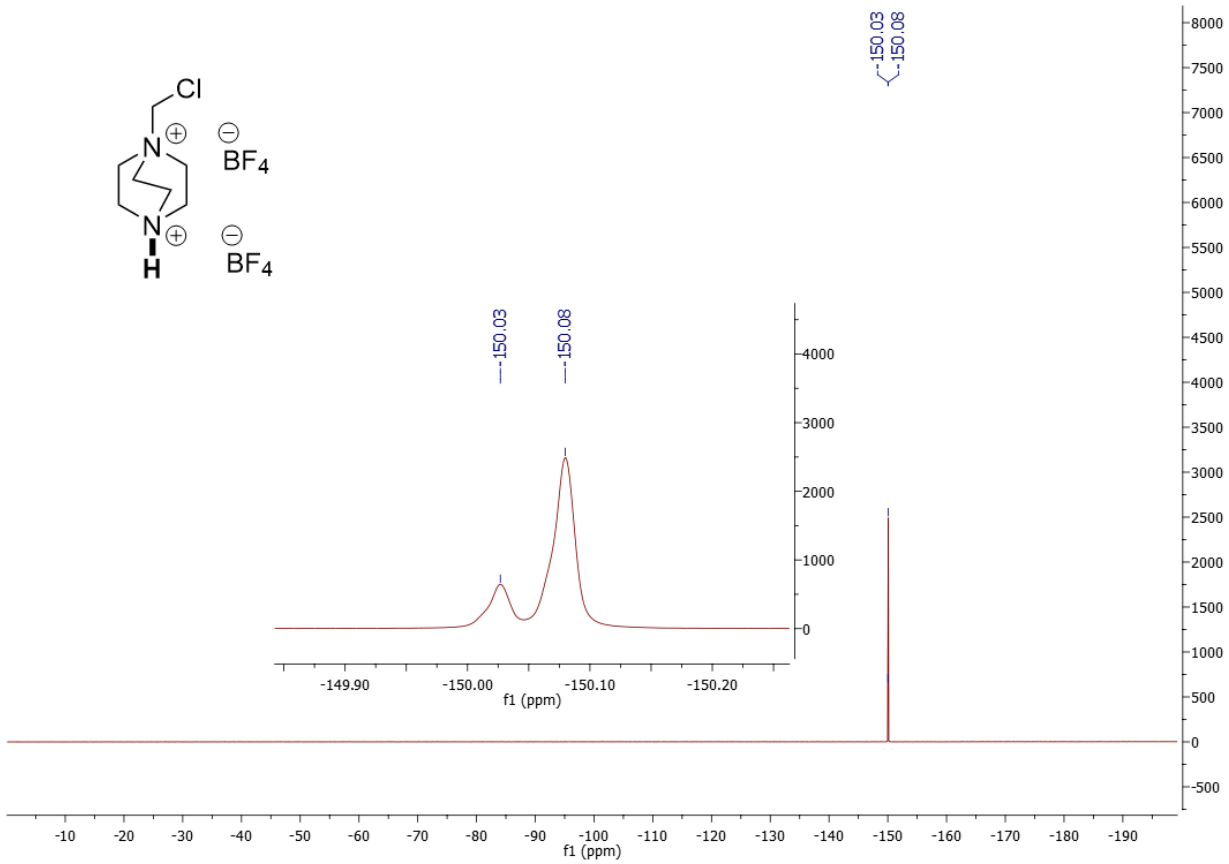

^{1}H NMR of compound **TEDA·Cl** in DMSO-d$_6$

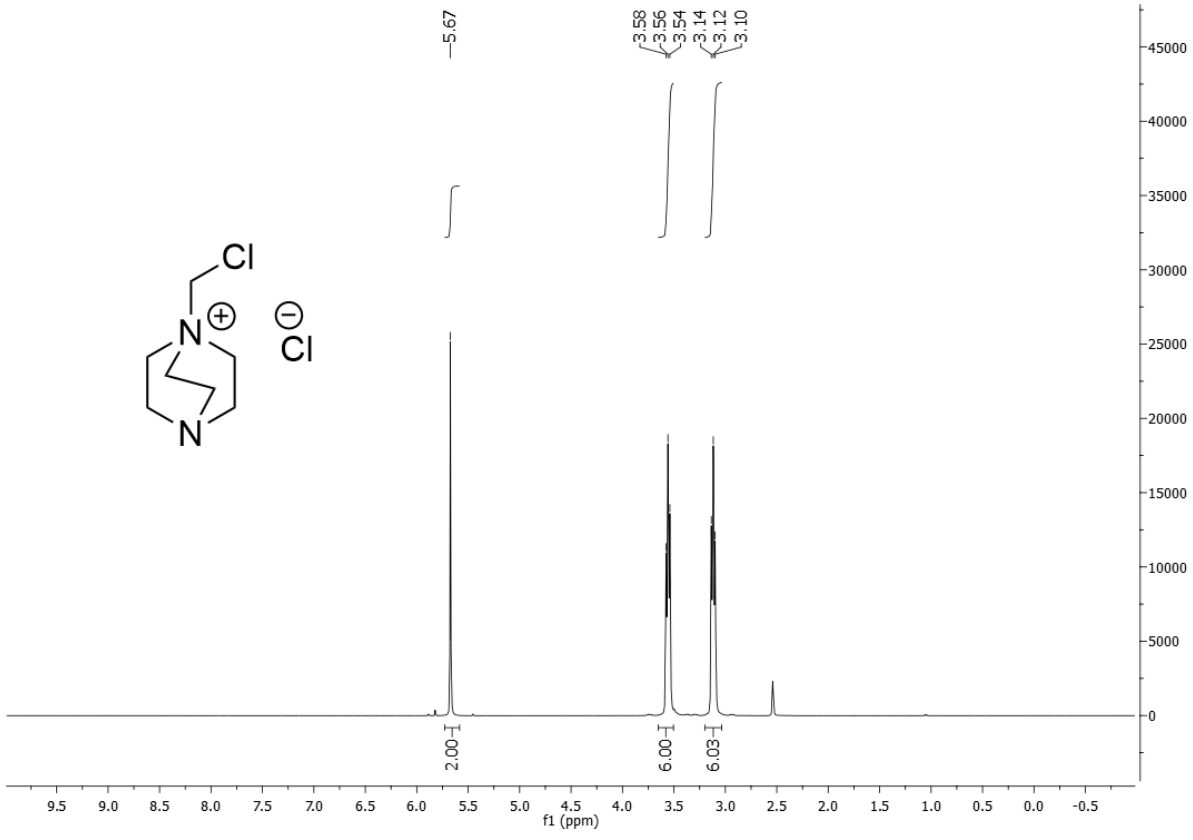

^{13}C NMR of compound **TEDA·Cl** in DMSO-d_6

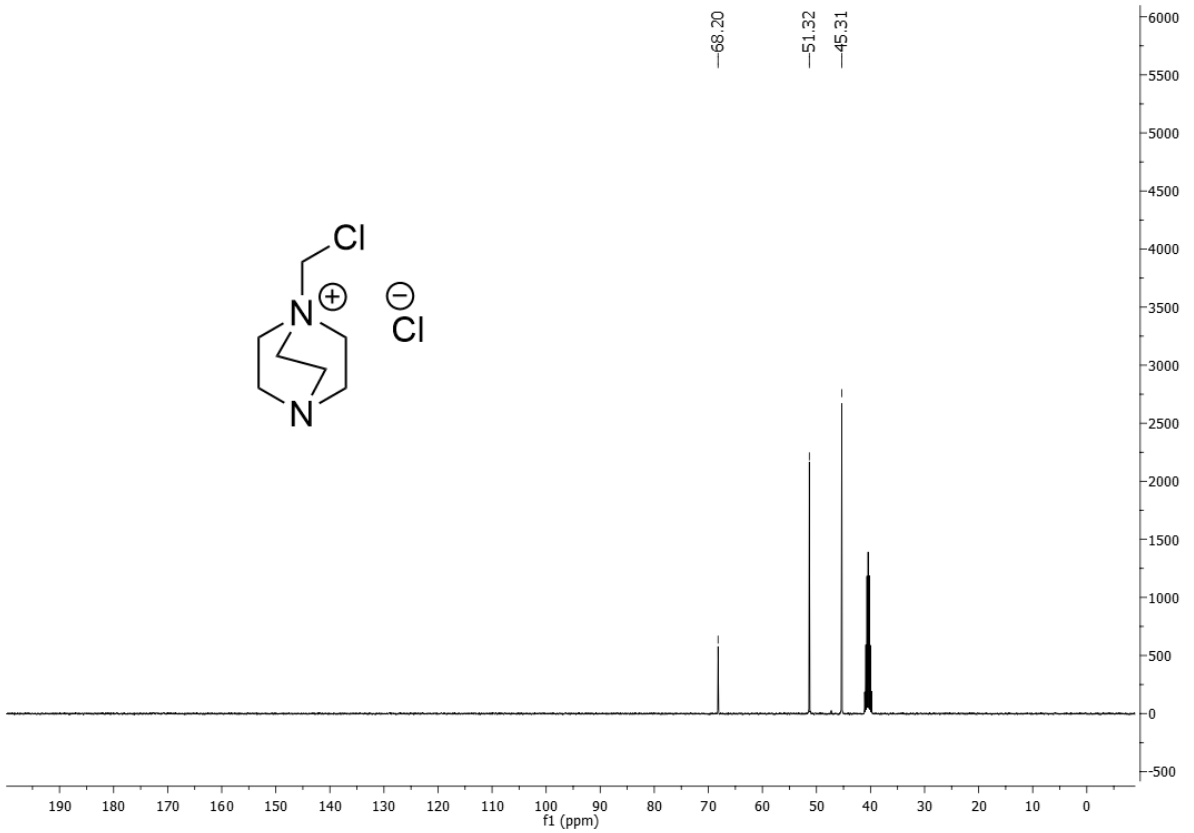

^{1}H NMR of compound **H-TEDA(Cl)$_2$** in D_2O

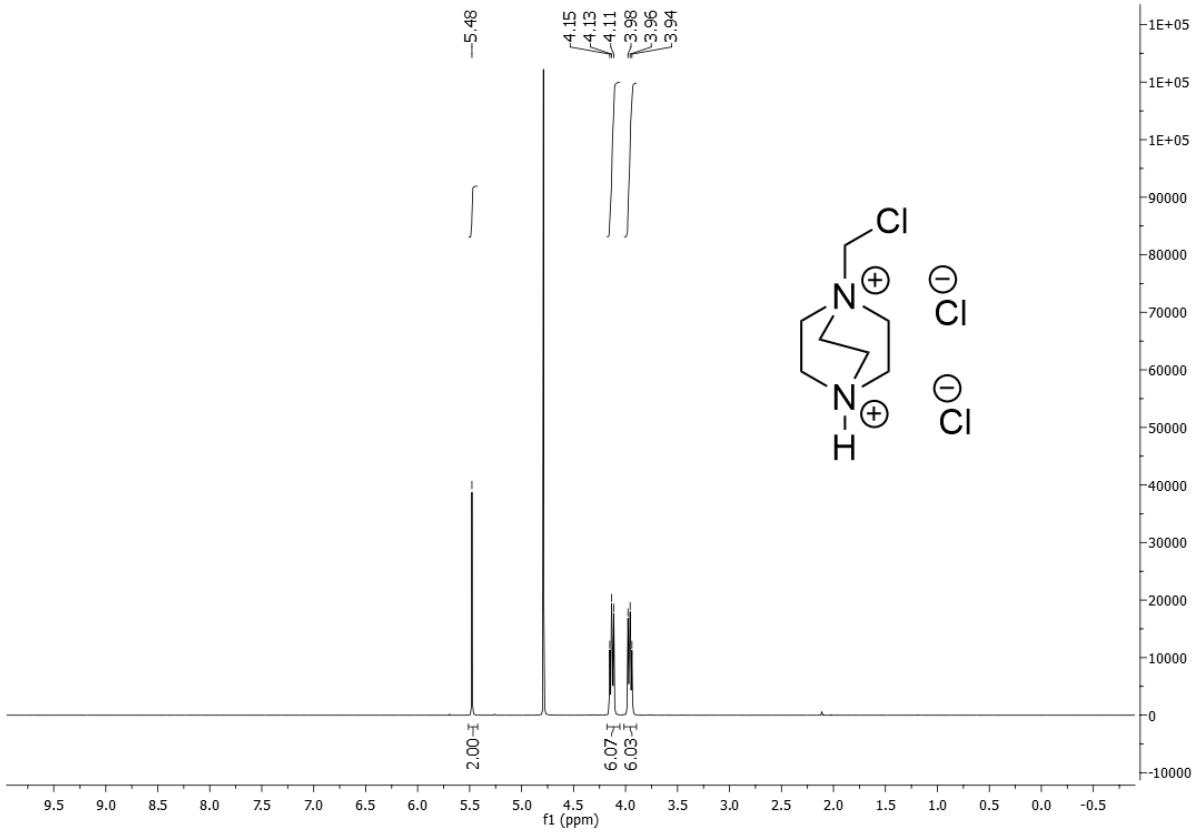

^{13}C NMR of compound **H-TEDA(Cl)$_2$** in D_2O

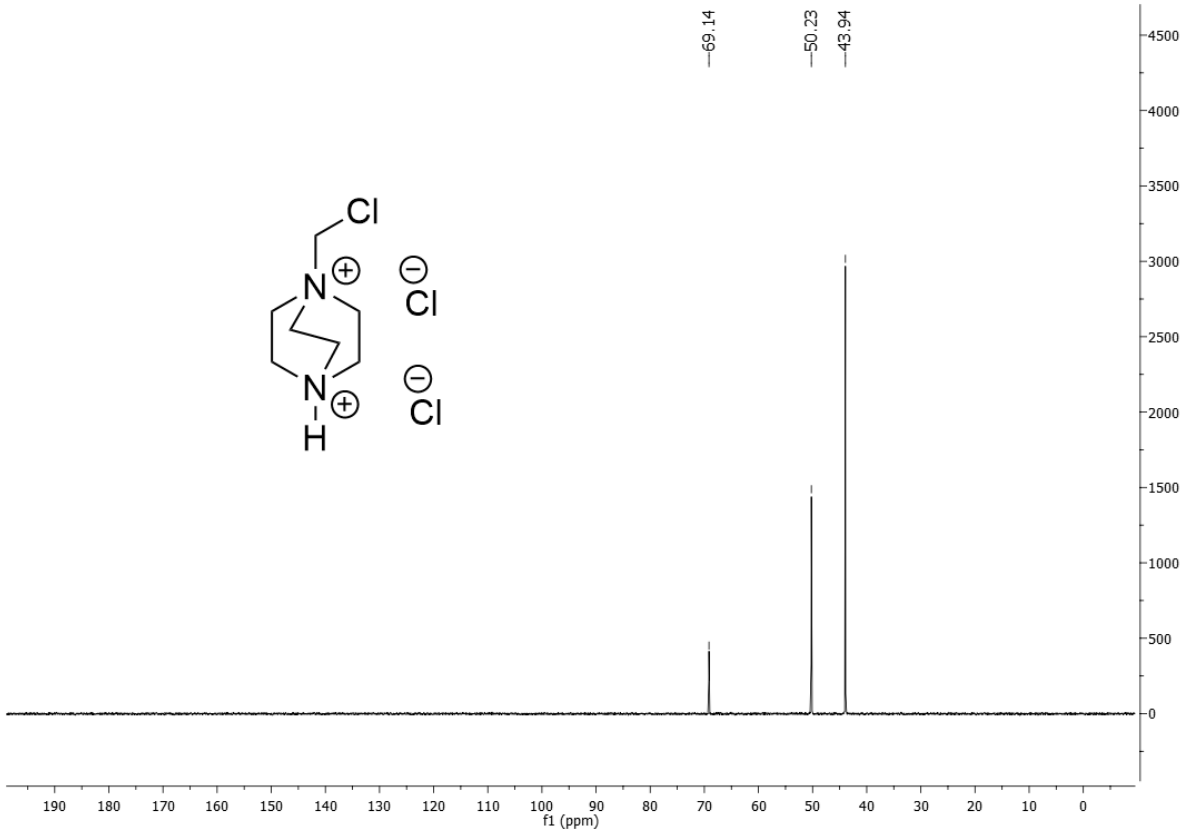

^{1}H NMR of compound **TEDA·BF$_4$** in DMSO-d$_6$

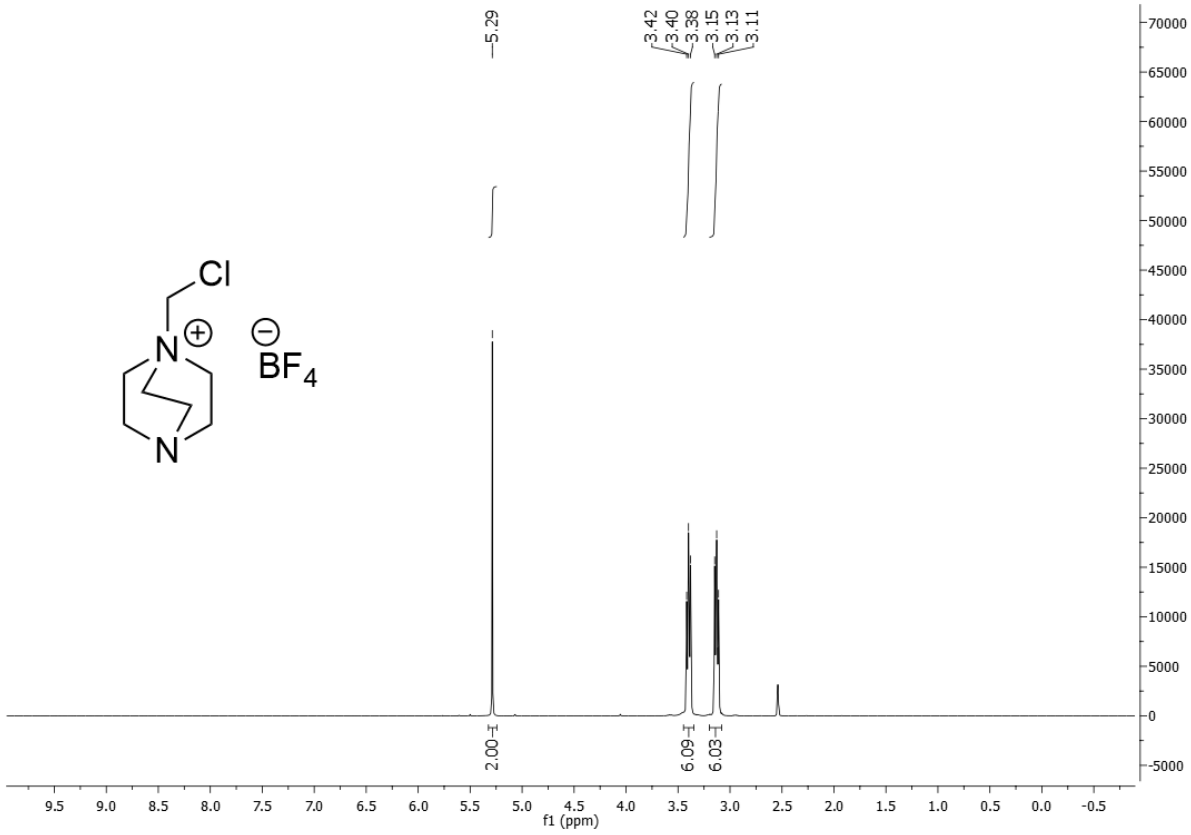

^{13}C NMR of compound **TEDA·BF$_4$** in DMSO-d$_6$

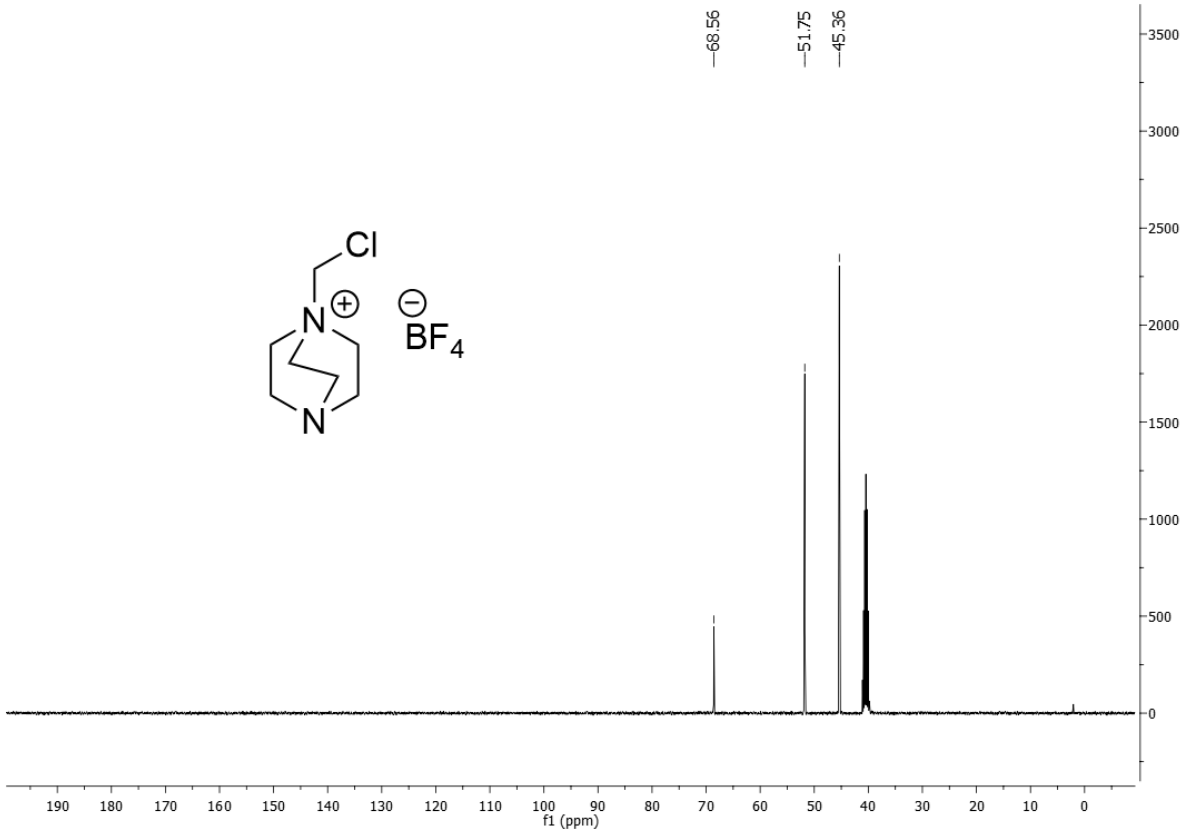

^{19}F NMR of compound **TEDA·BF$_4$** in DMSO-d$_6$

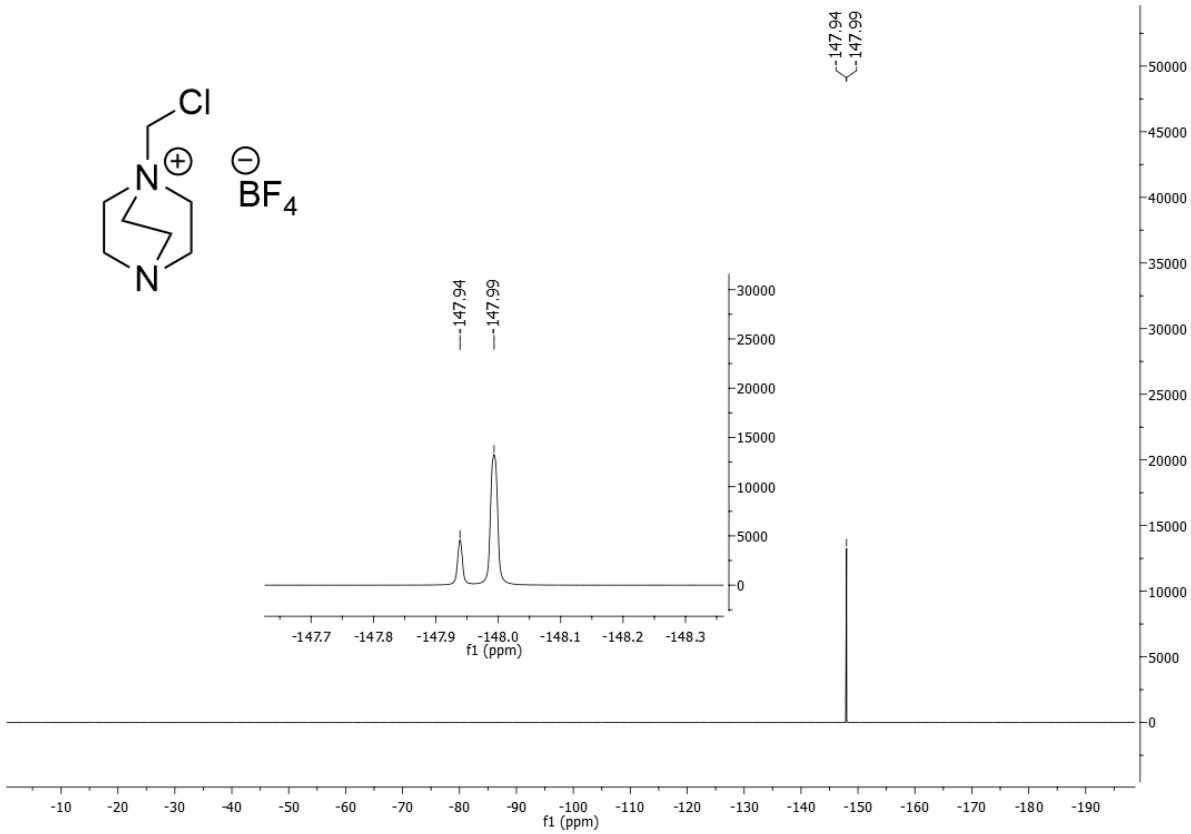

^{1}H NMR of compound **H-TEDA(PF$_6$)$_2$** in CD_3CN

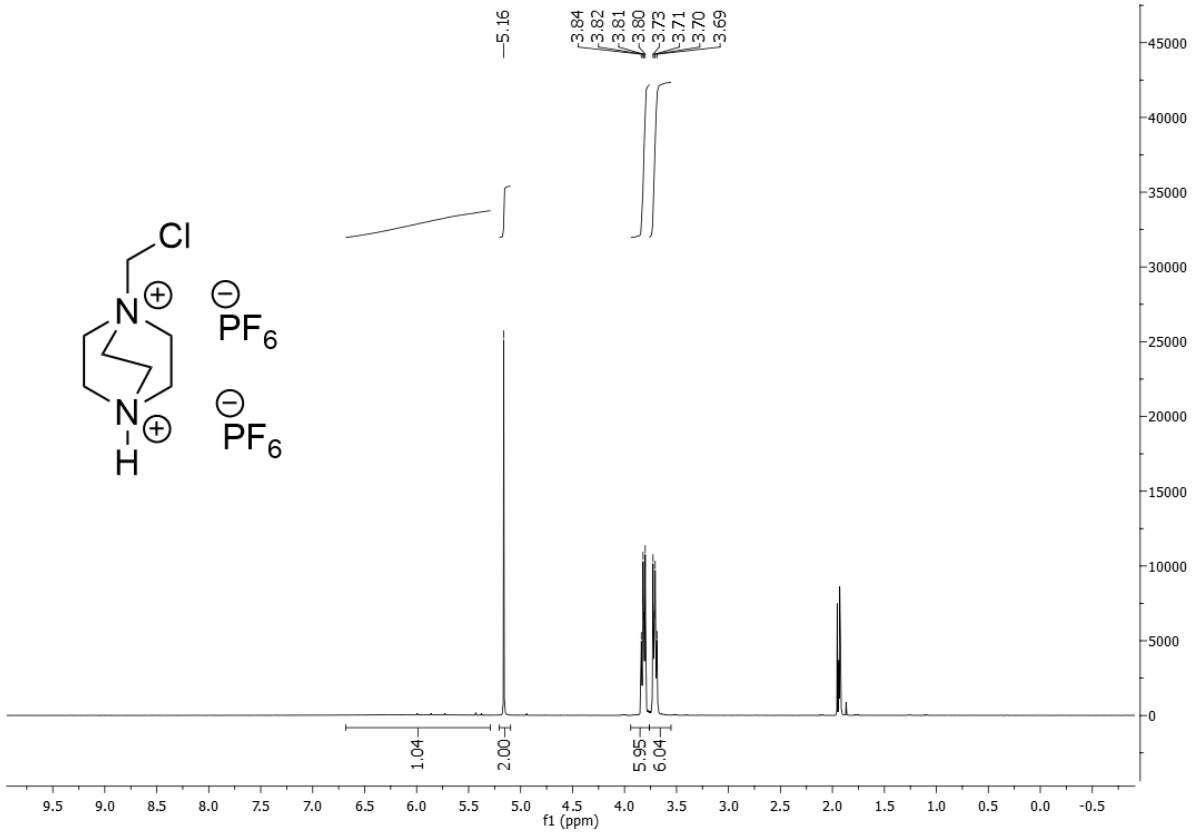

^{13}C NMR of compound **H-TEDA(PF$_6$)$_2$** in CD_3CN

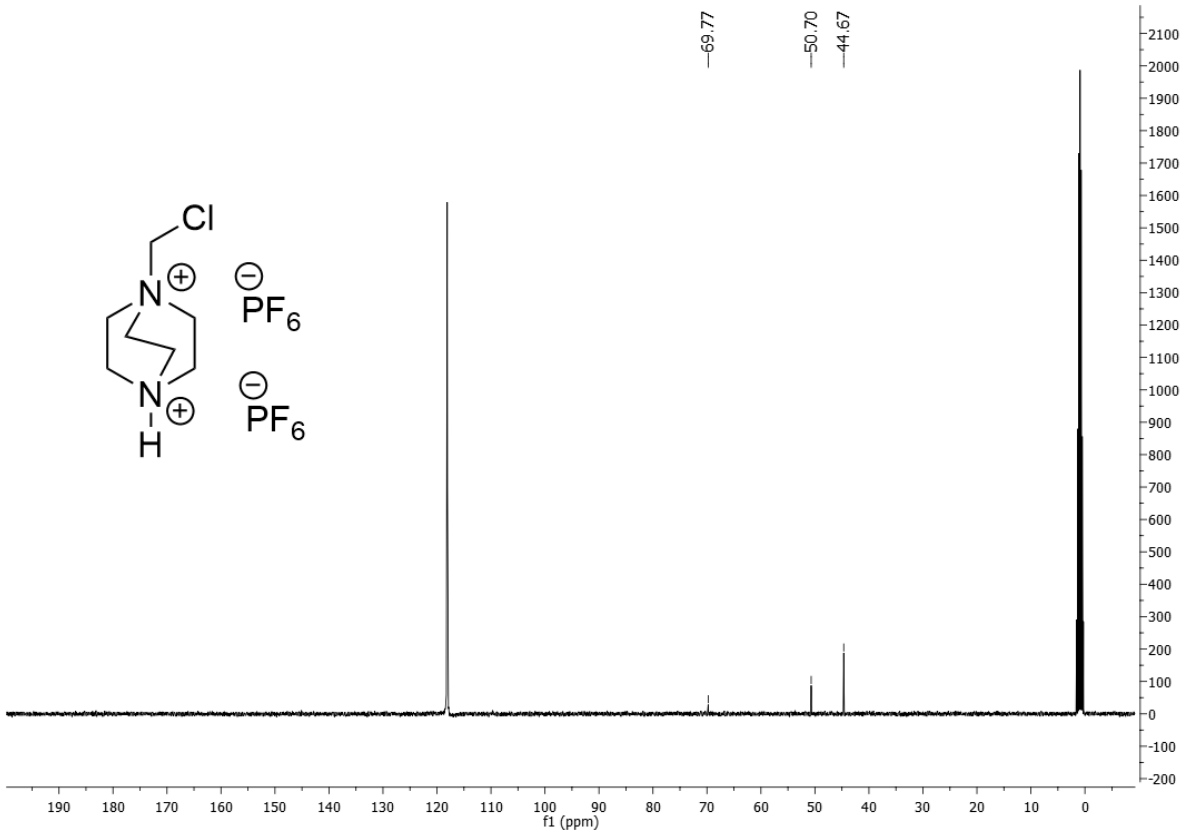

^{19}F NMR of compound **H-TEDA(PF$_6$)$_2$** in CD_3CN

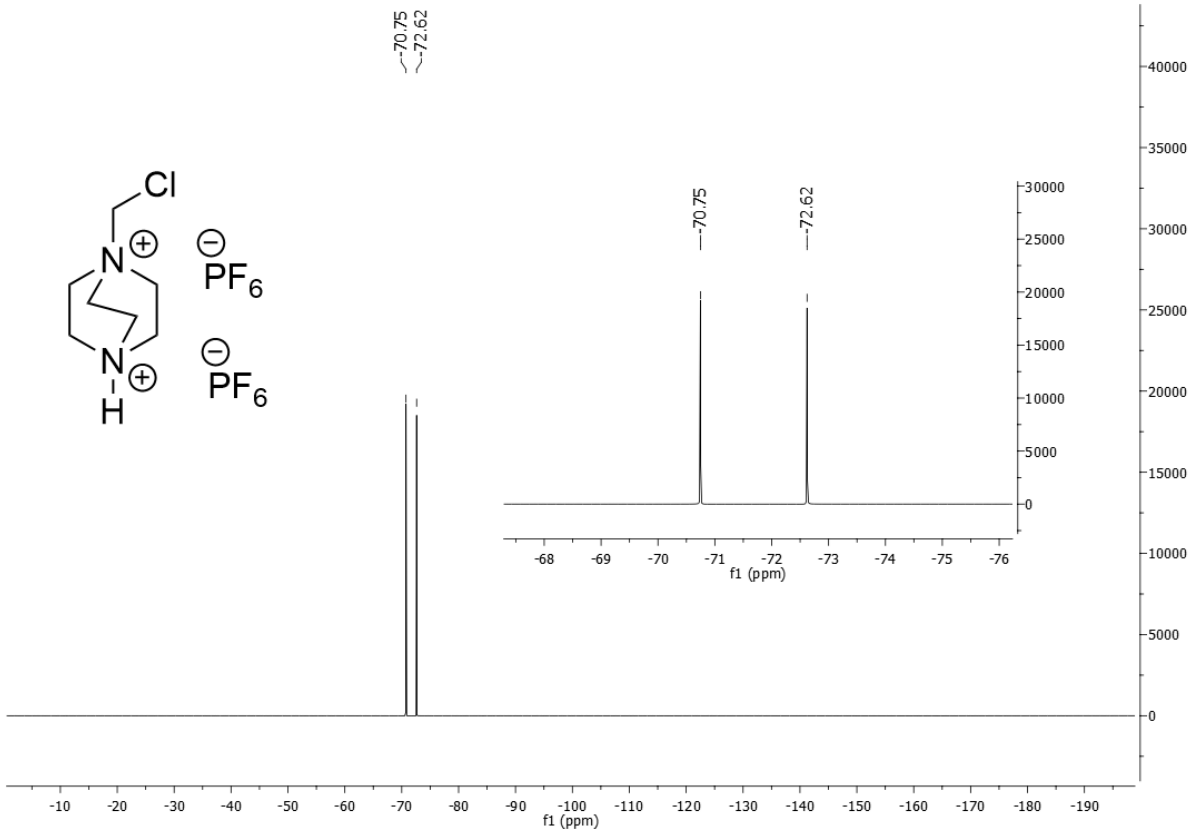

^{31}P NMR of compound **H-TEDA(PF$_6$)$_2$** in CD_3CN

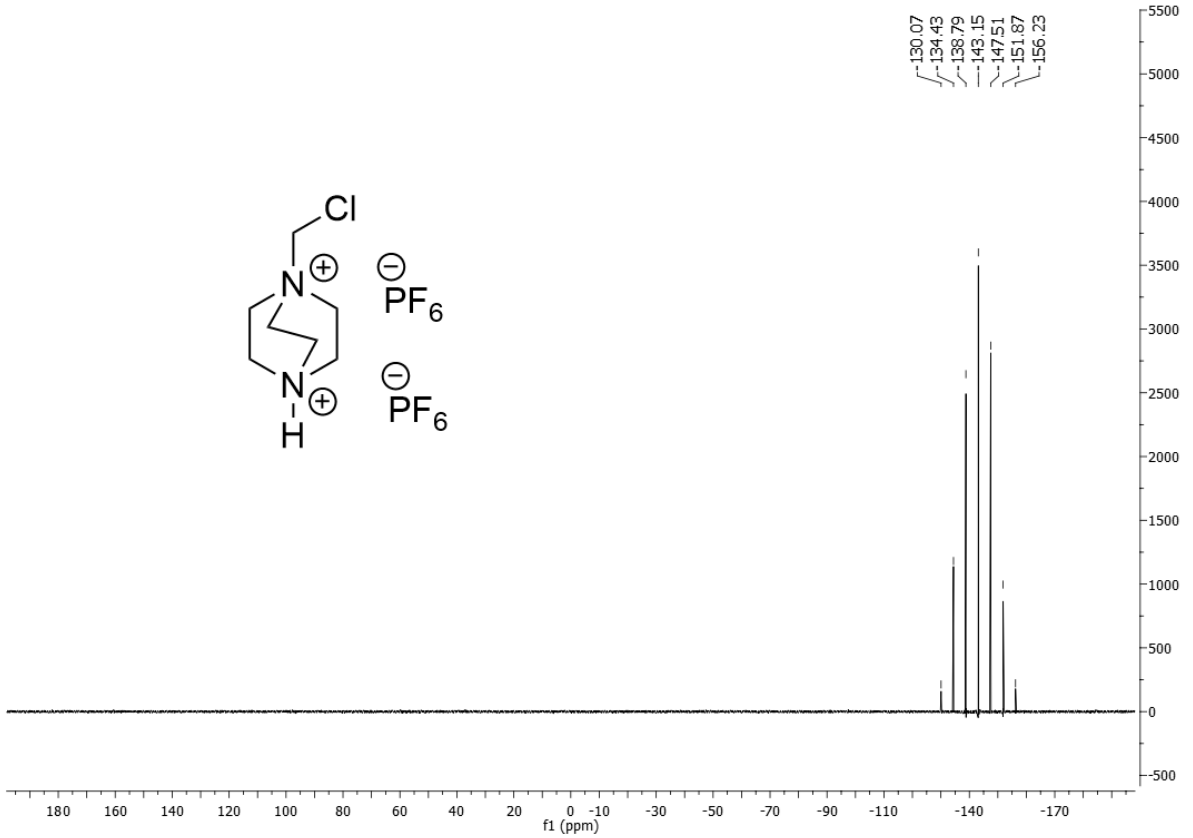

^{1}H NMR of compound **5** in CD_3CN

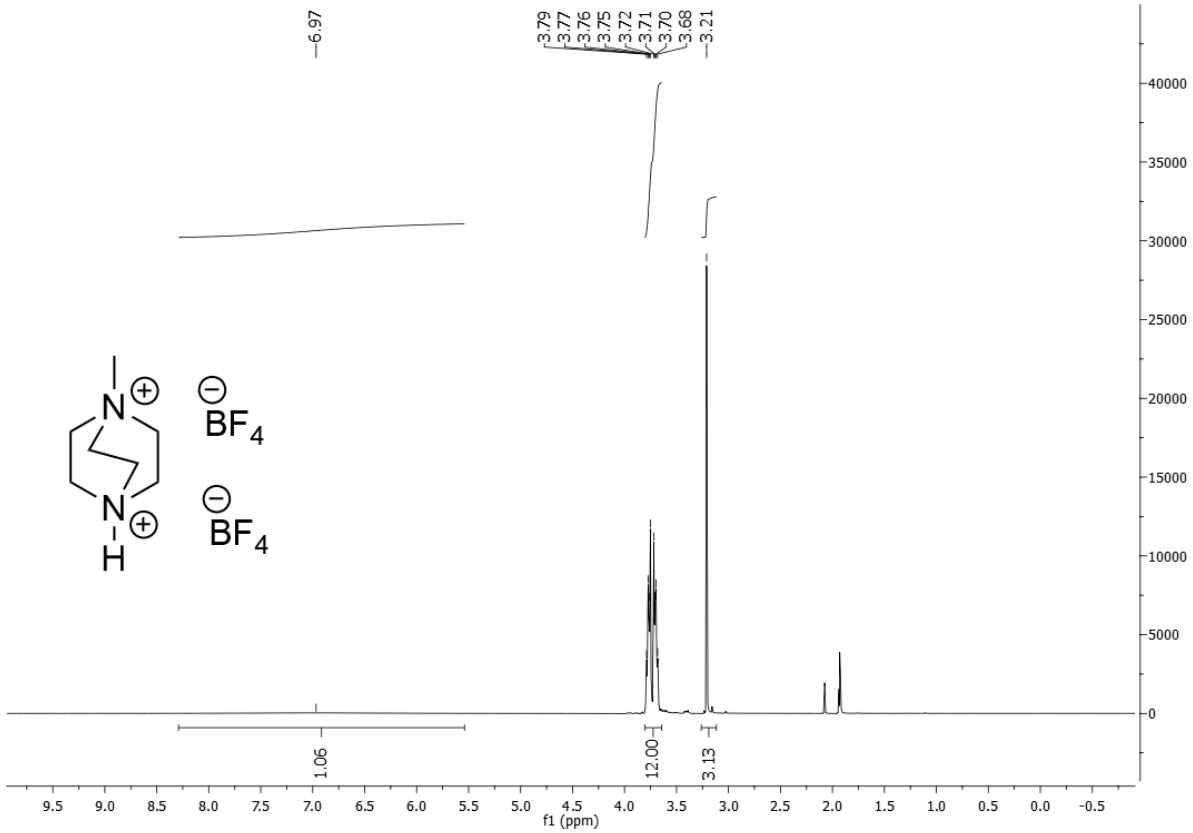

^{13}C NMR of compound **5** in CD_3CN

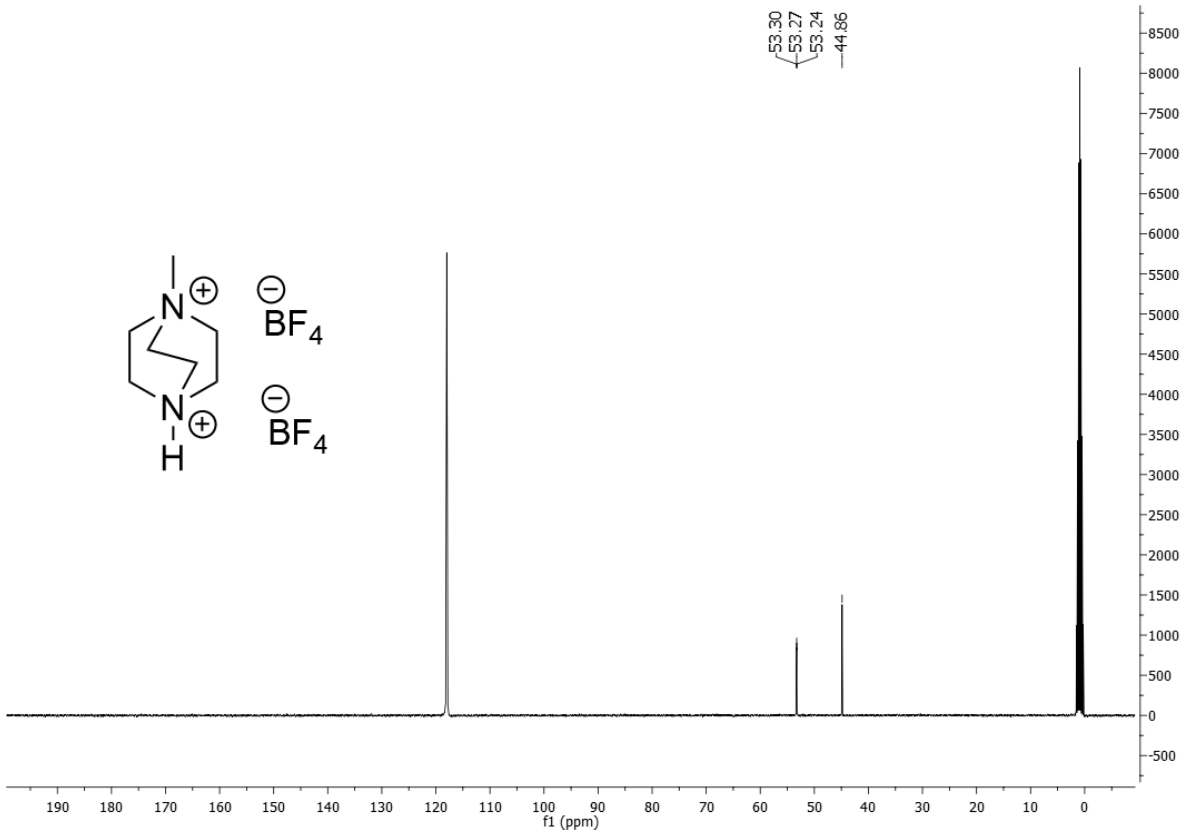

^{19}F NMR of compound **5** in CD_3CN

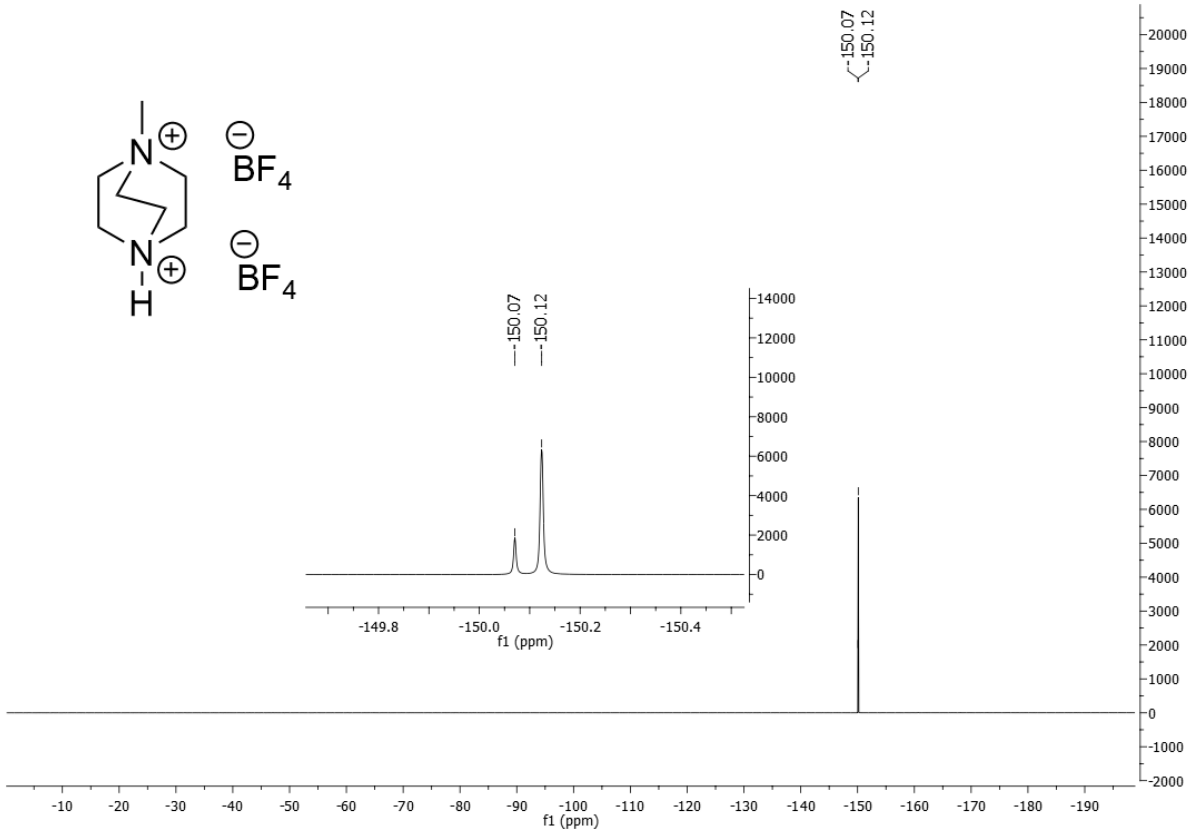

^{1}H NMR of compound **6** in CD_3CN

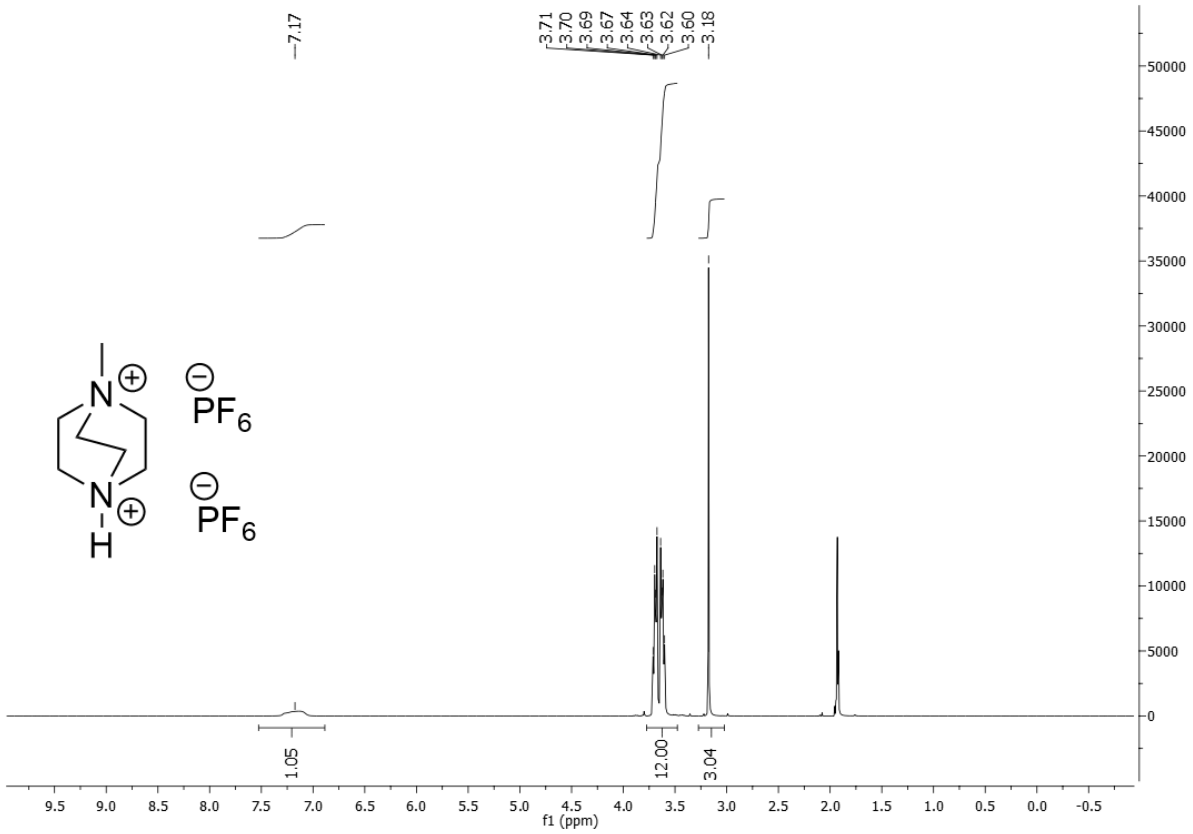

^{13}C NMR of compound **6** in CD_3CN

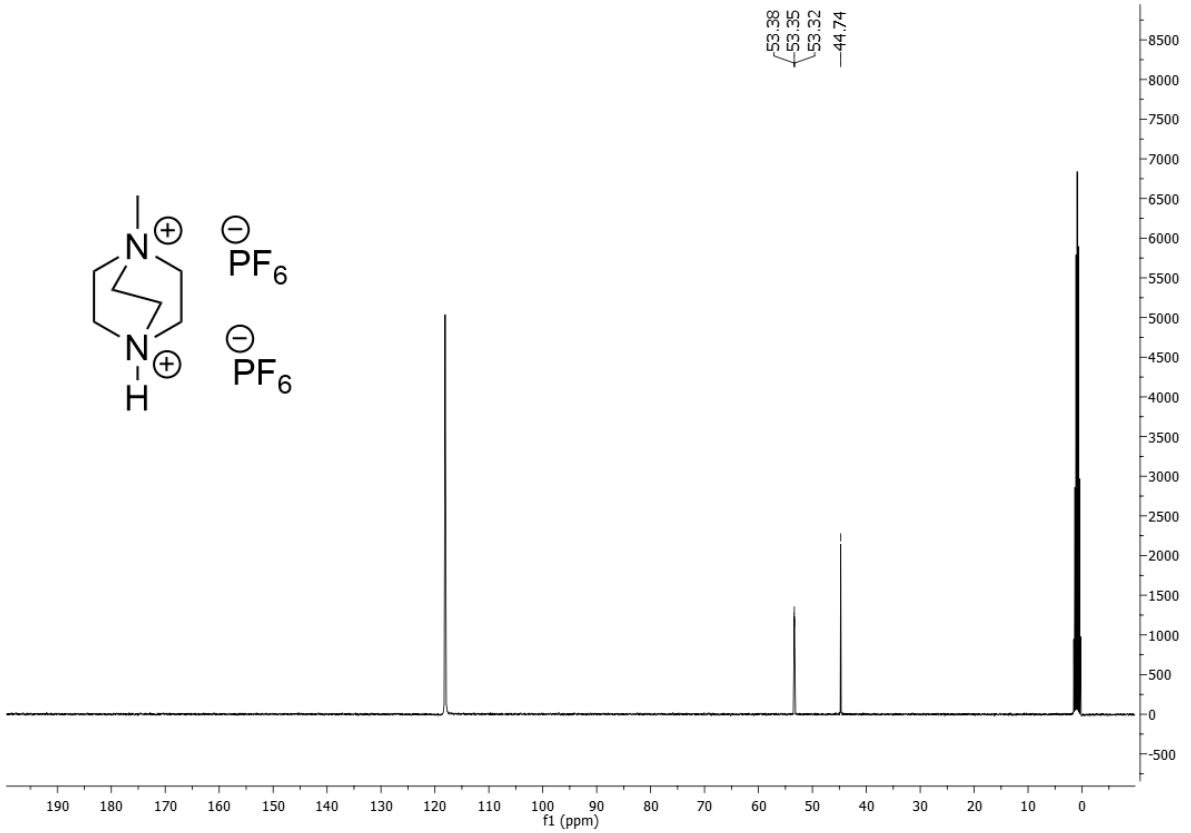

^{19}F NMR of compound **6** in CD_3CN

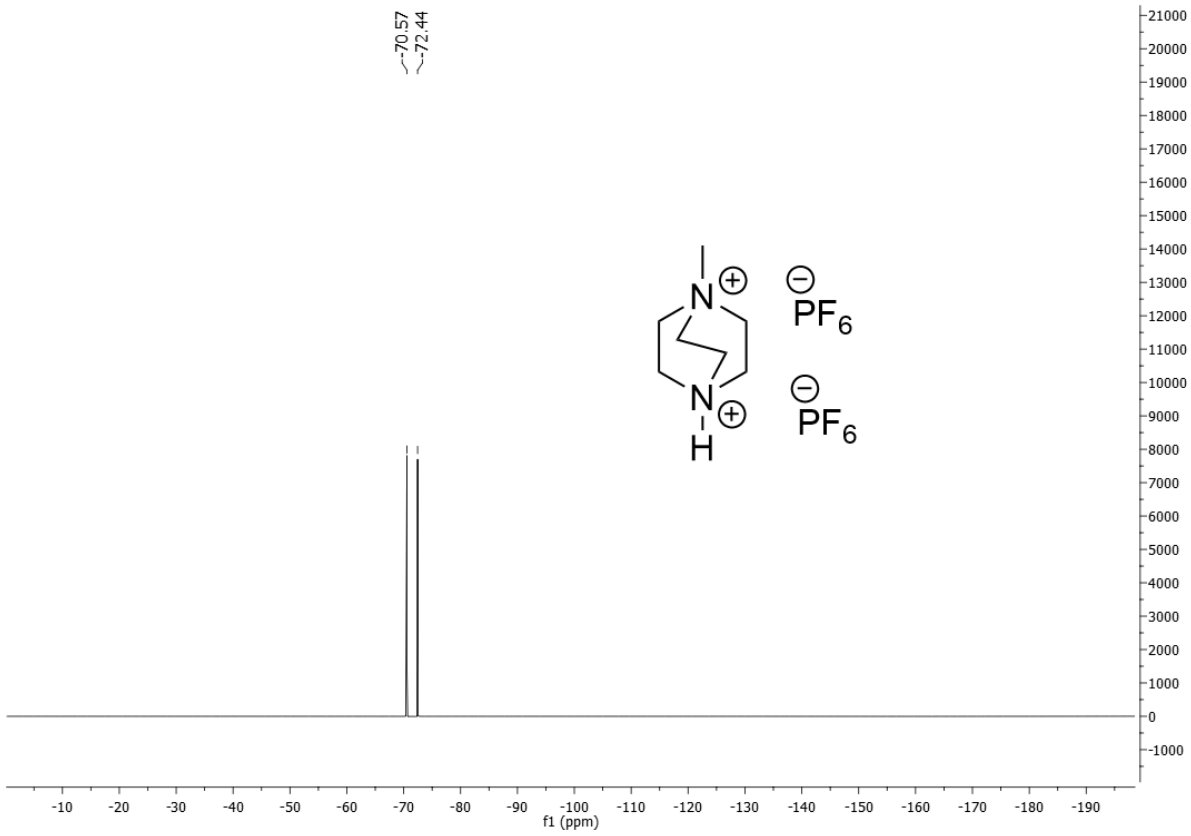

^{31}P NMR of compound **6** in CD_3CN

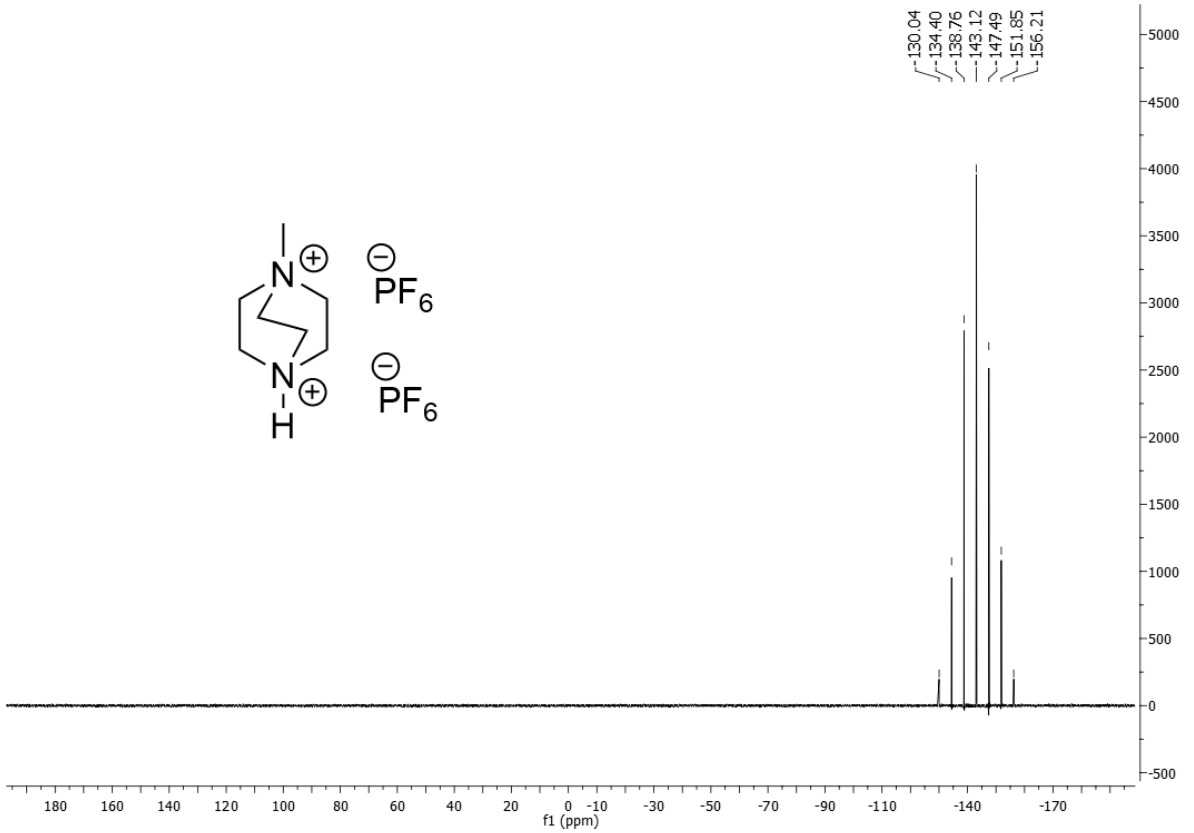

^{1}H NMR of compound **7** in D_2O

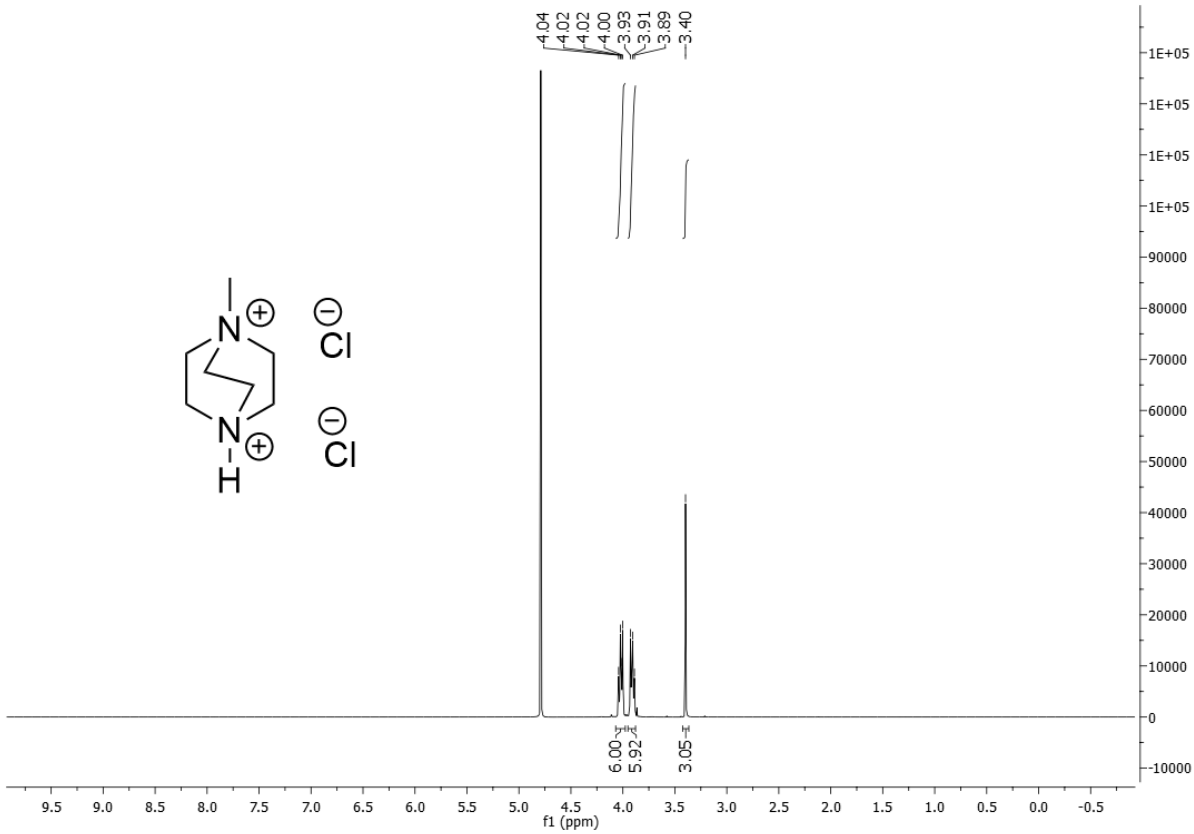

^{13}C NMR of compound **7** in D_2O

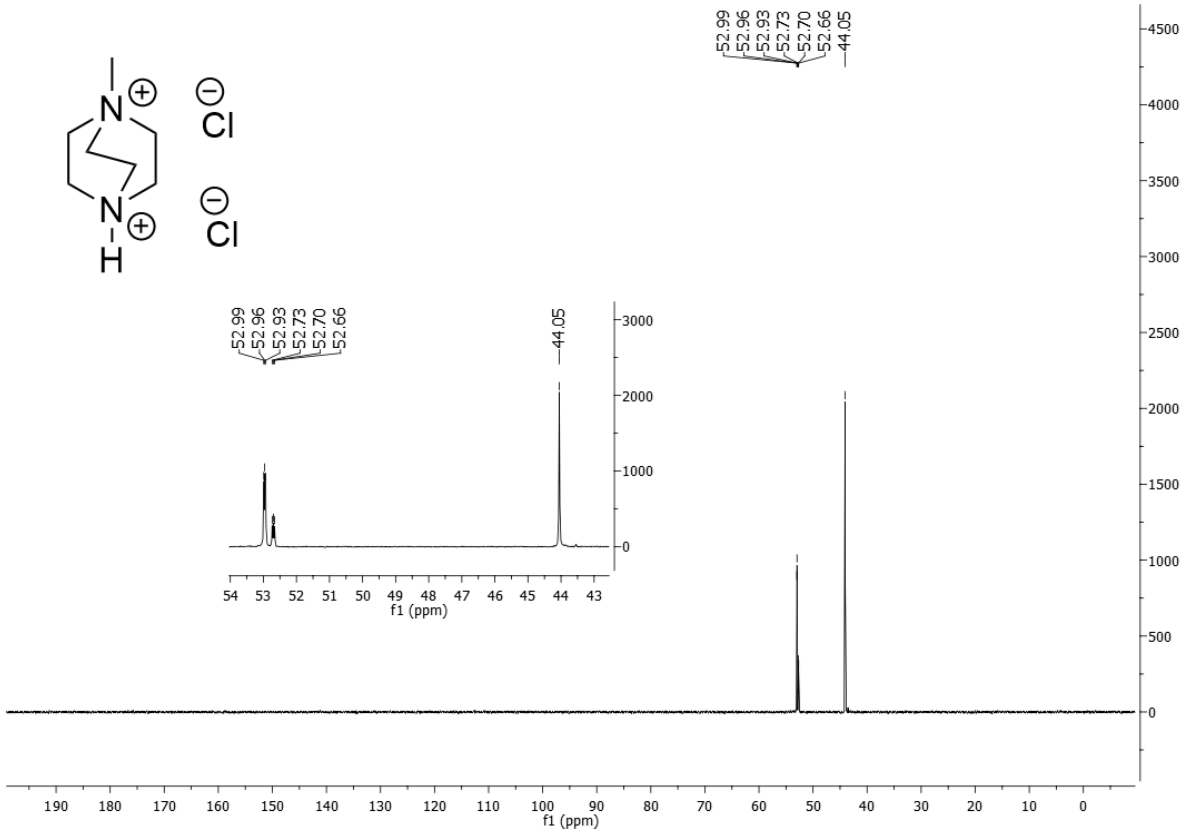

^{1}H NMR of compound **2d** in $CDCl_3$

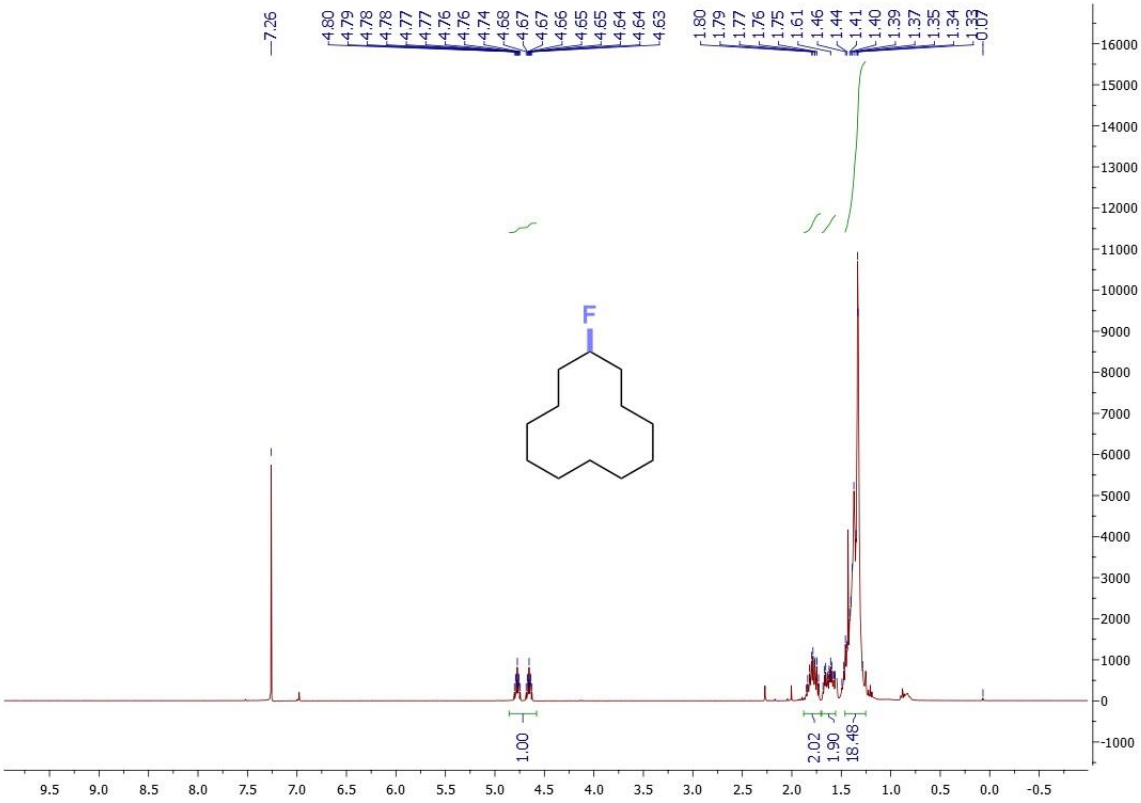

^{13}C NMR of compound **2d** in $CDCl_3$

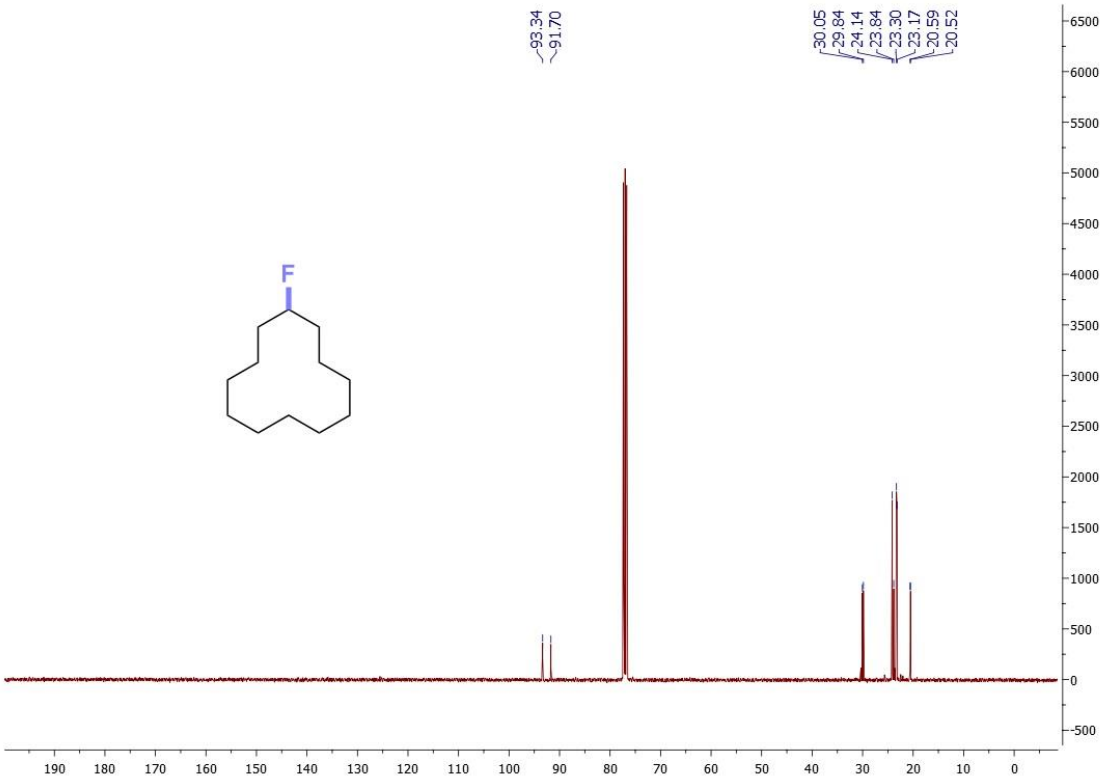

^{19}F NMR of compound **2d** in $CDCl_3$

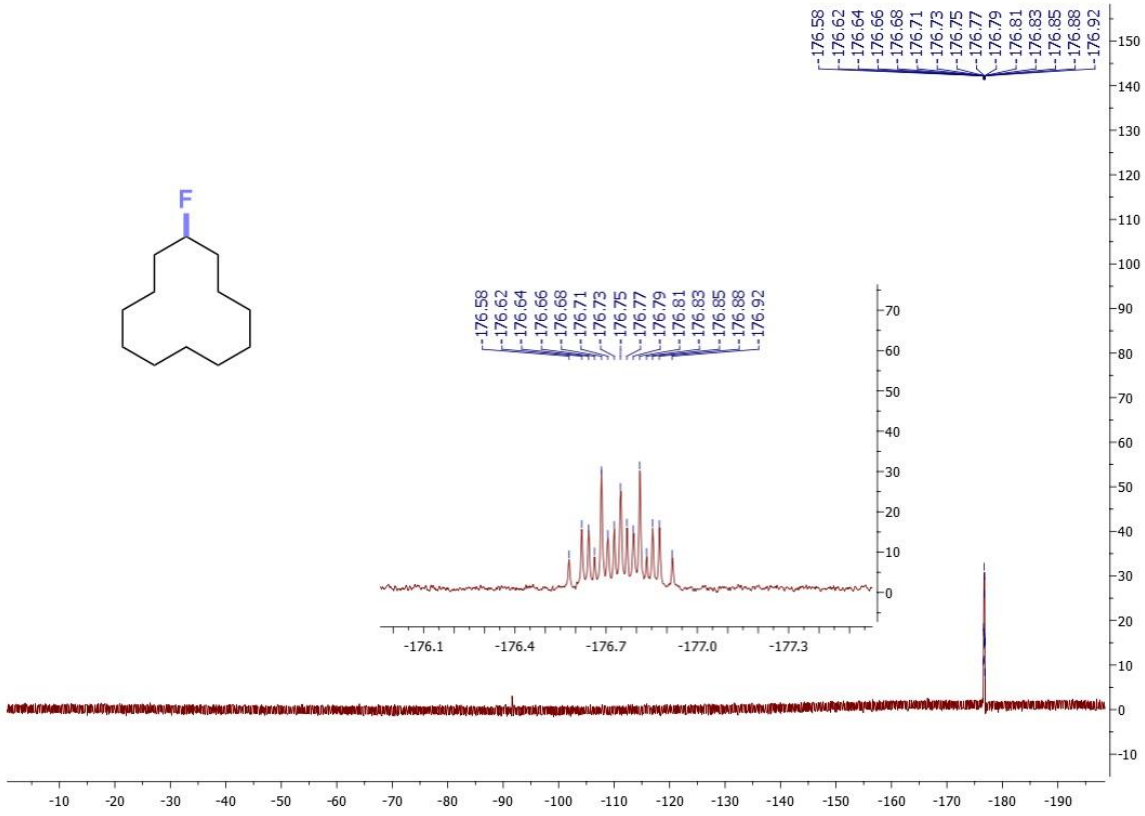

^{1}H NMR of compound **2h** in $CDCl_3$

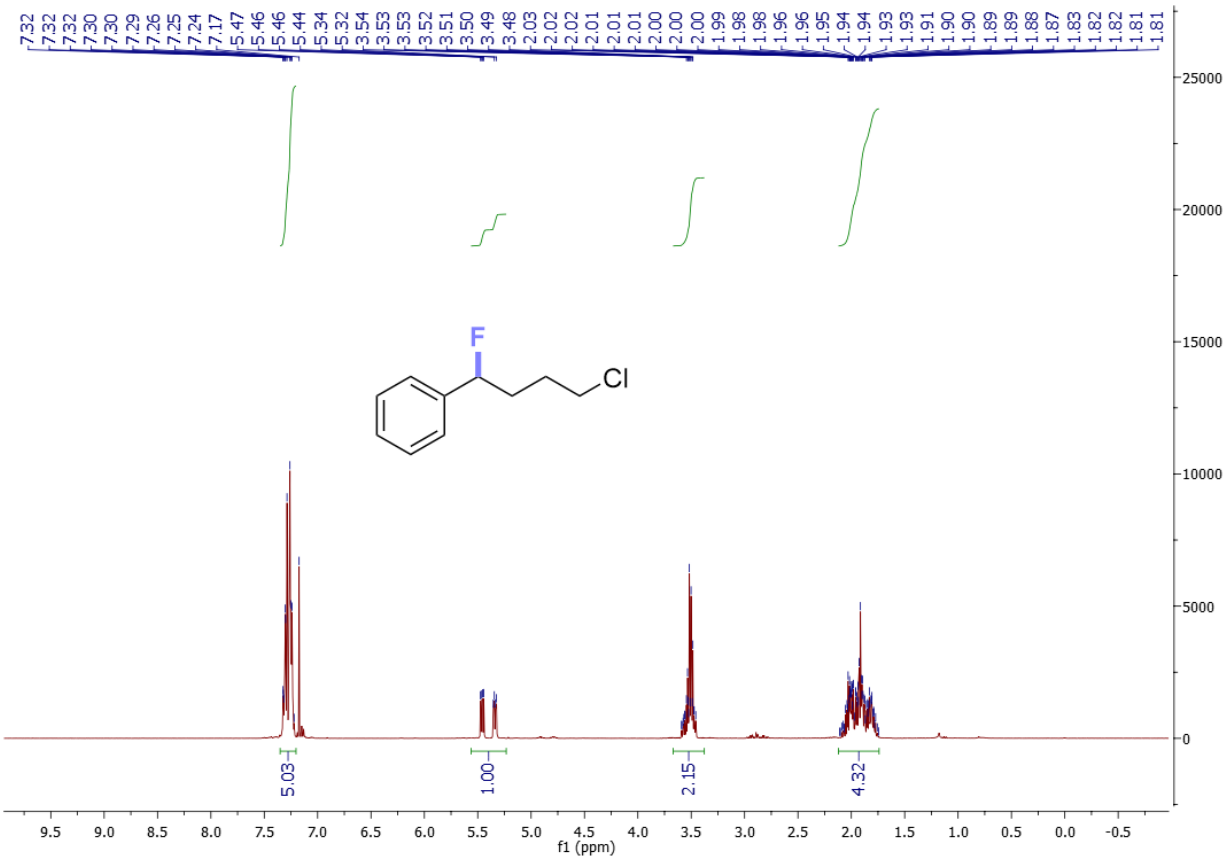

^{13}C NMR of compound **2h** in $CDCl_3$

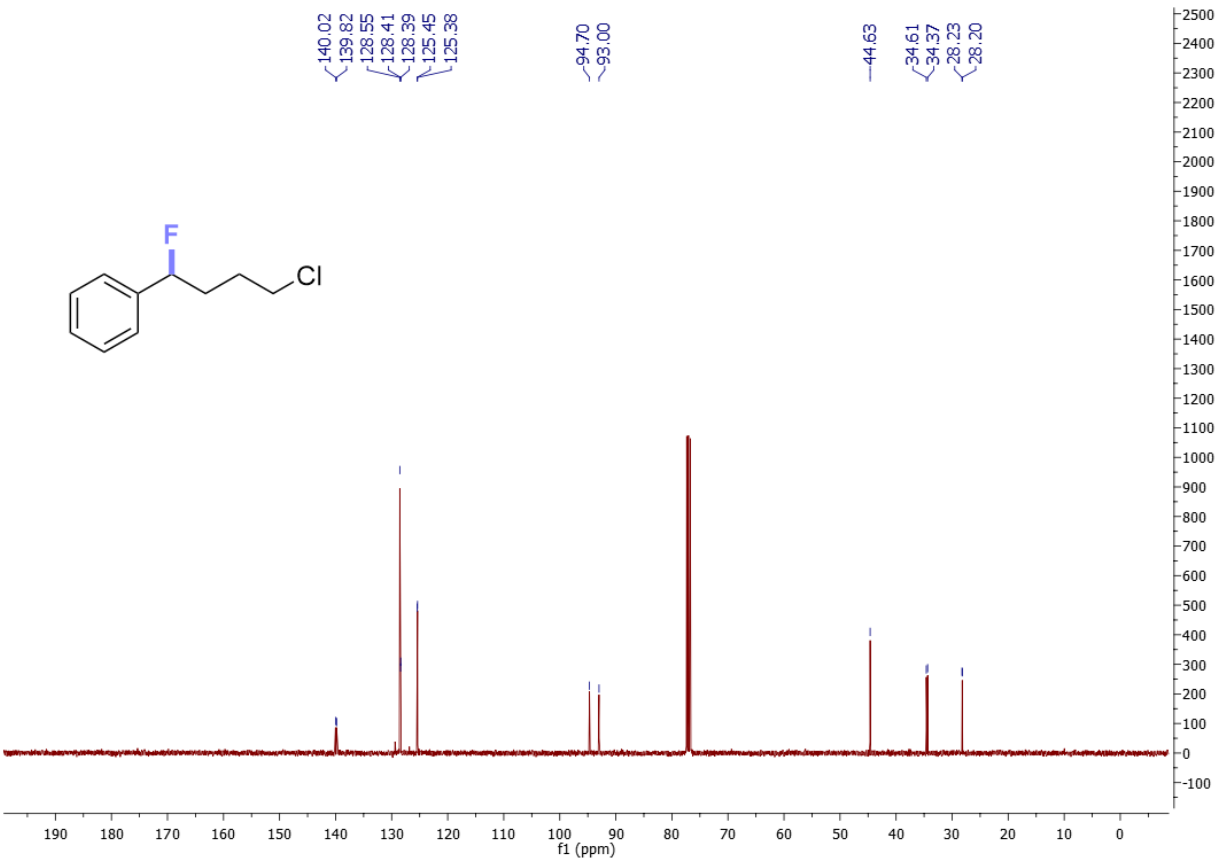

^{19}F NMR of compound **2h** in $CDCl_3$

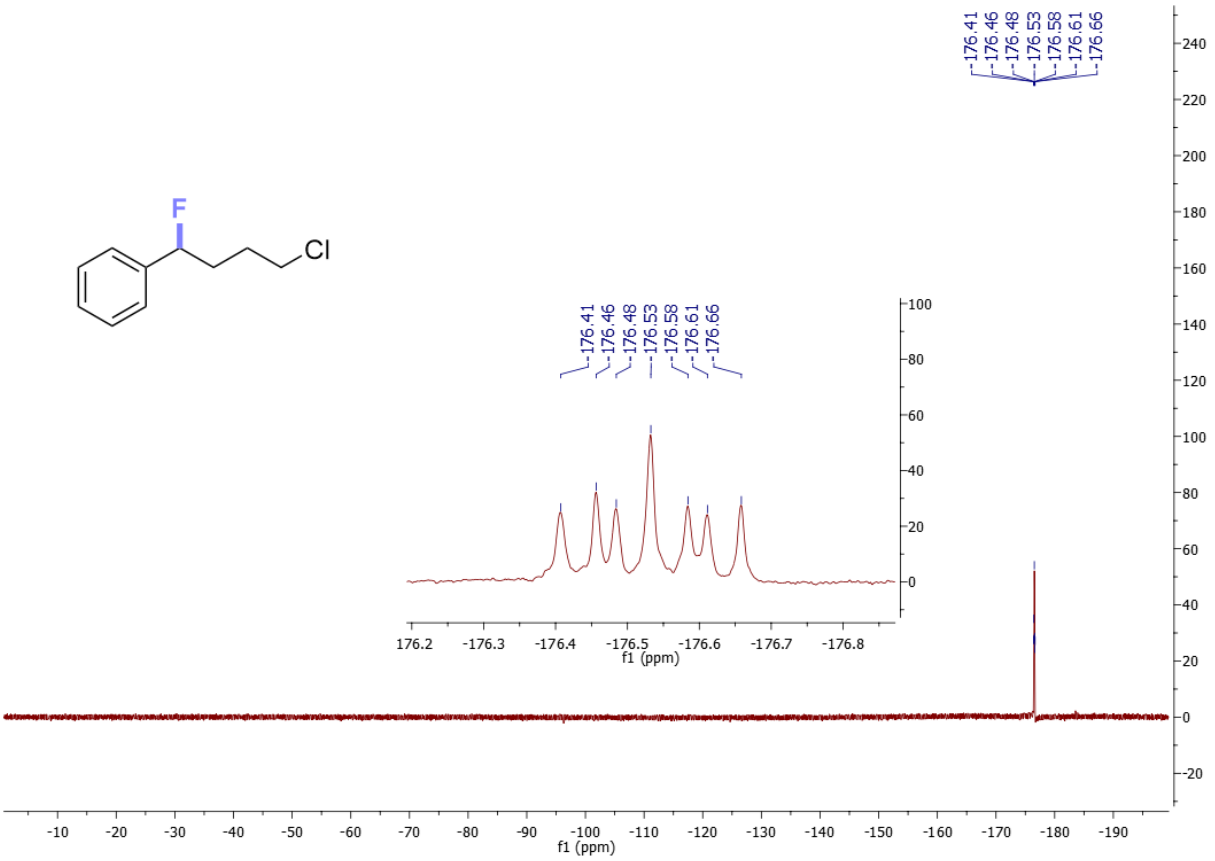

^{1}H NMR of compound **2q** in $CDCl_3$

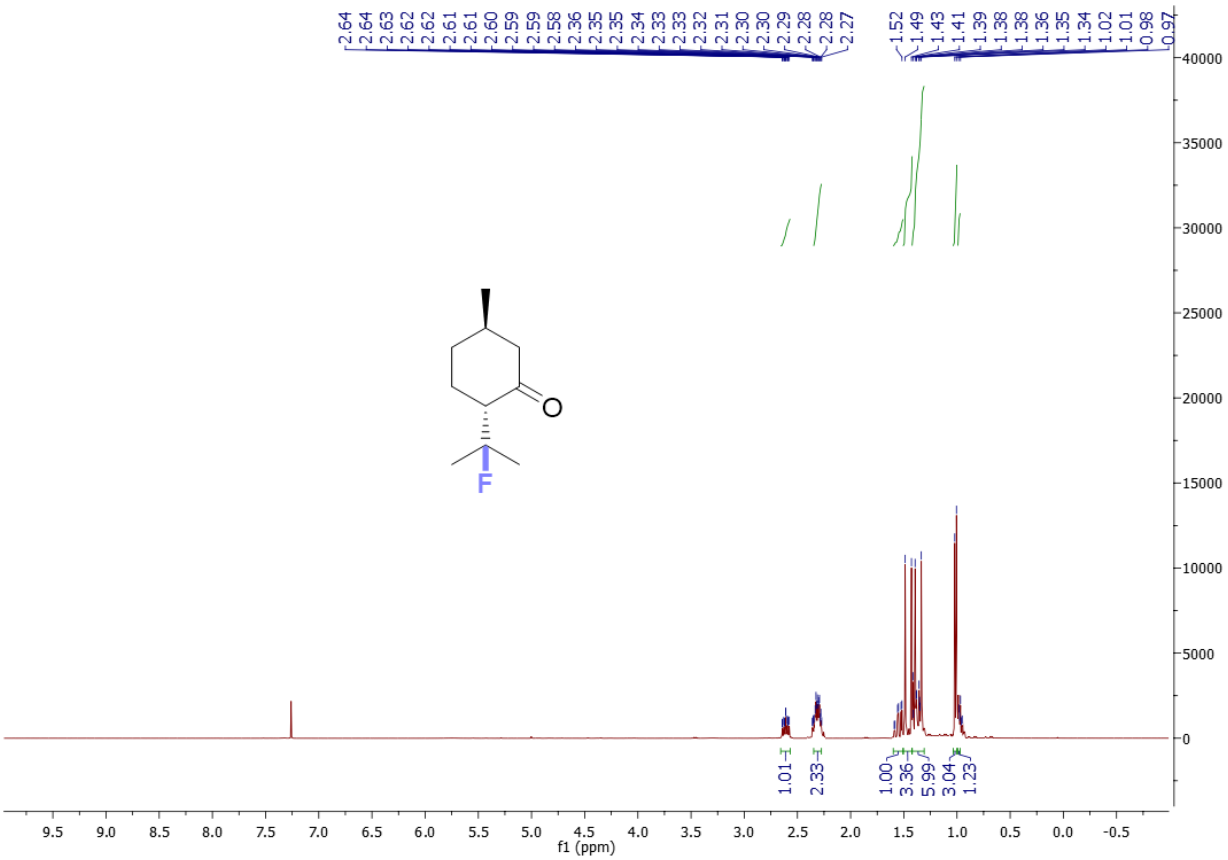

^{13}C NMR of compound **2q** in $CDCl_3$

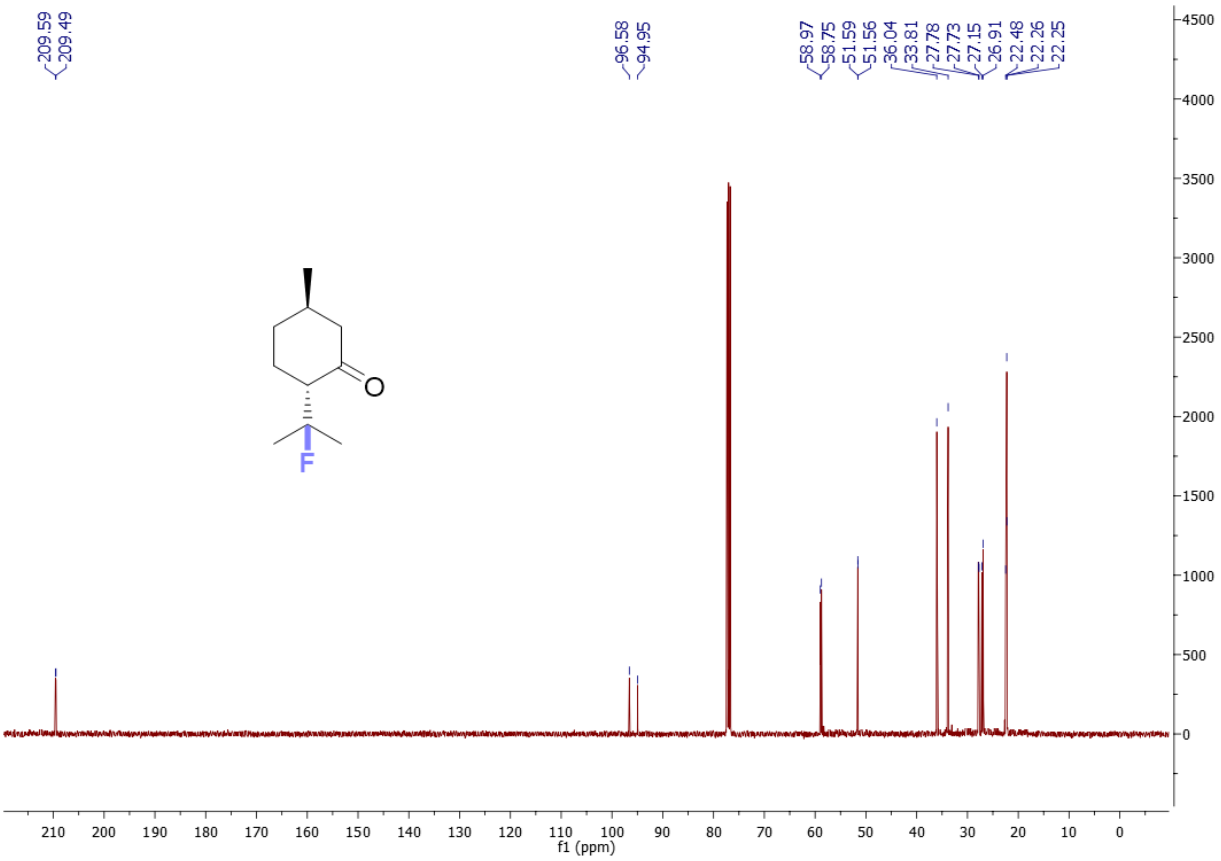

^{19}F NMR of compound **2q** in $CDCl_3$

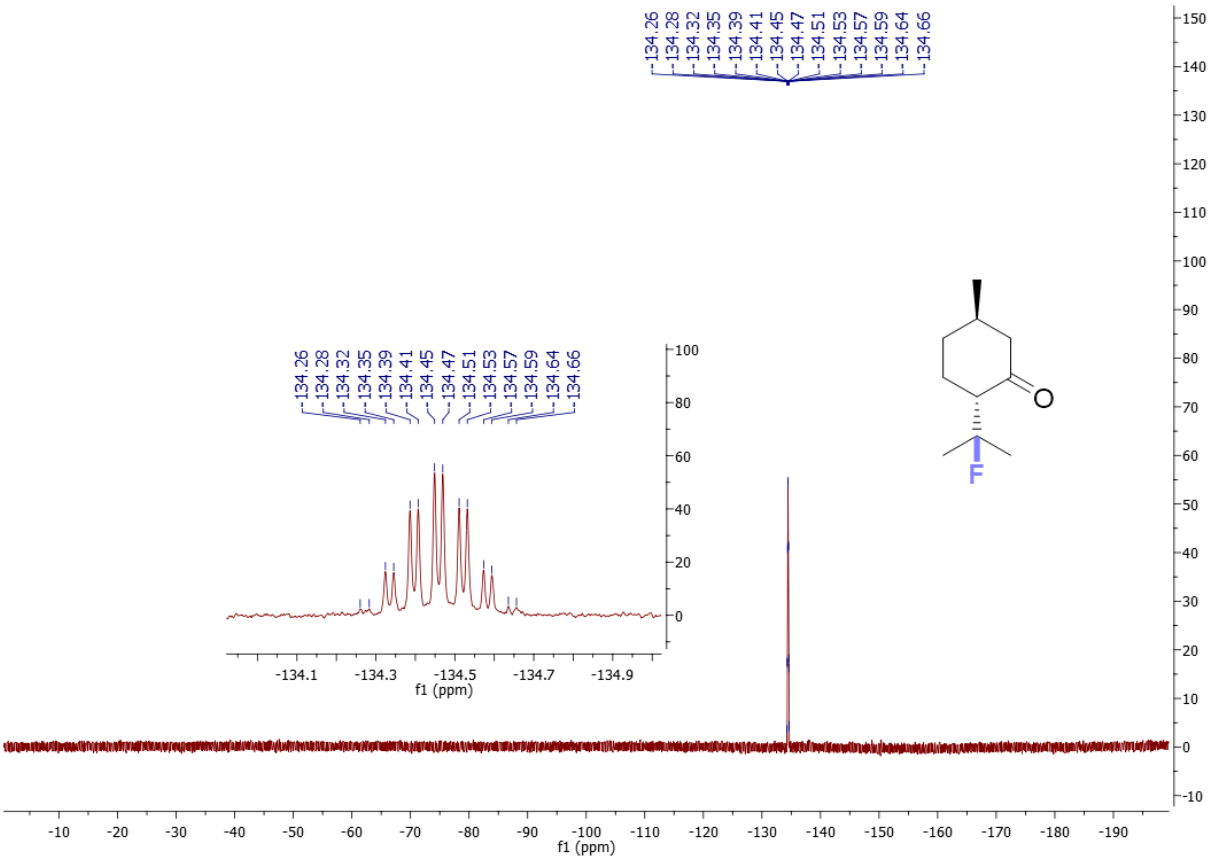

^{1}H NMR of compound **2r** in CD_3CN

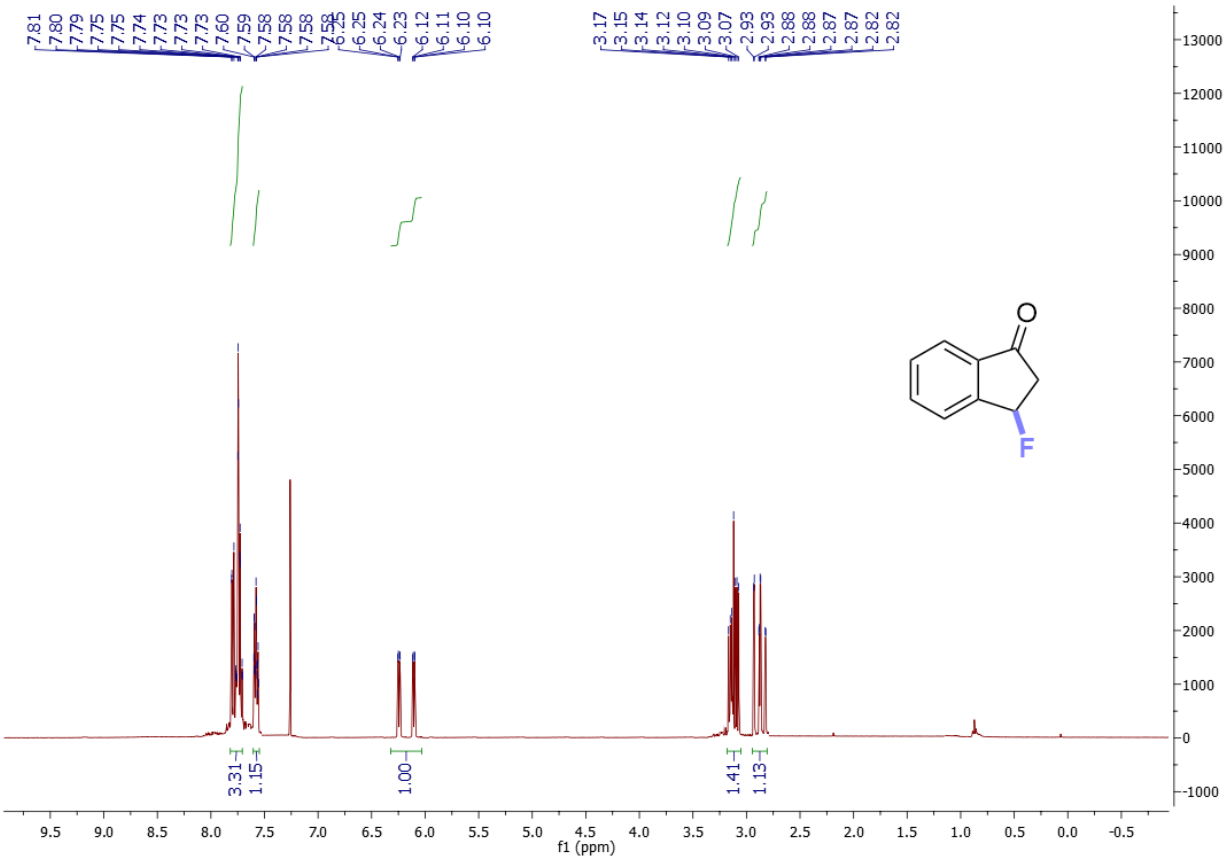

^{13}C NMR of compound **2r** in CD_3CN

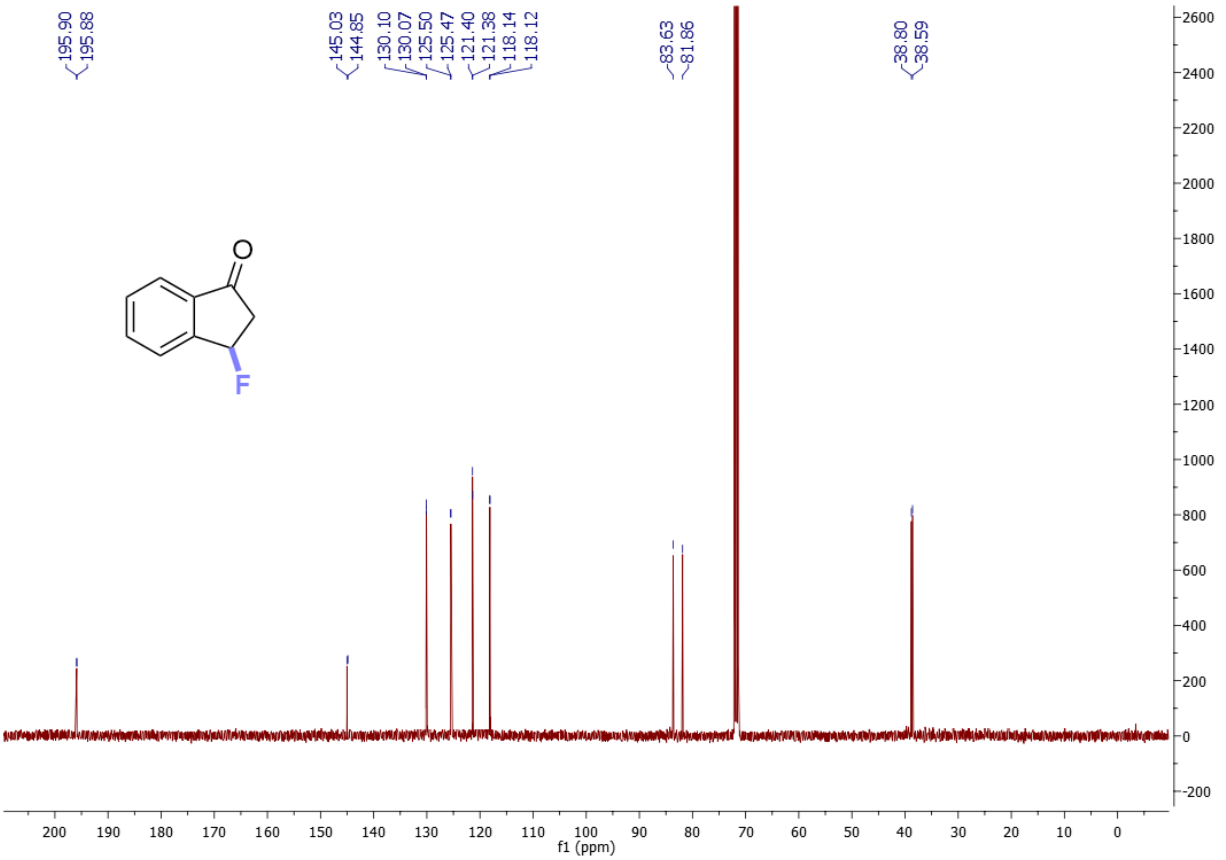

^{19}F NMR of compound **2r** in CD_3CN

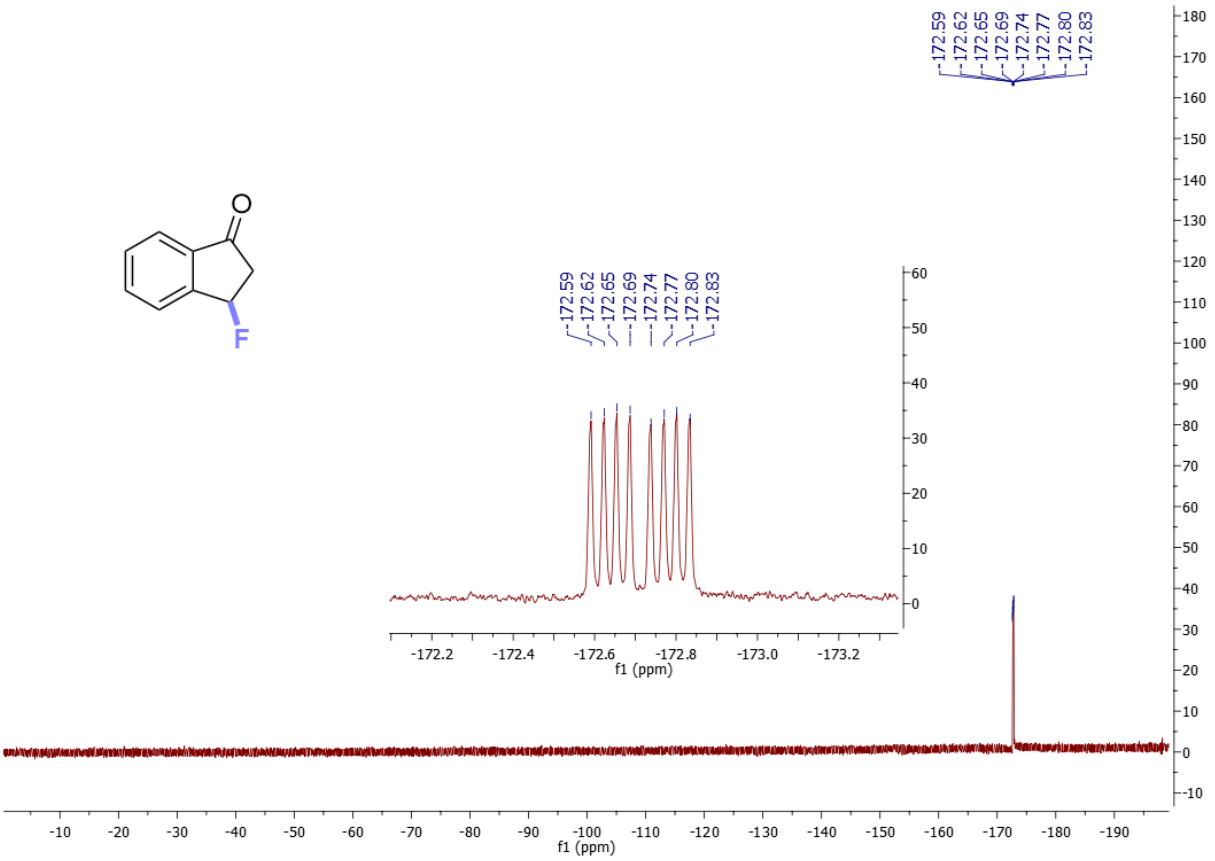

^{1}H NMR of compound **2t** in $CDCl_3$

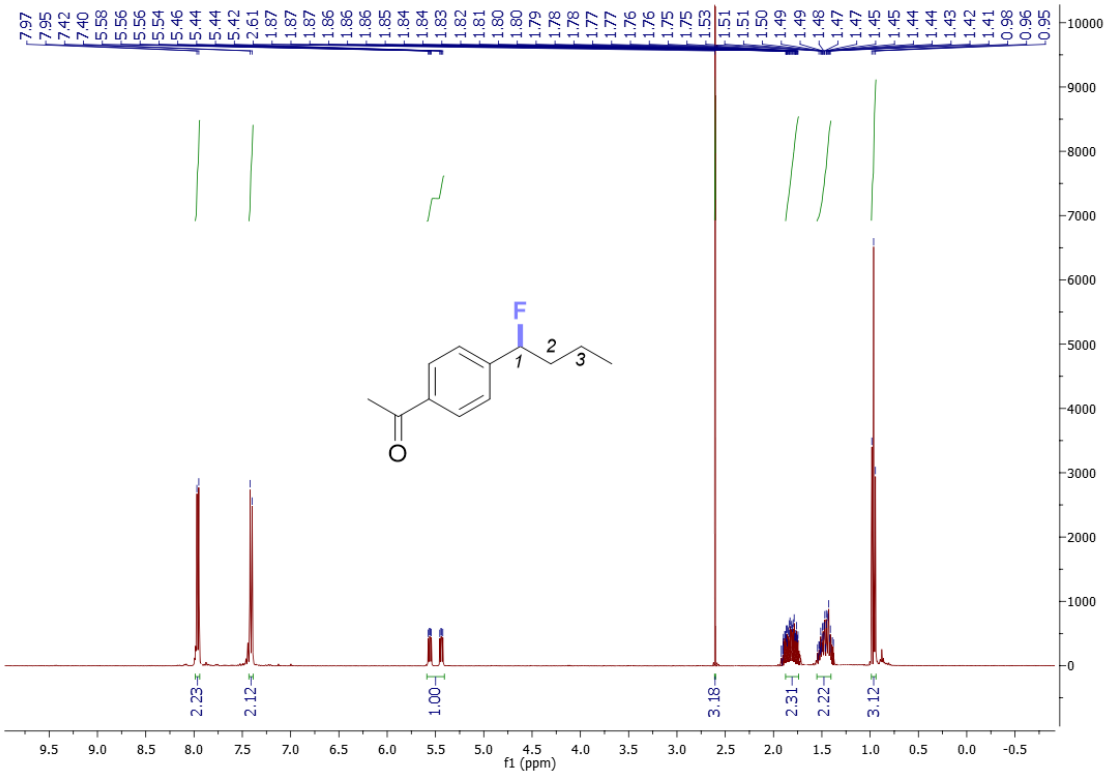

^{13}C NMR of compound **2t** in $CDCl_3$

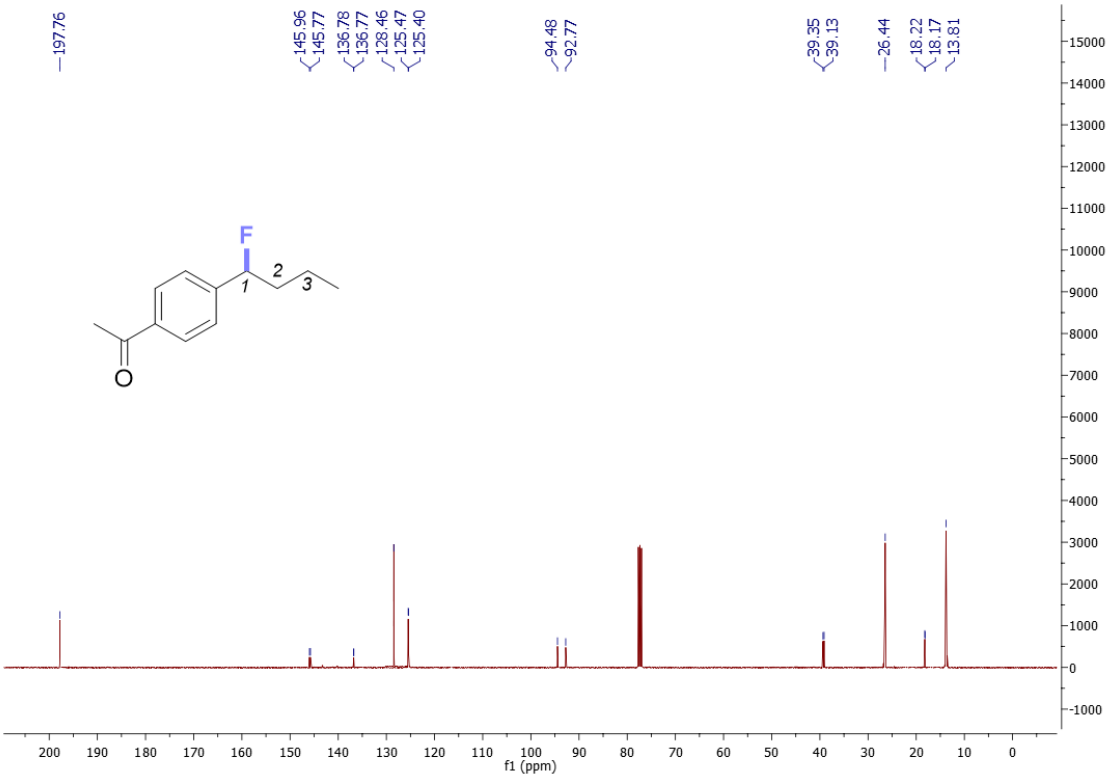

^{19}F NMR of compound **2t** in $CDCl_3$

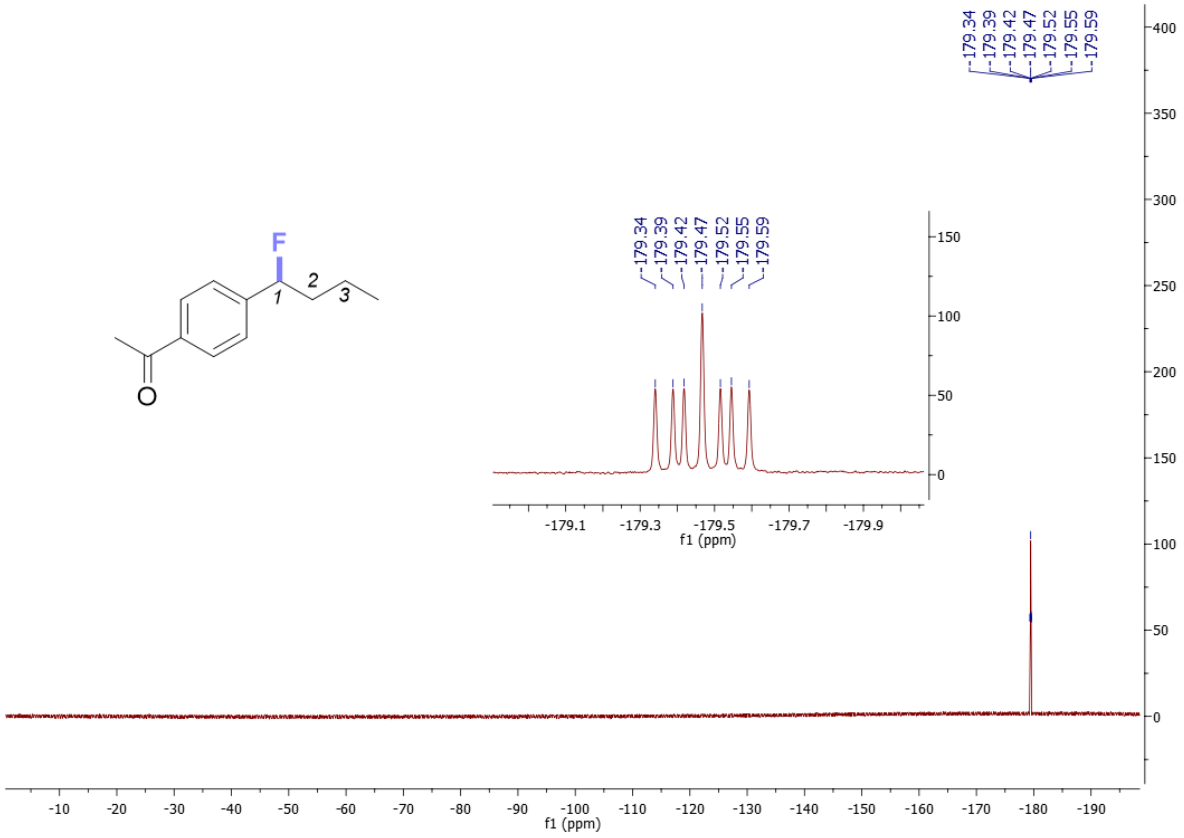

^{1}H NMR of compound **2v** in $CDCl_3$

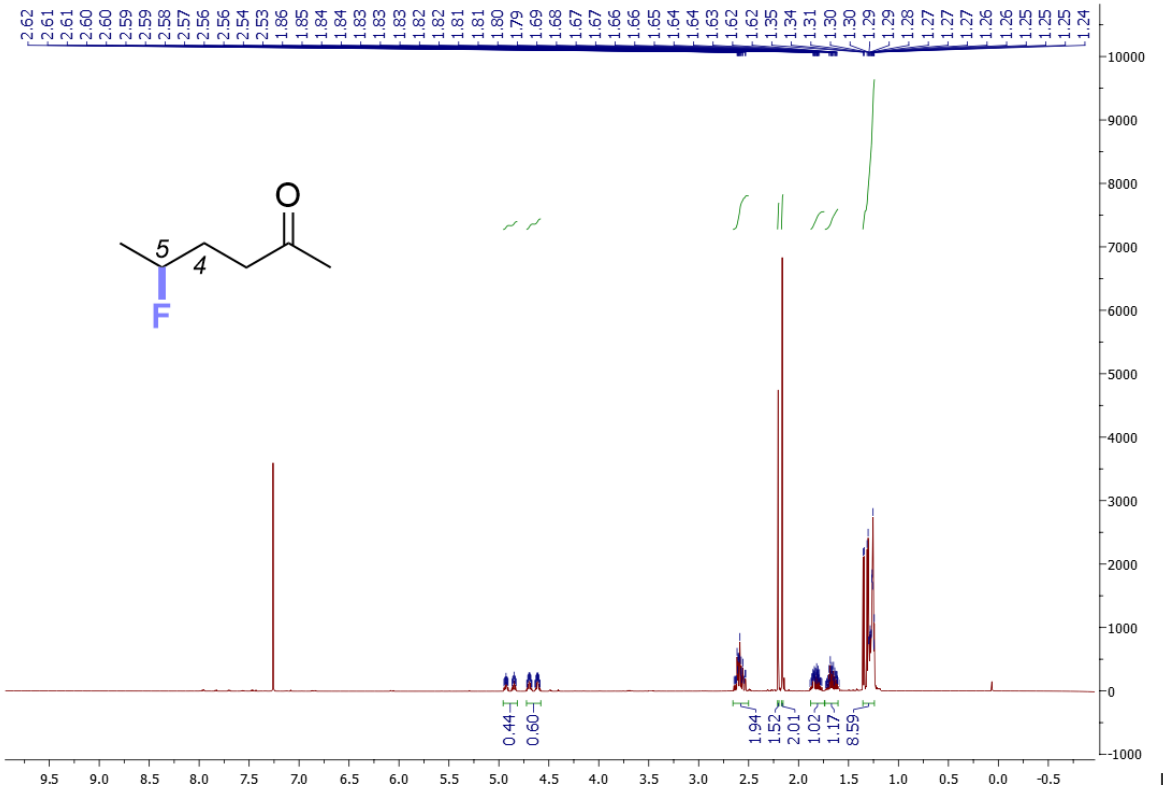

^{13}C NMR of compound **2v** in $CDCl_3$

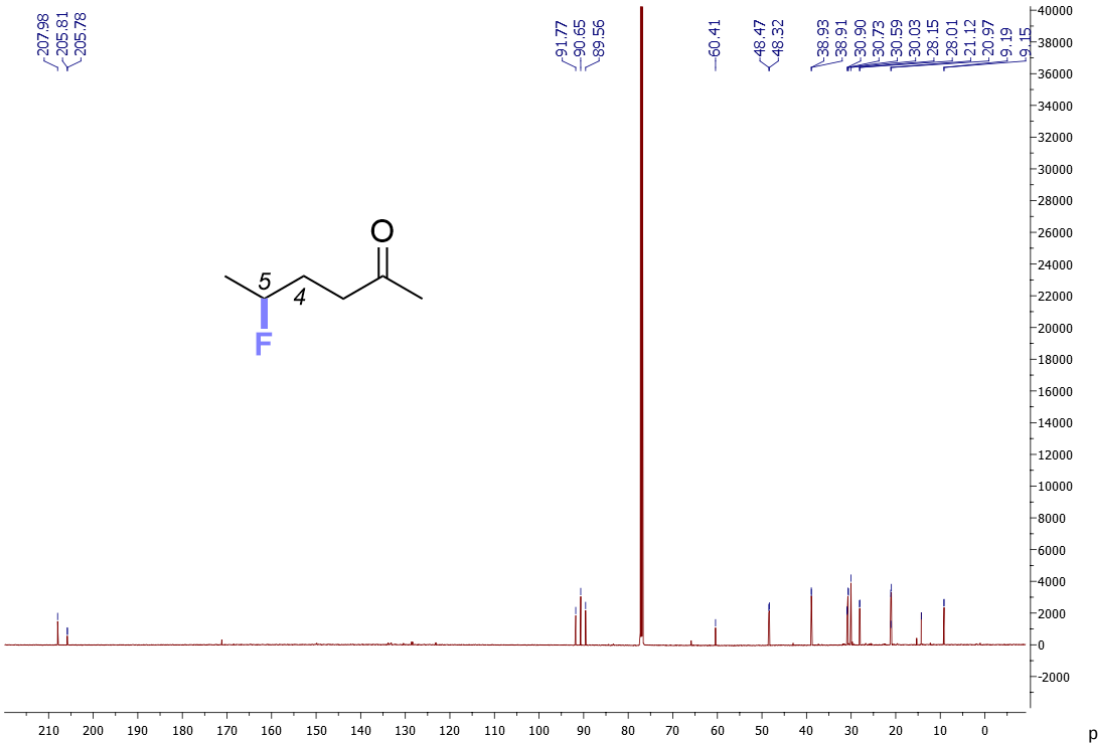

^{19}F NMR of compound **2v** in $CDCl_3$

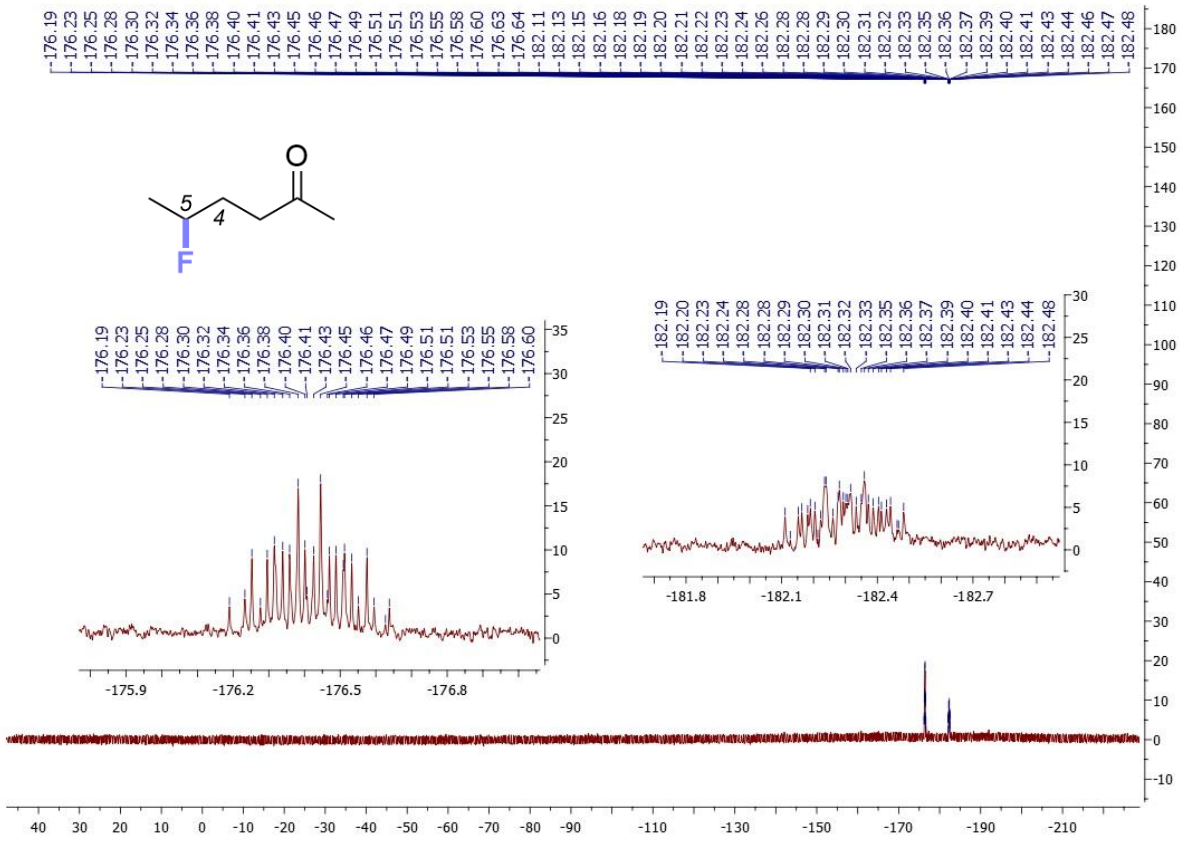

^{1}H NMR of compound **2y** in $CDCl_3$

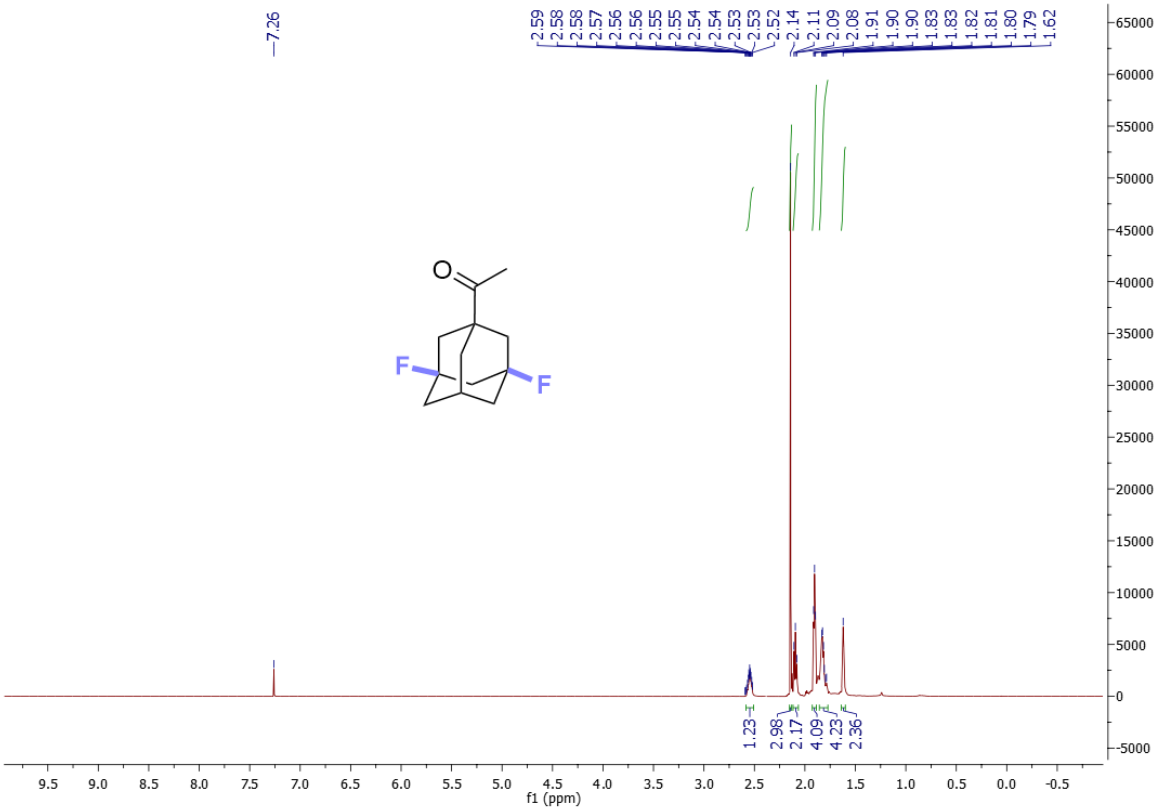

^{13}C NMR of compound **2y** in $CDCl_3$

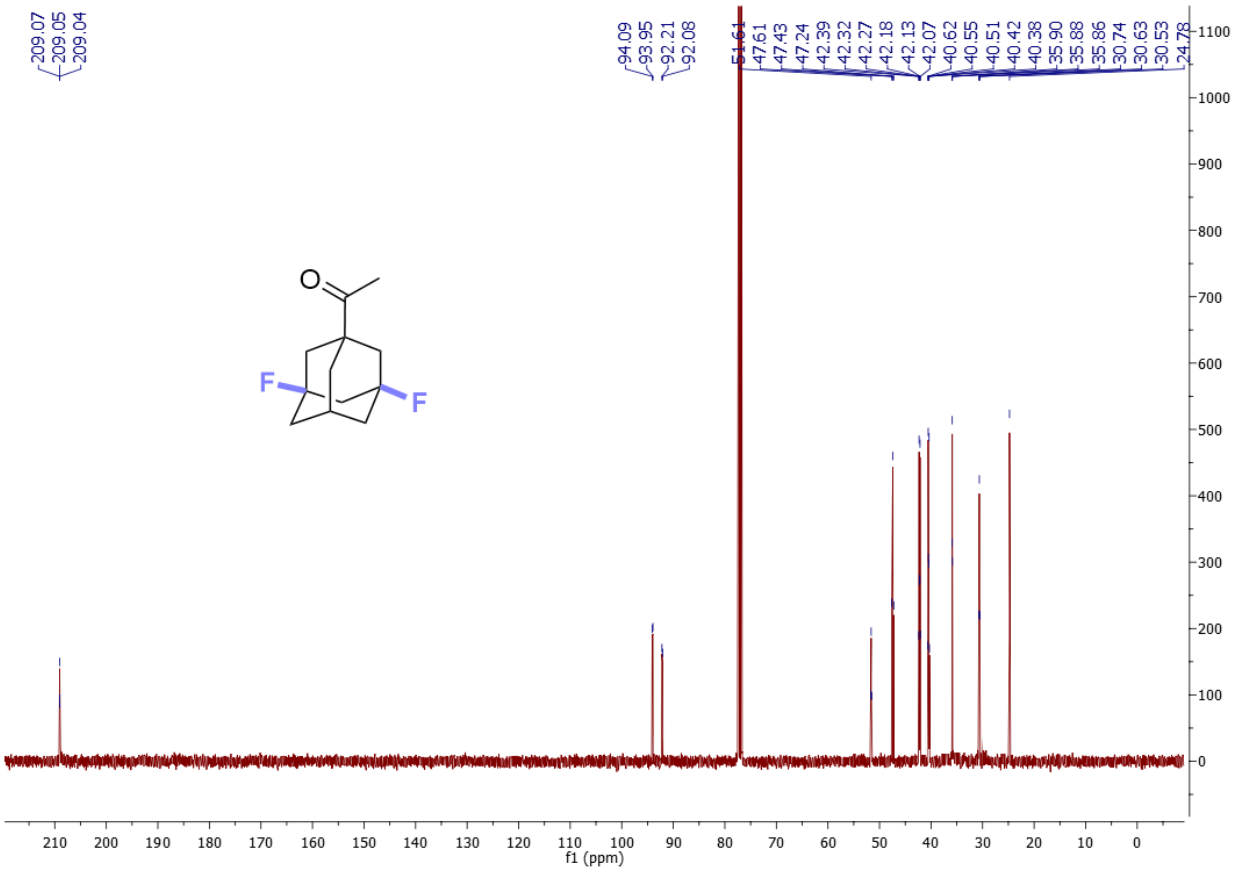

^{19}F NMR of compound **2y** in $CDCl_3$

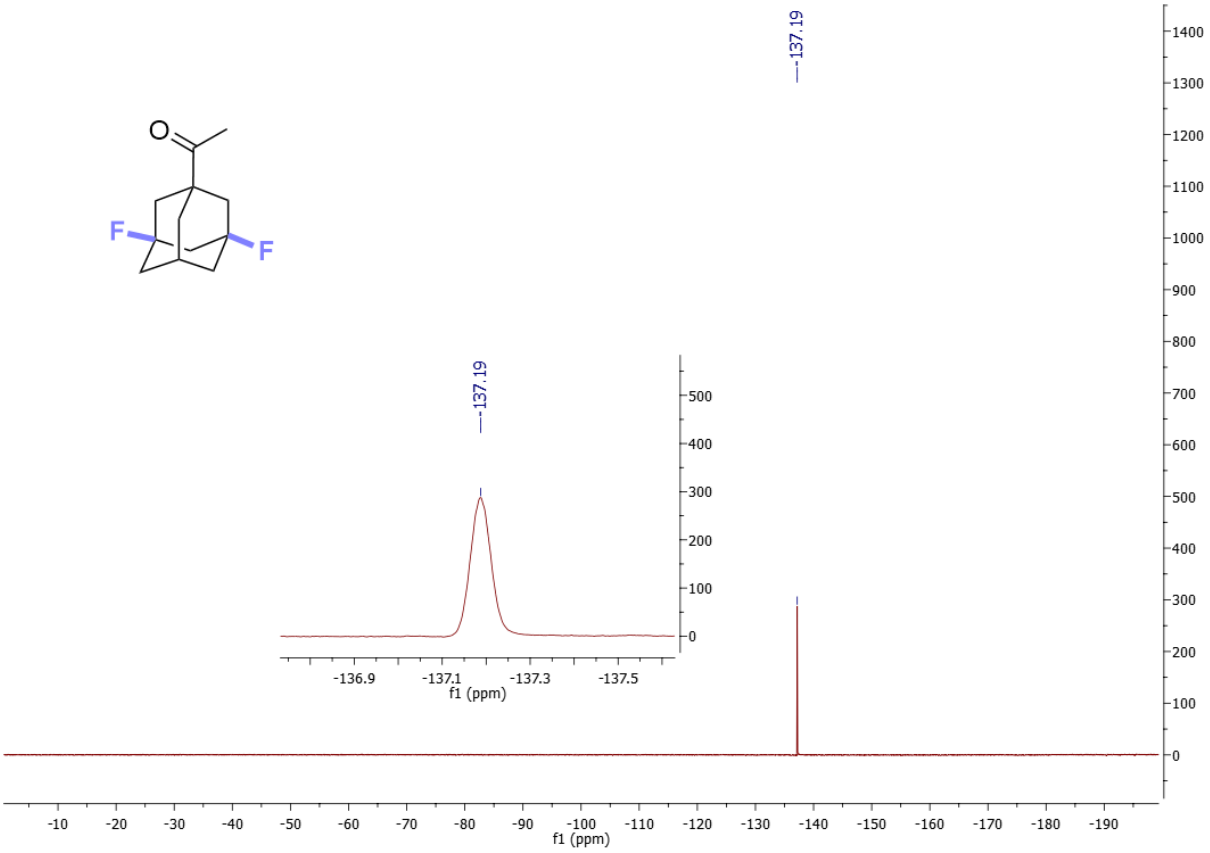

5 X-Ray Crystal Data and Experimental

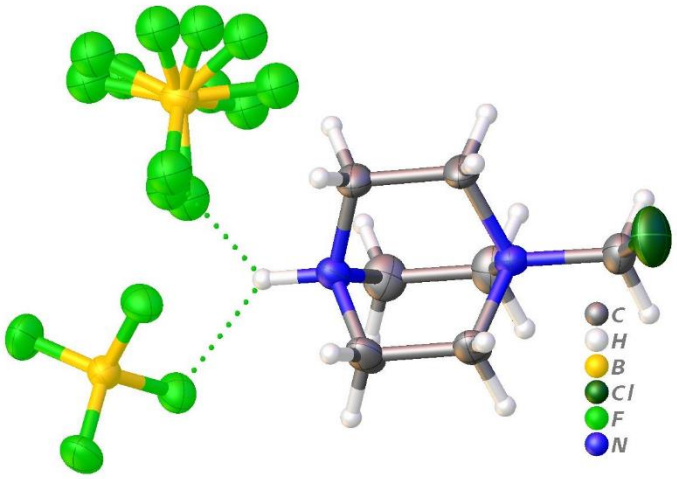

Experimental. Single clear colourless prism-shaped crystals of **H-TEDA(BF$_4$)$_2$** were used as supplied. A suitable crystal with dimensions 0.27 × 0.08 × 0.06 mm^3 was selected and mounted on a MITIGEN holder oil on a XtaLAB Synergy R, DW system, HyPix-Arc 150 diffractometer. The crystal was kept at a steady T = 143.01(10) K during data collection. The structure was solved with the ShelXT 2018/2 (Sheldrick, 2018) solution program using dual methods and by using Olex2 1.5-alpha (Dolomanov et al., 2009) as the graphical interface. The model was refined with ShelXL 2018/3 (Sheldrick, 2015) using full matrix least squares minimisation on $\boldsymbol{F^2}$.

Crystal Data. $C_7H_{15}B_2ClF_8N_2$, M_r = 336.23, orthorhombic, *Pbca* (No. 61), a = 13.1167(2) Å, b = 12.7140(2) Å, c = 15.6393(3) Å, $\alpha = \beta = \gamma = 90^\circ$, V = 2608.10(8) Å^3, T = 143.01(10) K, Z = 8, Z' = 1, μ(Cu K$_\alpha$) = 3.463, 30229 reflections measured, 2683 unique (R_{int} = 0.0477) which were used in all calculations. The final wR_2 was 0.1740 (all data) and R_1 was 0.0654 (I≥2 σ(I)).

CCDC deposition number: 2291634.

Compound	**H-TEDA(BF$_4$)$_2$**
Formula	$C_7H_{15}B_2ClF_8N_2$
$D_{calc.}$/ g cm^{-3}	1.713
μ/mm^{-1}	3.463
Formula Weight	336.23
Colour	clear colourless
Shape	prism-shaped
Size/mm^3	0.27×0.08×0.06
T/K	143.01(10)
Crystal System	orthorhombic
Space Group	*Pbca*
a/Å	13.1167(2)
b/Å	12.7140(2)
c/Å	15.6393(3)
α/°	90
β/°	90
γ/°	90
V/Å^3	2608.10(8)
Z	8
Z'	1
Wavelength/Å	1.54184
Radiation type	Cu K$_\alpha$
Θ_{min}/°	5.611
Θ_{max}/°	75.507
Measured Refl's.	30229
Indep't Refl's	2683
Refl's I≥2 σ(I)	2362
R_{int}	0.0477
Parameters	190
Restraints	1
Largest Peak	0.904
Deepest Hole	-0.522
GooF	1.053
wR_2 (all data)	0.1740
wR_2	0.1686
R_1 (all data)	0.0719
R_1	0.0654

Table 1: Fractional Atomic Coordinates (×10⁴) and Equivalent Isotropic Displacement Parameters (Å²×10³) for **H-TEDA(BF₄)₂**. U_{eq} is defined as 1/3 of the trace of the orthogonalised U_{ij}.

Atom	x	y	z	U_{eq}
Cl1	6088.4(8)	882.4(7)	5305.8(7)	54.6(3)
F5	6538.8(14)	5242.3(14)	8540.9(11)	33.7(4)
F6	8002.5(14)	5257.1(15)	7787.4(11)	36.0(4)
F7	8066.2(16)	5127.7(15)	9233.5(11)	40.9(5)
F8	7578.7(18)	6668.9(14)	8620.5(13)	45.3(5)
N1	6234.1(19)	4238.9(18)	6958.6(15)	27.0(5)
N2	5584.5(18)	2650.8(18)	6167.4(14)	24.8(5)
C1	6669(3)	4236(2)	6075.1(19)	33.1(7)
C3	4705(3)	3330(3)	6450(2)	38.2(7)
C6	6171(3)	2308(2)	6947.2(19)	32.8(7)
C4	5105(3)	4288(3)	6922(2)	39.5(7)
C5	6560(3)	3265(2)	7422(2)	38.1(8)
C7	5138(3)	1715(2)	5710(2)	35.6(7)
C2	6270(3)	3285(2)	5591.9(19)	36.3(7)
B1	7555(3)	5588(3)	8556(2)	27.7(7)
B2	5919(3)	7098(3)	6284(2)	30.6(7)
F2	6277(4)	6555(5)	6988(4)	44.7(5)
F3	6030(4)	8163(3)	6526(3)	44.7(5)
F1	6462(4)	6884(4)	5563(3)	44.7(5)
F4	4920(3)	6861(4)	6195(3)	44.7(5)
F1A	6073(9)	6570(8)	5494(6)	44.7(5)
F2A	5972(9)	6459(11)	7033(8)	44.7(5)
F4A	4864(8)	7400(9)	6235(6)	44.7(5)
F3A	6299(9)	8092(9)	6268(7)	44.7(5)
F4B	5193(8)	6470(8)	5866(7)	44.7(5)
F1B	6744(9)	7220(9)	5721(7)	44.7(5)
F3B	5550(10)	8060(9)	6405(7)	44.7(5)
F2B	6513(10)	6480(12)	6837(9)	44.7(5)

Table 2: Anisotropic Displacement Parameters (×10⁴) for **H-TEDA(BF₄)₂**. The anisotropic displacement factor exponent takes the form: $-2\pi^2[h^2a^{*2} \times U_{11} + \ldots + 2hka^* \times b^* \times U_{12}]$

Atom	U_{11}	U_{22}	U_{33}	U_{23}	U_{13}	U_{12}
Cl1	61.0(6)	38.8(5)	63.9(6)	-23.3(4)	-0.7(4)	-0.3(4)
F5	33.0(9)	37.1(10)	31.2(9)	-4.4(7)	3.5(7)	-2.8(7)
F6	35.7(10)	43.5(10)	28.9(9)	-1.8(7)	4.5(7)	-3.4(8)
F7	51.7(12)	41.9(10)	29.1(9)	4.1(8)	-13.5(8)	-0.7(9)
F8	63.3(13)	25.9(9)	46.5(11)	-1.5(8)	-5.7(10)	-5.2(9)
N1	34.7(13)	24.5(12)	22.0(11)	0.1(9)	-2.6(9)	1.2(10)
N2	28.5(12)	24.7(11)	21.1(10)	2.2(9)	0.5(9)	-2.1(9)
C1	41.2(17)	33.1(15)	25.0(14)	0.1(12)	5.6(12)	-8.3(13)
C3	30.3(16)	36.0(17)	48.3(19)	-3.2(14)	-2.7(14)	5.0(13)
C6	45.3(18)	25.3(14)	27.9(14)	4.7(11)	-8.3(13)	2.0(12)
C4	37.2(17)	37.1(17)	44.2(18)	-6.2(14)	6.0(14)	6.7(14)
C5	58(2)	29.1(15)	27.3(14)	3.3(12)	-14.4(14)	3.0(14)
C7	40.0(17)	30.7(15)	36.1(16)	0.0(12)	-7.1(13)	-8.9(13)
C2	49.8(19)	35.5(16)	23.6(14)	-1.5(12)	8.7(13)	-15.0(14)
B1	34.2(17)	25.4(15)	23.7(14)	-0.9(12)	-0.7(13)	-3.1(13)
B2	32.6(17)	31.5(16)	27.8(15)	1.0(13)	-0.5(13)	1.0(14)
F2	48.9(14)	42.9(10)	42.4(10)	-1.8(9)	-0.1(8)	-2.8(10)
F3	48.9(14)	42.9(10)	42.4(10)	-1.8(9)	-0.1(8)	-2.8(10)
F1	48.9(14)	42.9(10)	42.4(10)	-1.8(9)	-0.1(8)	-2.8(10)
F4	48.9(14)	42.9(10)	42.4(10)	-1.8(9)	-0.1(8)	-2.8(10)
F1A	48.9(14)	42.9(10)	42.4(10)	-1.8(9)	-0.1(8)	-2.8(10)

Atom	U_{11}	U_{22}	U_{33}	U_{23}	U_{13}	U_{12}
F^{2A}	48.9(14)	42.9(10)	42.4(10)	-1.8(9)	-0.1(8)	-2.8(10)
F^{4A}	48.9(14)	42.9(10)	42.4(10)	-1.8(9)	-0.1(8)	-2.8(10)
F^{3A}	48.9(14)	42.9(10)	42.4(10)	-1.8(9)	-0.1(8)	-2.8(10)
F^{4B}	48.9(14)	42.9(10)	42.4(10)	-1.8(9)	-0.1(8)	-2.8(10)
F^{1B}	48.9(14)	42.9(10)	42.4(10)	-1.8(9)	-0.1(8)	-2.8(10)
F^{3B}	48.9(14)	42.9(10)	42.4(10)	-1.8(9)	-0.1(8)	-2.8(10)
F^{2B}	48.9(14)	42.9(10)	42.4(10)	-1.8(9)	-0.1(8)	-2.8(10)

Table 3: Bond Lengths in Å for **H-TEDA(BF$_4$)$_2$**.

Atom	Atom	Length/Å
Cl^{1}	C^{7}	1.753(4)
F^{5}	B^{1}	1.404(4)
F^{6}	B^{1}	1.402(4)
F^{7}	B^{1}	1.384(4)
F^{8}	B^{1}	1.378(4)
N^{1}	C^{1}	1.495(4)
N^{1}	C^{4}	1.484(4)
N^{1}	C^{5}	1.497(4)
N^{2}	C^{3}	1.507(4)
N^{2}	C^{6}	1.506(3)
N^{2}	C^{7}	1.507(4)
N^{2}	C^{2}	1.506(4)
C^{1}	C^{2}	1.519(4)
C^{3}	C^{4}	1.518(5)
C^{6}	C^{5}	1.514(4)
B^{2}	F^{2}	1.382(7)
B^{2}	F^{3}	1.414(6)
B^{2}	F^{1}	1.361(5)
B^{2}	F^{4}	1.351(5)
B^{2}	F^{1A}	1.421(10)
B^{2}	F^{2A}	1.427(14)
B^{2}	F^{4A}	1.438(11)
B^{2}	F^{3A}	1.359(12)
B^{2}	F^{4B}	1.404(11)
B^{2}	F^{1B}	1.403(12)
B^{2}	F^{3B}	1.330(12)
B^{2}	F^{2B}	1.404(16)

Table 4: Bond Angles in ° for **H-TEDA(BF$_4$)$_2$**.

Atom	Atom	Atom	Angle/°
C^{1}	N^{1}	C^{5}	109.7(2)
C^{4}	N^{1}	C^{1}	110.2(2)
C^{4}	N^{1}	C^{5}	109.8(3)
C^{6}	N^{2}	C^{3}	108.6(2)
C^{6}	N^{2}	C^{7}	110.7(2)
C^{7}	N^{2}	C^{3}	107.1(2)
C^{2}	N^{2}	C^{3}	109.0(2)
C^{2}	N^{2}	C^{6}	109.5(2)
C^{2}	N^{2}	C^{7}	111.8(2)
N^{1}	C^{1}	C^{2}	109.3(2)
N^{2}	C^{3}	C^{4}	109.8(3)
N^{2}	C^{6}	C^{5}	109.7(2)
N^{1}	C^{4}	C^{3}	109.3(3)
N^{1}	C^{5}	C^{6}	109.4(2)
N^{2}	C^{7}	Cl^{1}	111.8(2)
N^{2}	C^{2}	C^{1}	109.5(2)
F^{6}	B^{1}	F^{5}	106.8(2)
F^{7}	B^{1}	F^{5}	109.9(2)
F^{7}	B^{1}	F^{6}	109.1(3)
F^{8}	B^{1}	F^{5}	109.6(3)
F^{8}	B^{1}	F^{6}	110.6(3)
F^{8}	B^{1}	F^{7}	110.8(2)
F^{2}	B^{2}	F^{3}	103.3(4)
F^{1}	B^{2}	F^{2}	112.5(4)
F^{1}	B^{2}	F^{3}	111.0(4)
F^{4}	B^{2}	F^{2}	107.5(4)
F^{4}	B^{2}	F^{3}	109.9(4)
F^{4}	B^{2}	F^{1}	112.2(4)
F^{1A}	B^{2}	F^{2A}	116.0(7)
F^{1A}	B^{2}	F^{4A}	102.5(6)
F^{2A}	B^{2}	F^{4A}	104.0(6)
F^{3A}	B^{2}	F^{1A}	111.8(6)
F^{3A}	B^{2}	F^{2A}	121.8(8)
F^{3A}	B^{2}	F^{4A}	96.0(7)
F^{4B}	B^{2}	F^{2B}	110.2(8)
F^{1B}	B^{2}	F^{4B}	107.1(7)
F^{1B}	B^{2}	F^{2B}	91.2(7)
F^{3B}	B^{2}	F^{4B}	110.1(7)
F^{3B}	B^{2}	F^{1B}	105.5(7)
F^{3B}	B^{2}	F^{2B}	128.9(9)

Table 5: Torsion Angles in ° for **H-TEDA(BF$_4$)$_2$**.

Atom	Atom	Atom	Atom	Angle/°
N^{1}	C^{1}	C^{2}	N^{2}	-1.0(4)
N^{2}	C^{3}	C^{4}	N^{1}	-0.5(4)
N^{2}	C^{6}	C^{5}	N^{1}	-0.1(4)

Atom	Atom	Atom	Atom	Angle/°
C^{1}	N^{1}	C^{4}	C^{3}	60.7(3)
C^{1}	N^{1}	C^{5}	C^{6}	-60.4(3)
C^{3}	N^{2}	C^{6}	C^{5}	-59.4(3)
C^{3}	N^{2}	C^{7}	Cl^{1}	177.5(2)
C^{3}	N^{2}	C^{2}	C^{1}	59.9(3)
C^{6}	N^{2}	C^{3}	C^{4}	60.0(3)
C^{6}	N^{2}	C^{7}	Cl^{1}	-64.2(3)
C^{6}	N^{2}	C^{2}	C^{1}	-58.8(3)
C^{4}	N^{1}	C^{1}	C^{2}	-59.9(3)
C^{4}	N^{1}	C^{5}	C^{6}	60.8(3)
C^{5}	N^{1}	C^{1}	C^{2}	61.0(3)
C^{5}	N^{1}	C^{4}	C^{3}	-60.2(3)
C^{7}	N^{2}	C^{3}	C^{4}	179.7(3)
C^{7}	N^{2}	C^{6}	C^{5}	-176.7(3)
C^{7}	N^{2}	C^{2}	C^{1}	178.1(3)
C^{2}	N^{2}	C^{3}	C^{4}	-59.2(3)
C^{2}	N^{2}	C^{6}	C^{5}	59.5(3)
C^{2}	N^{2}	C^{7}	Cl^{1}	58.2(3)

Table 6: Hydrogen Fractional Atomic Coordinates ($\times 10^{4}$) and Equivalent Isotropic Displacement Parameters ($Å^{2}\times 10^{3}$) for **H-TEDA(BF$_4$)$_2$**. U_{eq} is defined as 1/3 of the trace of the orthogonalised U_{ij}.

Atom	x	y	z	U_{eq}
H^{1}	6494.57	4868.54	7273.38	32
H^{1A}	7422.53	4209.01	6103.87	40
H^{1B}	6470.5	4888.76	5772.76	40
H^{3A}	4249.61	2921.62	6829.84	46
H^{3B}	4306.2	3556.15	5944.76	46
H^{6A}	6752.86	1860.03	6773.3	39
H^{6B}	5723.55	1889.2	7326.54	39
H^{4A}	4888.91	4936.62	6621.58	47
H^{4B}	4821.73	4305.58	7508.28	47
H^{5A}	6282.01	3271.02	8010.65	46
H^{5B}	7312.64	3240.29	7458.73	46
H^{7A}	4703.21	1962.48	5233.6	43
H^{7B}	4701.46	1314.67	6111.57	43
H^{2A}	5885.04	3518.33	5081.47	44
H^{2B}	6848.08	2845	5397.83	44

Table 7: Atomic Occupancies for all atoms that are not fully occupied in **H-TEDA(BF$_4$)$_2$**.

Atom	Occupancy
F^{2}	0.567(4)
F^{3}	0.567(4)
F^{1}	0.567(4)

Atom	Occupancy
F^{4}	0.567(4)
F^{1A}	0.226(4)
F^{2A}	0.226(4)
F^{4A}	0.226(4)

Atom	Occupancy
F^{3A}	0.226(4)
F^{4B}	0.206(4)
F^{1B}	0.206(4)
F^{3B}	0.206(4)

Atom	Occupancy
F^{2B}	0.206(4)

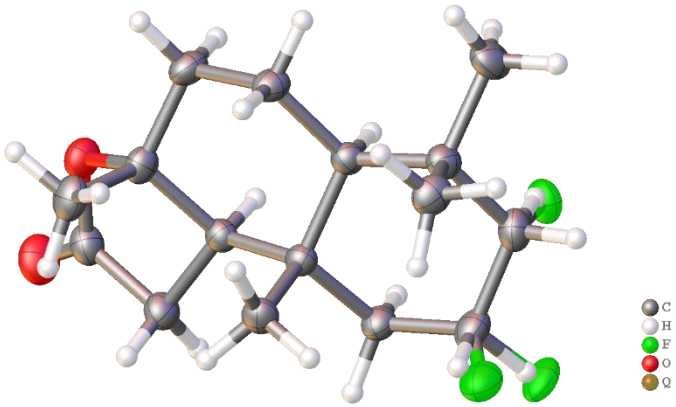

Experimental. Single clear colourless prism-shaped crystals of **2o** were used as supplied. A suitable crystal with dimensions 0.14 × 0.10 × 0.08 mm³ was selected and mounted on a MITIGEN holder inert oil on a XtaLAB Synergy R, DW system, HyPix-Arc 150 diffractometer. The crystal was kept at a steady T = 123.00(10) K during data collection. The structure was solved with the ShelXT 2018/2 (Sheldrick, 2018) solution program using iterative methods and by using Olex2 1.5-alpha (Dolomanov et al., 2009) as the graphical interface. The model was refined with olex2.refine 1.5-alpha (Bourhis et al., 2015) using full matrix least squares minimisation on $\boldsymbol{F^2}$.

Crystal Data. $C_{16}H_{25.05}F_{0.95}O_2$, M_r = 267.385, orthorhombic, $P2_12_12_1$ (No. 19), a = 5.9658(1) Å, b = 13.5775(1) Å, c = 17.6402(1) Å, $\alpha = \beta = \gamma = 90^\circ$, V = 1428.87(3) Å³, T = 123.00(10) K, Z = 4, Z' = 1, μ(Cu K_α) = 0.709, 26733 reflections measured, 2919 unique (R_{int} = 0.0229) which were used in all calculations. The final wR_2 was 0.0707 (all data) and R_1 was 0.0279 (I≥2 σ(I)).

CCDC deposition number: 2381200.

Compound	**2o**
Formula	$C_{16}H_{25.05}F_{0.95}O_2$
$D_{calc.}$/ g cm^{-3}	1.243
μ/mm^{-1}	0.709
Formula Weight	267.385
Colour	clear colourless
Shape	prism-shaped
Size/mm³	0.14×0.10×0.08
T/K	123.00(10)
Crystal System	orthorhombic
Flack Parameter	-0.14(4)
Hooft Parameter	-0.14(4)
Space Group	$P2_12_12_1$
a/Å	5.9658(1)
b/Å	13.5775(1)
c/Å	17.6402(1)
α/°	90
β/°	90
γ/°	90
V/Å³	1428.87(3)
Z	4
Z'	1
Wavelength/Å	1.54184
Radiation type	Cu K_α
Θ_{min}/°	4.11
Θ_{max}/°	75.01
Measured Refl's.	26733
Indep't Refl's	2919
Refl's I≥2 σ(I)	2813
R_{int}	0.0229
Parameters	284
Restraints	0
Largest Peak	0.1599
Deepest Hole	-0.1812
GooF	1.0738
wR_2 (all data)	0.0707
wR_2	0.0698
R_1 (all data)	0.0293
R_1	0.0279

Table 8: Fractional Atomic Coordinates (×10⁴) and Equivalent Isotropic Displacement Parameters (Å²×10³) for **2o**. U_{eq} is defined as 1/3 of the trace of the orthogonalised U_{ij}.

Atom	x	y	z	U_{eq}
O1	1783.6(15)	3665.7(6)	8036.0(5)	30.0(2)
O2	563.6(17)	2117.4(7)	8151.0(5)	41.0(3)
F1	3959(2)	3316.9(8)	4102.2(6)	38.5(4)
C9	4608.7(19)	3968.6(8)	6144.9(6)	22.1(2)
C8	3865(2)	5063.4(8)	6029.9(6)	22.7(2)
C1	1673(2)	2709.8(9)	7812.6(7)	30.4(3)
C3	3159(2)	3621.1(8)	6813.2(6)	22.5(2)
C7	4141(2)	5673.9(9)	6757.8(7)	27.3(3)
C10	3930(2)	3376.1(9)	5437.5(7)	26.8(2)
C4	3440(2)	4190.1(9)	7558.8(6)	25.6(2)
C13	4741(2)	5564.5(8)	5294.9(7)	26.4(3)
C14	7127(2)	3817.3(10)	6298.7(7)	27.9(3)
C2	3043(2)	2560.6(9)	7093.0(7)	29.2(3)
C11	4818(2)	3842.7(10)	4713.4(7)	31.6(3)
C6	2776(2)	5254.7(9)	7428.6(7)	29.1(3)
C15	7273(2)	5762.5(10)	5280.2(7)	31.9(3)
C12	4077(2)	4900.3(9)	4623.5(7)	31.0(3)
C5	5656(2)	4110.1(11)	7989.8(7)	34.1(3)
C16	3556(3)	6560.2(10)	5185.3(8)	36.3(3)
F2	1764(6)	4764(3)	4495(2)	34.3(13)
F3	6620(30)	3727(7)	4513(6)	42(4)

Table 9: Anisotropic Displacement Parameters (×10⁴) for **2o**. The anisotropic displacement factor exponent takes the form: $-2\pi^2[h^2a^{*2} \times U_{11} + \ldots + 2hka^* \times b^* \times U_{12}]$

Atom	U_{11}	U_{22}	U_{33}	U_{23}	U_{13}	U_{12}
O1	32.3(5)	32.8(4)	24.9(4)	-4.4(4)	5.3(4)	1.9(4)
O2	46.0(6)	40.0(5)	37.1(5)	-11.0(5)	4.2(4)	9.6(4)
F1	60.4(8)	32.9(6)	22.3(6)	-10.0(6)	-0.7(5)	-8.6(4)
C9	21.5(5)	22.8(5)	21.8(5)	1.5(4)	-0.5(4)	-0.5(4)
C8	22.3(5)	22.8(5)	23.1(5)	0.6(4)	1.0(4)	0.4(4)
C1	33.3(7)	30.5(6)	27.5(6)	-2.5(5)	-2.7(5)	5.6(5)
C3	21.8(5)	22.7(5)	23.1(5)	0.1(5)	-1.8(4)	0.9(4)
C7	31.9(6)	22.0(5)	28.1(6)	-1.5(5)	4.9(5)	-1.9(5)
C10	32.8(6)	23.7(5)	24.1(5)	-1.1(5)	-0.4(5)	-2.0(4)
C4	25.2(6)	29.7(6)	21.9(5)	-2.8(5)	3.5(4)	0.3(5)
C13	29.4(6)	23.4(6)	26.5(6)	-0.5(4)	2.6(5)	2.7(5)
C14	22.9(5)	31.8(6)	29.0(6)	4.0(5)	1.0(5)	1.0(5)
C2	35.8(7)	24.7(6)	27.2(6)	-1.8(5)	0.8(5)	3.1(5)
C11	40.3(7)	31.5(6)	23.0(6)	-4.3(5)	0.9(6)	-4.6(5)
C6	34.1(7)	26.5(6)	26.5(6)	-1.4(5)	6.8(5)	-4.8(5)
C15	32.7(7)	32.0(6)	31.0(6)	-5.8(5)	6.0(5)	-0.0(6)
C12	34.1(6)	34.9(7)	24.2(6)	-3.4(5)	-1.5(5)	4.3(5)
C5	33.7(7)	43.5(7)	25.1(6)	-4.7(6)	-4.8(5)	-0.9(6)
C16	43.6(8)	27.9(6)	37.4(7)	4.4(6)	5.5(6)	9.4(5)
F2	31(2)	41(2)	31(2)	2.0(16)	-9.1(15)	4.4(15)
F3	61(8)	30(5)	35(6)	-1(5)	2(6)	-5(4)

Table 10: Bond Lengths in Å for **2o**.

Atom	Atom	Length/Å
O1	C1	1.3580(16)
O1	C4	1.4808(14)
O2	C1	1.2007(15)
F1	C11	1.3911(17)
C9	C8	1.5643(15)
C9	C3	1.5363(16)
C9	C10	1.5389(16)
C9	C14	1.5407(16)
C8	C7	1.5372(16)
C8	C13	1.5548(16)
C1	C2	1.5234(17)
C3	C4	1.5346(15)
C3	C2	1.5237(15)
C7	C6	1.5451(17)
C10	C11	1.5210(17)
C4	C6	1.5162(17)
C4	C5	1.5289(17)
C13	C15	1.5346(18)
C13	C12	1.5404(17)
C13	C16	1.5378(17)
C11	C12	1.5109(18)
C11	F3	1.141(18)
C12	F2	1.411(4)

Table 11: Bond Angles in ° for **2o**.

Atom	Atom	Atom	Angle/°
C4	O1	C1	109.08(9)
C3	C9	C8	103.40(9)
C10	C9	C8	108.48(9)
C10	C9	C3	108.28(9)
C14	C9	C8	115.22(10)
C14	C9	C3	111.89(9)
C14	C9	C10	109.24(10)
C7	C8	C9	111.95(9)
C13	C8	C9	115.38(9)
C13	C8	C7	115.13(9)
O2	C1	O1	121.52(12)
C2	C1	O1	110.06(10)
C2	C1	O2	128.39(12)
C4	C3	C9	116.20(10)
C2	C3	C9	124.35(10)
C2	C3	C4	101.72(9)
C6	C7	C8	112.62(10)
C11	C10	C9	111.81(10)
C3	C4	O1	99.92(9)
C6	C4	O1	111.72(10)
C6	C4	C3	108.76(9)
C5	C4	O1	105.08(9)
C5	C4	C3	119.02(10)
C5	C4	C6	111.66(11)
C15	C13	C8	114.94(10)
C12	C13	C8	107.37(9)
C12	C13	C15	110.05(10)
C16	C13	C8	109.57(10)
C16	C13	C15	107.24(11)
C16	C13	C12	107.44(10)
C3	C2	C1	99.71(10)
C10	C11	F1	107.98(11)
C12	C11	F1	107.36(11)
C12	C11	C10	112.47(11)
F3	C11	F1	92.1(6)
F3	C11	C10	122.1(6)
F3	C11	C12	111.9(5)
C4	C6	C7	109.24(10)
C11	C12	C13	113.60(10)
F2	C12	C13	116.89(19)
F2	C12	C11	100.27(19)

Table 12: Torsion Angles in ° for **2o**.

Atom	Atom	Atom	Atom	Angle/°
O1	C1	C2	C3	-20.15(11)
O1	C4	C3	C9	178.75(8)
O1	C4	C3	C2	-43.14(10)
O1	C4	C6	C7	-163.83(10)
O2	C1	C2	C3	157.62(16)
F1	C11	C10	C9	-174.52(11)
F1	C11	C12	C13	175.31(11)
F1	C11	C12	F2	49.81(19)
C9	C8	C7	C6	-58.79(11)
C9	C8	C13	C15	-69.18(11)
C9	C8	C13	C12	53.61(11)
C9	C8	C13	C16	170.01(11)
C9	C3	C4	C6	61.62(11)
C9	C3	C4	C5	-67.73(11)
C9	C3	C2	C1	171.83(13)
C9	C10	C11	C12	-56.24(12)

Atom	Atom	Atom	Atom	Angle/°
C9	C10	C11	F3	81.1(6)
C8	C7	C6	C4	56.08(11)
C8	C13	C12	C11	-53.14(11)
C8	C13	C12	F2	62.95(19)
C1	C2	C3	C4	38.36(10)
C3	C4	C6	C7	-54.50(11)
C7	C6	C4	C5	78.82(11)
C10	C11	C12	C13	56.68(12)
C10	C11	C12	F2	-68.83(18)
C13	C12	C11	F3	-85.1(6)

Table 13: Hydrogen Fractional Atomic Coordinates ($\times 10^4$) and Equivalent Isotropic Displacement Parameters ($Å^2 \times 10^3$) for **2o**. U_{eq} is defined as 1/3 of the trace of the orthogonalised U_{ij}.

Atom	x	y	z	U_{eq}
H8	2180(20)	5027(10)	5930(7)	21(3)
H3	1600(20)	3770(10)	6658(7)	22(3)
H7a	5810(20)	5710(10)	6896(8)	26(3)
H7b	3620(30)	6365(11)	6672(8)	32(4)
H10a	4490(20)	2661(10)	5475(7)	25(3)
H10b	2140(20)	3316(9)	5386(7)	14(3)
H14a	8010(30)	3731(11)	5829(9)	36(4)
H14b	7790(30)	4380(12)	6574(9)	36(4)
H14c	7370(30)	3209(11)	6600(9)	37(4)
H2a	4480(30)	2288(12)	7238(9)	38(4)
H2b	2250(30)	2084(11)	6751(8)	36(4)
H11a	6650(50)	3813.9(13)	4717.8(7)	37.9(3)
H11b	4233(16)	3417(12)	4228(14)	37.9(3)
H6a	3030(30)	5658(11)	7889(8)	28(3)
H6b	1100(30)	5282(11)	7305(8)	30(4)
H15a	7730(30)	6143(12)	5747(9)	42(4)
H15b	8250(30)	5158(12)	5221(9)	44(4)
H15c	7650(30)	6145(14)	4813(10)	51(5)
H12a	2380(20)	4916.9(10)	4563.3(11)	37.3(3)
H12	4763(9)	5178(4)	4141(7)	30(4)
H5a	5380(30)	4361(12)	8506(10)	46(5)
H5b	6260(30)	3419(12)	8001(9)	39(4)
H5c	6830(30)	4540(11)	7771(8)	32(4)
H16a	1900(30)	6504(11)	5258(9)	37(4)
H16b	4140(30)	7064(13)	5542(9)	46(5)
H16c	3850(30)	6812(12)	4675(10)	45(4)

Table 14: Atomic Occupancies for all atoms that are not fully occupied in **2o**.

Atom	Occupancy
F1	0.660(4)
H11a	0.921(4)
H11b	0.340(4)
H12a	0.793(3)
F2	0.207(3)
F3	0.079(4)

6 References

1. S. Yakubov, W. J. Stockerl, X. Tian, A. Shahin, M. J. P. Mandigma, R. M. Gschwind and J. P. Barham, *Chem. Sci.,* 2022, **13**, 14041.
2. Selected examples: (a) C. W. Kee, K. F. Chin, M. W. Wong and C. H. Tan, *Chem. Commun.,* 2014, **50**, 8211; (b) J. B. Xia, C. Zhu and C. Chen, *Chem. Commun.,* 2014, **50**, 11701; (c) S. Bloom, J. L. Knippel and T. Lectka, *Chem. Sci.,* 2014, **5**, 1175; (d) J. B. Xia, Y. Ma and C. Chen, *Org. Chem. Front.,* 2014, **1**, 468.
3. R. S., Sreeperumbuduru, Z. M., Abid, K. M., Claunch, H. H., Chen, S. M., McGillivray and E. E. Simanek, *RSC Adv.*, 2016, **6**, 8806.
4. Y. F. Liang and N. Jiao, *Angew. Chem., Int. Ed.,* 2014, **53**, 548.
5. S. Ikonen, Nonappa, A. Valkonen, R. Juvonen, H. Salo and E. Kolehmainen, *Org. Biomol. Chem.,* 2010, **8**, 2784.
6. Y. Amaoka, M. Nagatomo and M. Inoue, *Org. Lett.,* 2013, **15**, 2160.
7. A. M. Hua, D. N. Mai, R. Martinez and R. D. Baxter, *Org. lett.,* 2017, **19**, 2949.